

Manuscript Number: GR-D-13-00117R1

Title: A PROVENANCE STUDY OF THE PALEOZOIC VENTANIA SYSTEM (ARGENTINA): TRANSIENT COMPLEX SOURCES FROM WESTERN AND EASTERN GONDWANA

Article Type: Research Paper

Corresponding Author: Dr. Victor A. Ramos, Dr.

Corresponding Author's Institution: Universidad de Buenos Aires

First Author: Victor A Ramos, Dr.

Order of Authors: Victor A Ramos, Dr.; Farid Chemale Jr., Dr.; Maximiliano Naipauer, Dr.; Pablo Pazos, Doctor

Abstract: The U-Pb and Lu-Hf isotopic analyses of the different sedimentary sequences of the Ventania System, an old Paleozoic orogenic belt exposed in the southern region of the Río de la Plata Craton in the province of Buenos Aires, Argentina, provide new evidence for the understanding of the tectonic evolution of the western sector of the Gondwanides mountain belt. These ranges formed as result of the late Paleozoic collision of the Patagonia terrane against the continental margin of Gondwana. The provenance analysis together with the sedimentary paleocurrents confirm a dominant source from the Tandilia System, a Paleoproterozoic mountain belt formed during the amalgamation of the Río de la Plata Craton at about 1,800-2,200 Ma, and incorporated to Western Gondwana during the Brasiliano Orogeny at 550-530 Ma. The local dominant source at the base of the early Paleozoic changed to more distant supplies toward the top of the sequences, when is recorded an increasing participation of detritus from first, Cambrian (560-520 Ma) zircons from the Pampean Orogen, and later on Ordovician (480-460 Ma) zircons from the Famatinian Orogen. The detrital zircon patterns and the maximum age of the units shed light on some previous discrepancies in the early Paleozoic stratigraphy. The Balcarce Formation, an early Paleozoic sedimentary cover of the Tandilia metamorphic and igneous basement, shows striking differences when compared with the new data from the Ventania System. The two data-sets reveal different sources for the two regions. The late Paleozoic foreland basin deposits mark an abrupt change of 180° in the paleocurrent directions, in the petrographic composition of the sediments, and in the provenance of detrital zircons. These data indicate a southern provenance with the first evidence of Carboniferous and Permian magmatic zircons. The oldest Archean zircons together with the finding of clasts with archeocyathids support the provenance from Patagonia, which was derived from Eastern Gondwana. The U-Pb ages of the ash-fall tuffs in the Tunas Formation confirm the Early Permian age of the Eurydesma Fauna in the Ventania System. The U-Pb data together with the Lu-Hf isotopic data enhance the comprehension of the tectonic evolution of the Ventania System as part of the larger Gondwanides Belt that amalgamated to Western Gondwana during Late Permian times with some independent pieces derived from Eastern Gondwana.

Response to Reviewers: In the attach "answer to the reviewers" we give a detail report of the changes made. We have no major differences with the recommended corrections.

July 6th, 2013.-

Ms. Ref. No.: GR-D-13-00117

Title: A PROVENANCE STUDY OF THE PALEOZOIC VENTANIA SYSTEM
(ARGENTINA): TRANSIENT COMPLEX SOURCES FROM WESTERN AND
EASTERN GONDWANA

Gondwana Research

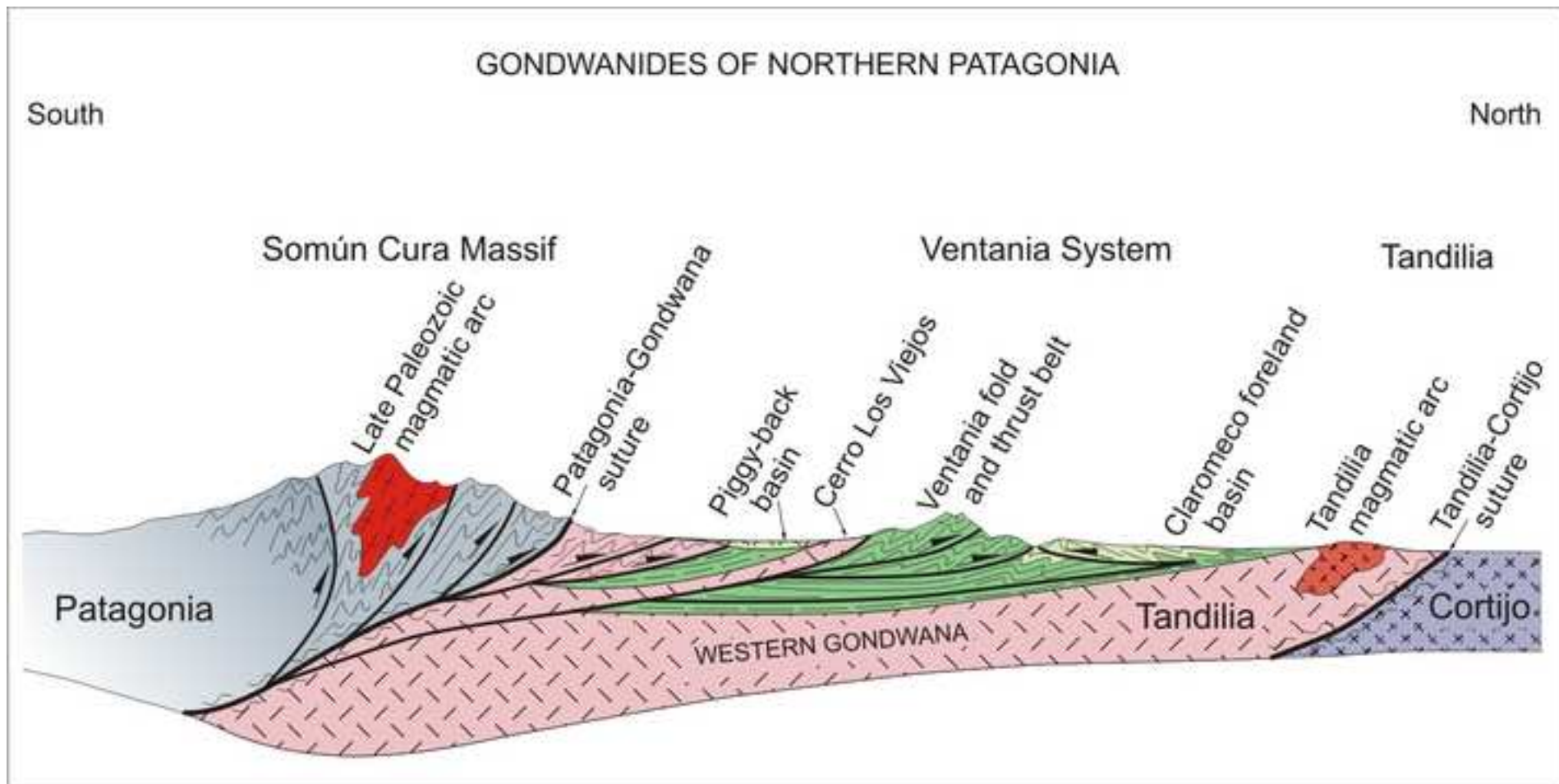
Dear Dr Collins,

We are submitting the comments to the reviewers, new figures and the revised version of the manuscript. We have had very constructive and positive reviews and we acknowledge the reviewers for their excellent reviews. It is a pity that one of the reviewers is anonymous, because he has done positive comments that improved the manuscript.

Best regards,

A handwritten signature in blue ink, appearing to read "Victor Ramos", with a horizontal line underneath.

Victor A. Ramos



HIGHLIGHTS

- Comprehensive detrital zircon U-Pb age database of the Paleozoic Ventania Fold Belt.
- Changing sources through time shed light in the paleogeography of this sector of Gondwana.
- An abrupt change in provenance associated with the collision of Patagonia.
- Different Precambrian sources and Paleozoic similarities when compared with the Cape Fold Belt.

Ms. Ref. No.: GR-D-13-00117

Title: A PROVENANCE STUDY OF THE PALEOZOIC VENTANIA SYSTEM
(ARGENTINA): TRANSIENT COMPLEX SOURCES FROM WESTERN AND
EASTERN GONDWANA

Gondwana Research

Answers to the reviewers' comments

Reviewer #1:

The article in question presents a complete set of U-Pb detrital zircon ages from rocks of the Ventania System located at the southern portion of the Buenos Aires Province. At the same time makes comparisons with Table Mountain Belt of South Africa. This is an article where the data, predominantly LAICPMS zircon ages, are interpreted based on local and regional geological contexts, providing robustness to the paleogeographic reconstructions presented.

1) The cited articles are relevant and updated with minor problems reported in the text. Most of these problems concerns articles of the U-Pb and Lu-Hf methodologies not mentioned in the text but presented in the list of references.

The following cites that were missing are now included:

Deleted cites:

Blichert-Toft and Albarede, 1997.

Bodet and Scharer, 2000

Eggins et al., 1998

Patchett and Ruiz, 1987

Scherer et al., 2001

Woodhead et al., 2004

Woodhead and Hergt, 2005

Add cites:

Goodge, J.W., Vervoort, J.D., 2006. Origin of Mesoproterozoic A-type granites in Laurentia: Hf isotope evidence. Earth and Planetary Science Letters 243, 711–731.

Stacey, J.S., Kramers, J.D., 1975. Approximation of terrestrial lead isotope evolution by a two-stage model. Earth and Planetary Science Letters 26, 207–221.

Harrington, H.J., 1955. The Permian Eurydesma fauna of Eastern Argentina. Journal of Paleontology 29, 112-128.

Ramos, V. A., 1988. Tectonic of the Late Proterozoic-Early Paleozoic: a collisional history of the southern South American. Episodes, 12: 168-174.

2) Comments and discussions of the internal structures of the zircon crystals that can help to interpret the ages obtained are missing. Ideally the tables showing the analytical data have an additional column next to the spot number with the indications concerning the place of the grain effectively analyzed. For example, a detailed examination of the images of back-scatter, could clarify some of the authors doubts concerning the Pan de Azucar sample. If the analyzed domains correspond to igneous portions (oscillatory zoning) would most likely consider this rock a quartzite belonging to low-grade metamorphic units of La Lola Fm, and probably derived from a source other than the underlying metamorphic basement. On the other hand if the analyzed portion corresponds to metamorphic rims (overgrowths), the age of 545Ma likely indicate the time of the main metamorphic event of the underlying paragneiss basement.

The suggestion of the reviewer was correct. We are showing the BSE images of zircon crystals from sample VE-02 (Pan de Azúcar sample) to support interpretation. The internal textures and Th/U ratio in each dated zircon indicate an igneous origin; apparently deformational and metamorphic process has not reached the detrital zircons. The images have been incorporated in the new Figure 6, where is indicated the spot places in each grain.

3) The plots presented in Figures 6b, 8, 9, 10, 11, 13, 14, 15, and 18 represent the frequency diagrams constructed with U-Pb detrital zircon ages for the different samples. This manner of representation is interesting but, the absence of the histograms in the same figure, prevents the reader easily see how many points were used in each sample.

The recommendation was followed and now we have drawn all the histograms in the frequency diagrams in all these figures.

4) Furthermore, it is important to inform which age ($^{206}\text{Pb}/^{238}\text{U}$ or $^{207}\text{Pb}/^{206}\text{Pb}$) was used in the preparation of the diagram. A question arises - to build the plot was used only the value presented in the column "best age" of Table 2?

For zircons older than Early Paleozoic we use $^{207}\text{Pb}/^{206}\text{Pb}$ ages and for Late Paleozoic zircons we use $^{206}\text{Pb}/^{238}\text{U}$ ages. We build the plot diagrams with the value presented in the column "best age" of Table 2.

5) As consequences of this, two cases stand out: 1) the sample SLV VE 07 has only 4 points and the curve corresponding to this sample in Figure 12 does not allow the reader to recognize the discrepancy in data quality of this sample compared with the other samples presented in this figure, 2) the plot of Piedra Azul Formation (sample VE 17) in Figure 13 was also made with only 3 points. We suggest suppressing the curve of sample VE 07 of Figure 12 and the plot of the sample VE-17 of Figure 13.

The plot of the sample SLV-VE-07 was deleted of Figure 12 as the reviewer recommended but we did not suppress the plot of the sample SLV-17 of Figure 13

because is the only sample of this formation. We put the number of dated grains into the plot diagram and preserve the sample.

6) The reviewer was unable to locate the plot of the sandstone of Tunas Fm. (sample SLV-VE-24) whose data are in Table 2 (guess it is the Gonzalez Chaves sample). If I'm right, please write SLV-VE-24 in the figure 15.

The reviewer is right. We wrote SLV-VE 24 in the legend of figure 15 to indicate that it is the González Chaves sandstone as indicated in the Figure 2.

7) On the other hand the data of the formations Sierra Grande and El Jaguelito (Figure 14) are not listed in table 2. Also absent from table 2 are the data of Punta Mogotes Fm. If these data have been presented in other articles, make that very clear in the text and in the figure. If they are new results, the analytical data need to be included in Table 2 otherwise the plots must be deleted.

These data are from previous works such as Pankhurst et al., 2006; Uriz et al., 2011; Rapela et al., 2007, 2011; Naipauer et al., 2010, 2011. Therefore we indicated the source not only in the text, but into the plot diagrams to facilitate the comprehension (see Figures 11, 14, and 18).

7) In the comparison of Curamalal and Ventana groups performed in section 5.4 the authors indicate the large difference observed in the detrital zircon pattern of these units. However, when compared in detail, the Mascota and Bravard Fms. are quite similar, with both showing the same peaks of Cambrian age (predominant), and Paleoproterozoic-Grenviliano.

We do not entirely agree with the reviewer. Although Bravard Formation has a frequency that is transitional to the top of the Curamalal Group, the detail examination indicates conspicuous differences. Those differences are even higher when the top of both groups are compared.

8) In Chapter 5.6 the authors consider the rhyolites of the Somún Cura Massif as the only source area for the volcanic ash levels interlayered in the Tunas Fm. It is plausible to consider that Massif has been important source area of these rocks, but another possible source is the Choiyoi Group (NW Argentina) since it represents a Permian explosive volcanism with large volume of pyroclastic rocks, which was responsible for numerous ash-falls levels intercalated in the Upper Paleozoic units of Paraná Basin.

This is the classic interpretation to explain the pyroclastic levels in the Paraná Basin in southern Brazil. Based on the U-Pb dates of Rocha Campos et al. (2011) with ages around 281.4 ± 2.5 Ma Los Reyunos Fm, and the northeast paleocurrent directions measured in the aeolian sandstones of the Reyunos Fm by Pazos (2011), it looks quite probable that Choiyoi is the source of the tuffs in the Paraná Basin. However, if we want to use the same Choiyoi source to the pyroclastic deposits of Las Tunas the dominant winds should be southeast (different from what it was measured in the Choiyoi intercalated aeolian sandstones). The distance is much shorter from Somún

Cura, ages are similar to the one measured, and the required paleowind direction is also northeast). Therefore we prefer as a potential source the Early Permian calderas and volcanic rocks of the same age found in the Somún Cura Massif. This interpretation also explains the source of the igneous Carboniferous detrital zircons found in Las Tunas Formation.

Nevertheless, we modified the text to briefly explain the potential source for the Permian zircons.

Added:

Rocha Campos, A.C., Basei, M.A., Nutman, A.P., Kleiman, L.E., Varela, R., Llambias, E., Canile, F.M., da Rosa, O. de C.R., 2011. 30 million years of Permian volcanism recorded in the Choiyoi igneous province (W Argentina) and their source for younger ash fall deposits in the Paraná Basin: SHRIMP U–Pb zircon geochronology evidence. Gondwana Research 19, 509-523.

Pazos, P.J., Rey, F., Marsicano C., Ottone G., de la Fuente M. 2011. Permian unroofing, palaeoenvironmental and palaeoclimate evolution in the San Rafael foreland basin, Mendoza, Argentina. In: da Silva, R., Schmitt, R.Trow, R.A, de Souza Carvalho I., and Collins A.,(eds.), Gonwana 14, Reuniting Gondwana: East meets West, Abstracts , p. 149. Buzios.

9) The Chapter 7 is very well grounded in the data available, having been built in order to lead the reader, even those unfamiliar with the local geology, follow the paleogeographic evolution proposed by the authors. In this context, in the opinion of the reviewer, the interpretation of the meaning of the angular unconformity between the Balcarce Fm. and lower units as a result of the Pampia Block collision against the Rio de la Plata Craton deserves a more detailed explanation. What is the regional expression of this unconformity? Is there other evidence to support this interpretation?

The reviewer is right. The unconformity could be either Pampean (early Cambrian) or Famatinian (middle Ordovician). The sedimentary record of Balcarce Fm indicate a post Hirnantian glaciation age. The Pampean unconformity is seen in different places and dated in 530 Ma by Escayola et al. (2007) and Ianizzotto et al. (2013), but as the main source is coming from eastern Sierras Pampeanas which is closer to Tandilia is more probable that deformation is related to the Pampean orogen (see for further details Pazos and Rapalini,2011).

10) In Figure 20, the orogenic front of the Permian belt truncates the Pampean belt but appears to be truncated by Pampia Block. This termination deserves a refinement in the design presented.

The reviewer is absolutely right! With Dr Pangaro (coauthor of that figure) we have discussed the western extreme of this orogenic front, and we learnt that we may have another syntaxis. But unfortunately the excellent geophysical data base we have used to build the map ends at this boundary and we do not have enough information to define the trace of the syntaxis.

11) The structural profile that summarizes the Gondwanides northern portion of Patagonia (Figure 5) is very interesting and is based on a large number of information obtained by several previous works. However, the discussion of this figure is contained in a few lines discussing the relationship between Patagonia and Gondwana tectonics. This discussion is far from the importance of this figure. In addition, to facilitate the reader, it is necessary to clarify some of the details contained in it, such as:

The reviewer is right and the following paragraph has been added to the text:

Based on the new offshore seismic data presented by Pángaro and Ramos (2012) a series of interesting observations can be summarized (Fig. 5). One of the main objections that have been put forwards to interpret the Ventania System as a collisional orogen was the lack of some lower to middle crustal metamorphic rocks related to the main Permian deformation (Trow and De Witt, 2008). However, the seismic line shows the inner part of the orogen where lower to middle crust is overriding the Paleozoic sedimentary sequences. The correlation with Cerro Los Viejos exposures supports the age of these units, as well as the magmatic arc developed in the Somún Cura Massif as result of the closure of the Colorado Ocean (Ramos, 2008, Rapalini, 2005). The low-grade dynamic metamorphism exposed in the southern part of Sierra de la Ventana is just a second order upper crust middle-to-high pressure deformation, which is related to the intense folding of the Paleozoic quartzites (Von Gosen et al., 1991; Ramos, 2008). The structural triangle zone with opposite vergence is known since the early work of Keidel (1916), and is supported by the detail structural study of Tomezzoli and Cristallini (2004). The seismic lines through the Claromecó foreland basin depict and confirm these structures (Ramos and Kostadinoff, 2005). Regarding the Tandilia System, the pioneer work of Teruggi et al. (1988) interpreted the granitoids of Tandilia as a Paleoproterozoic magmatic arc, which collided with the island arc terrane of Cortijo (Cingolani, 2011). Recently, the geophysical work of Chernicoff (2012b) has identified the precise location of the suture between the Tandilia and Cortijo blocks, as well as other complexities in the basement. The structural cross-section depicts the deformation at the end of the Late Paleozoic. The opening of the South Atlantic Ocean during Late Jurassic – Early Cretaceous had an aborted branch that developed an aulacogenic basin between the Somún Cura Massif and the Ventania System, which is the present Colorado Basin (Ramos, 1996).

11.1) The expression in the area of Somún Cura Massif is compatible with a magmatic arc resulting from the closure of Ocean Colorado?

The reviewer is right. The Somún Cura is the magmatic arc developed by subduction of the Colorado Ocean and the following phrase and the corresponding cites were added to the revised text:

The correlation with Cerro Los Viejos exposures supports the age of these units, as well as the magmatic arc developed in the Somún Cura Massif as result of the closure of the Colorado Ocean (Rapalini, 2005, Ramos, 2008).

11.2) The reason as the Claromeco foreland basin is represented as an allochthonous fragment with transport contrary to the thrusts of Ventania System?

The sedimentary rocks of the Claromecó Basin developed a structural triangle zone. The following text was added:

The structural triangle zone with opposite vergence is known since the early work of Keidel (1916), and is supported by the detail structural study of Tomezzoli and Cristallini (2004). The seismic lines through the Claromecó foreland basin depict and confirm these structures (Ramos and Kostadinoff, 2005).

11.3) What is the difference between the basements of Tandilla and Cortijo? 4) The Suture between Tandilla and Cortijo is Paleoproterozoic?

The Tandilia is a continental block that collided with the Cortijo Island arc in the Paleoproterozoic. The following text and the corresponding new cite was added:

Regarding the Tandilia System, the pioneer work of Teruggi et al. (1988) interpreted the granitoids of Tandilia as a Paleoproterozoic magmatic arc, which collided with the island arc terrane of Cortijo (Cingolani, 2011). Recently, the geophysical work of Chernicoff (2012b) has identified the precise location of the suture between the Tandilia and Cortijo blocks, as well as other complexities in the basement.

12) In summary, it is an article with a large number of new data and presenting a tectonic interpretation quite suitable for most of the available information. The specific comments are indicated in the revised text, the figures and tables attached.

We have modified the tables following the comments of the reviewer and the specific comments in the text. We are sorry that we cannot acknowledge the excellent review of this anonymous reviewer.

**Reviewer #2:
Eric Tohver
University of Western Australia**

I have completed my review of the manuscript "A provenance study of the Paleozoic Ventania system (Argentina): transient complex sources from western and eastern Gondwana" by V. Ramos et al., submitted for publication in Gondwana Research. The manuscript is well-written, and reports a large body of data that will prove of great interest to the GR reader. Most of the assertions made by the authors are borne out by data, and I will concentrate the majority of my more critical comments to those more tangential conclusions of the authors. These comments can be accommodated by minor revisions.

1) There are two major issues that the authors are trying to address; first, the provenance of the different Paleozoic supergroups of the Ventania region, and second, less credibly, the East Antarctica origin of the Patagonian massif.

We agree with this statement. The second, less credibly East Antarctica origin of Patagonia is developed in a parallel paper specifically devoted to this subject that is in press. Therefore we added this text and cited that paper for those seeking more data in the origin of Patagonia.

This match indicates that Patagonia should have originated in Eastern Gondwana, and that it was transferred to Western Gondwana during the Gondwanan orogeny (for further details see Ramos and Naipauer, 2013).

Ramos, V.A. and Naipauer, M. 2013. Patagonia: Where does it come from? Iberian Geology (in press).

2) A third theme pertains to the non-rotation of the Falklands/Malvinas block. The first issue, the detrital provenance of the Ventania stratigraphy, is expertly treated. There are some minor questions about some awkwardly inconsistent ages for the tuffs in the Tunas Formation between the LA-ICP-MS ages and the previously determined SHRIMP ages.

See answers to previous reviewer.

3) The second issue regarding the putative allochthonous origin of Patagonia is really immaterial to the article (especially lines 684-690). None of the data presented, with the exception of the occurrence of Archeocyathids in clasts of the Sauce Grande Fm., really say much about the original whereabouts of Patagonia in Paleozoic times. I confess to some self-aggrandizing interest here in drawing Dr. Ramos' attention to a recent paper by Augusto Rapalini in press at Terra Nova that suggests Patagonia was always part of South America (Augusto Rapalini, Monica Lopez de Luchi, Eric Tohver, Peter Cawood, 2013. The South American ancestry of the North Patagonian Massif: geochronological evidence for an autochthonous origin? Terra Nova, Feb. 8, 2013. doi: 10.1111/ter.12043).

This paragraph was added:

Although some recent paper proposed a continuation of the magmatic activity for the early Paleozoic from the Sierras Pampeanas to the Somún Cura area (Rapalini et al., 2013), classic proposal advanced by Bracaccini (1960), is not able to elucidate the presence of archeocyathids (see discussion in Ramos and Naipauer, 2013). Rapalini et al. (2013) follows the arguments of Dalziel et al. (2013) who propose a continuous archeocyathid reef along the margin of Antarctica. However, this argument needs a magmatic arc located in the Somún Cura arc more than thousand kilometers away from the Pacific margin (see discussion in Ramos, 2008).

4) With regards to the position of the Falklands/Malvinas block (Lines 428-434 and elsewhere), I think that this issue is so far removed from the subject matter of the text that it does not bear mention. I regard this is as an important, highly interesting subject matter, but it distracts the reader from the topic at hand, that is, the data from stratigraphic units in the Ventania region. This should be removed entirely.

All the statement of Lines 428-434 has been modified and the mention to the rotation of the Malvinas Island has been deleted.

5) Line 13 - replace "show" with "provide"

Done.

6) Lines 14-16 - See 2nd point from above discussion.

The two alternatives have been discussed in the text.

7) Lines 18-23 - The record of reversals in paleocurrent should be mentioned more prominently here.

Done.

8) Line 27 - The two datasets reveal different sources for the two regions.

Done.

9) Line 31 - Replace "confirm" with "support"

Done.

10) Lines 35-37 - Again, see 2nd point from above.

The two alternatives have been discussed in the text.

11) Line 60 - Replace "has consensus" with "agree"

Done.

12) Line 114 - "4500 m thick, with the two lowermost sequence measuring 2400 m thick"

Done.

13) Line 126 - "monomict" and "situated at"

Done.

14) Line 131 - "crossbeds up to 4 m in amplitude are common..."

Done.

15) Line 137 - Replace "bipolar crossbedding" with "herringbone crossbeds"

Done.

16) Line 138 - Remove "which", insert "and" after "Ventana Group"

Done.

17) Line 149 - Replace "irregularly" with "unconformably"

Done.

18) Lines 161 - Paleomagnetism, not paleomag. The explanation of the 180 degree rotation misleads the reader into supposing that there is some mismatch between the SE

position of the Falklands and the paleomagnetic data. A clearer explanation would be helpful.

The paragraph has been simplified.

19) Line 166 and elsewhere - Replace "overlaid" with "overlain"

Done.

19') Materials and Methods section and throughout text - Isotope masses are in superscript.

Done.

20) Line 312 - 317 - The precision of the LA-ICP-MS data does not really preclude the intrusive relation for the Cerro Colorado Granite reported by Tohver et al. (2012). As written, there is no mention given of this interpretation (One that I am not particularly confident about, I must say, not having seen the contact myself) and its implications for a possible pre-Mascota Fm. Quartzite unit.

Text has been modified.

21) Lines 430-434 - Remove, separate subject.

Paragraph has been modified and rotation eliminated.

22) Line 453-454 - Awkward phrasing.

Done.

23) Line 464 - Awkward phrasing. What are "lepidofites"

Done.

24) Line 472 - There is some controversy over the APWP for South America, so some of R. Tomezzoli's age assignments could be incorrect. See M. Domeier, R. Van der Voo, E. Tohver, R.N. Tomezzoli, H. Vizán, T.H. Torsvik, Jordan Kirshner., 2011, New Late Permian Constraints on the Apparent Polar Wander Path and Paleo-Marginal Deformation of Gondwana, *Geochem. Geophys. Geosyst.*, 12, Q07002.

Done and new cite included.

25) Lines 485 - 492 - The imprecision of the LA-ICP-MS data is highlighted here, since the difference between 304 Ma (laser) and 282 Ma (SHRIMP) is outside of the probable analytical error. The "mixed" age explanation provided does not seem correct, since the laser analyses were probably individual grains. Since these are magmatic, the likelihood of metamorphic rims is low. Something is wrong with the explanation, the data, or both.

The reviewer is right, since only the juvenile Laser ablation ages are closed to the SHRIMP ages.

26) Line 508 - 510 - See recent papers by Rocha-Campos (Gondwana Research, 2011) and Domeier et al. 2011 (above) and M. Domeier, R. Van der Voo, R.N. Tomezzoli, E. Tohver, B.W.H. Hendriks, T. Torsvik, H. Vizan, A. Dominguez, 2011, Support for an "A-type" Pangea reconstruction from high-fidelity paleomagnetic records. Journal of Geophysical Research, 116, B12, art. no. B12114.

Paragraph has been modified as requested by reviewer 1 and the Rocha Campos et al 2011 paper cited.

27) Line 595 - Here, and elsewhere in the text, replace "inexistent" with "non-existent".
Done.

28) Line 629 - What is "immature" relief? High? "High relief of the Somún Cura Massif in Permian times..."

Juvenile poorly dissected relief in geomorphic grounds, which produce immature sandstones.

28) Lines 684-690 - Remove?

The text was modified and for further details the paper of Ramos and Naipauer (2013) was recommended. That paper analyzes and discusses the origin of Patagonia in the Transantarctic Mountains.

Both reviewers are strongly acknowledged, and we are sorry that first reviewer was anonymous because his excellent revision should be recognized.

1 **A provenance study of the Paleozoic Ventania System (Argentina): transient complex**
2 **sources from Western and Eastern Gondwana**

3
4
5 4 Victor A. Ramos^a, Farid Chemale^b, Maximiliano Naipauer^a and Pablo J. Pazos^a
6
7 5

8
9 6 ^a Instituto de Estudios Andinos Don Pablo Groeber, Universidad de Buenos Aires and
10 7 CONICET.

11
12 8 ^b Instituto de Geociências, Universidade de Brasília, Brasília-DF, 70904-970, Brazil
13
14 9

15
16 10 **ABSTRACT**

17
18 11 The U-Pb and Lu-Hf isotopic analyses of the different sedimentary sequences of the Ventania
19 12 System, an old Paleozoic orogenic belt exposed in the southern region of the Río de la Plata
20 13 Craton in the province of Buenos Aires, Argentina, provide new evidence for the
21 14 understanding of the tectonic evolution of the western sector of the Gondwanides mountain
22 15 belt. These ranges formed as result of the late Paleozoic collision of the Patagonia terrane
23 16 against the continental margin of Gondwana. The provenance analysis together with the
24 17 sedimentary paleocurrents confirm a dominant source from the Tandilia System, a
25 18 Paleoproterozoic mountain belt formed during the amalgamation of the Río de la Plata Craton
26 19 at about 1,800-2,200 Ma, and incorporated to Western Gondwana during the Brasiliano
27 20 Orogeny at 550-530 Ma. The local dominant source at the base of the early Paleozoic changed
28 21 to more distant supplies toward the top of the sequences, when is recorded an increasing
29 22 participation of detritus from first, Cambrian (560-520 Ma) zircons from the Pampean
30 23 Orogen, and later on Ordovician (480-460 Ma) zircons from the Famatinian Orogen. The
31 24 detrital zircon patterns and the maximum age of the units shed light on some previous
32 25 discrepancies in the early Paleozoic stratigraphy. The Balcarce Formation, an early Paleozoic
33 26 sedimentary cover of the Tandilia metamorphic and igneous basement, shows striking
34 27 differences when compared with the new data from the Ventania System. The two data-sets
35 28 reveal different sources for the two regions. The late Paleozoic foreland basin deposits mark
36 29 an abrupt change of 180° in the paleocurrent directions, in the petrographic composition of the
37 30 sediments, and in the provenance of detrital zircons. These data indicate a southern
38 31 provenance with the first evidence of Carboniferous and Permian magmatic zircons. The
39 32 oldest Archean zircons together with the finding of clasts with archeocyathids support the
40 33 provenance from Patagonia, which was derived from Eastern Gondwana. The U-Pb ages of
41 34 the ash-fall tuffs in the Tunas Formation confirm the Early Permian age of the *Eurydesma*

35 Fauna in the Ventania System. The U-Pb data together with the Lu-Hf isotopic data enhance
36 the comprehension of the tectonic evolution of the Ventania System as part of the larger
37 Gondwanides Belt that amalgamated to Western Gondwana during Late Permian times with
38 some independent pieces derived from Eastern Gondwana.

39
40 **Keywords:** Gondwanides, *Eurydesma* Fauna, Patagonia, collision, Famatinian and Pampean
41 belts, zircon geochronology, tectonics.

42 43 **1. Introduction**

44 The Ventania System is a complex fold and thrust belt developed in the southwestern
45 margin of Gondwana during late Paleozoic times (Keidel, 1916; Harrington, 1942,1947;
46 Suero, 1972; Killmurray, 1975; Ramos 1986; Von Gosen et al., 1990). Since the early work of
47 Du Toit (1927) it is assumed that Ventania was part of a larger system, which encompasses
48 the Cape Fold Belt of South Africa. Du Toit (1937) named this orogen as the Gondwanides
49 following pioneer work of Keidel (1921), and confirmed later by several works (see Veevers
50 2003, 2004; Milani and De Witt, 2008). In recent years many studies have analyzed the
51 evolution of the Ventania System (Fig. 1) and the adjacent Claromecó foreland basin (Varela
52 et al., 1987; Tomezzoli and Vilas, 1999; Tomezzoli and Cristallini, 1998; Dimieri et al., 2005;
53 Cingolani 2005; Ramos and Kostadinoff, 2005). Current studies were able to track the extent
54 of the Ventania Fold Belt in the offshore based on new seismic and geophysical data,
55 depicting the Colorado Syntaxis (Pángaro and Ramos, 2012). This feature is the mirror image
56 of the Cape Syntaxis and has similar characteristics (De Beer, 1995; Johnston, 2000).

57
58
59
60
61
62
63
64
65
66
67
68
69
70
71
72
73
74
75
76
77
78
79
80
81
82
83
84
85
86
87
88
89
90
91
92
93
94
95
96
97
98
99
100
101
102
103
104
105
106
107
108
109
110
111
112
113
114
115
116
117
118
119
120
121
122
123
124
125
126
127
128
129
130
131
132
133
134
135
136
137
138
139
140
141
142
143
144
145
146
147
148
149
150
151
152
153
154
155
156
157
158
159
160
161
162
163
164
165
166
167
168
169
170
171
172
173
174
175
176
177
178
179
180
181
182
183
184
185
186
187
188
189
190
191
192
193
194
195
196
197
198
199
200
201
202
203
204
205
206
207
208
209
210
211
212
213
214
215
216
217
218
219
220
221
222
223
224
225
226
227
228
229
230
231
232
233
234
235
236
237
238
239
240
241
242
243
244
245
246
247
248
249
250
251
252
253
254
255
256
257
258
259
260
261
262
263
264
265
266
267
268
269
270
271
272
273
274
275
276
277
278
279
280
281
282
283
284
285
286
287
288
289
290
291
292
293
294
295
296
297
298
299
300
301
302
303
304
305
306
307
308
309
310
311
312
313
314
315
316
317
318
319
320
321
322
323
324
325
326
327
328
329
330
331
332
333
334
335
336
337
338
339
340
341
342
343
344
345
346
347
348
349
350
351
352
353
354
355
356
357
358
359
360
361
362
363
364
365
366
367
368
369
370
371
372
373
374
375
376
377
378
379
380
381
382
383
384
385
386
387
388
389
390
391
392
393
394
395
396
397
398
399
400
401
402
403
404
405
406
407
408
409
410
411
412
413
414
415
416
417
418
419
420
421
422
423
424
425
426
427
428
429
430
431
432
433
434
435
436
437
438
439
440
441
442
443
444
445
446
447
448
449
450
451
452
453
454
455
456
457
458
459
460
461
462
463
464
465
466
467
468
469
470
471
472
473
474
475
476
477
478
479
480
481
482
483
484
485
486
487
488
489
490
491
492
493
494
495
496
497
498
499
500
501
502
503
504
505
506
507
508
509
510
511
512
513
514
515
516
517
518
519
520
521
522
523
524
525
526
527
528
529
530
531
532
533
534
535
536
537
538
539
540
541
542
543
544
545
546
547
548
549
550
551
552
553
554
555
556
557
558
559
560
561
562
563
564
565
566
567
568
569
570
571
572
573
574
575
576
577
578
579
580
581
582
583
584
585
586
587
588
589
590
591
592
593
594
595
596
597
598
599
600
601
602
603
604
605
606
607
608
609
610
611
612
613
614
615
616
617
618
619
620
621
622
623
624
625
626
627
628
629
630
631
632
633
634
635
636
637
638
639
640
641
642
643
644
645
646
647
648
649
650
651
652
653
654
655
656
657
658
659
660
661
662
663
664
665
666
667
668
669
670
671
672
673
674
675
676
677
678
679
680
681
682
683
684
685
686
687
688
689
690
691
692
693
694
695
696
697
698
699
700
701
702
703
704
705
706
707
708
709
710
711
712
713
714
715
716
717
718
719
720
721
722
723
724
725
726
727
728
729
730
731
732
733
734
735
736
737
738
739
740
741
742
743
744
745
746
747
748
749
750
751
752
753
754
755
756
757
758
759
760
761
762
763
764
765
766
767
768
769
770
771
772
773
774
775
776
777
778
779
780
781
782
783
784
785
786
787
788
789
790
791
792
793
794
795
796
797
798
799
800
801
802
803
804
805
806
807
808
809
810
811
812
813
814
815
816
817
818
819
820
821
822
823
824
825
826
827
828
829
830
831
832
833
834
835
836
837
838
839
840
841
842
843
844
845
846
847
848
849
850
851
852
853
854
855
856
857
858
859
860
861
862
863
864
865
866
867
868
869
870
871
872
873
874
875
876
877
878
879
880
881
882
883
884
885
886
887
888
889
890
891
892
893
894
895
896
897
898
899
900
901
902
903
904
905
906
907
908
909
910
911
912
913
914
915
916
917
918
919
920
921
922
923
924
925
926
927
928
929
930
931
932
933
934
935
936
937
938
939
940
941
942
943
944
945
946
947
948
949
950
951
952
953
954
955
956
957
958
959
960
961
962
963
964
965
966
967
968
969
970
971
972
973
974
975
976
977
978
979
980
981
982
983
984
985
986
987
988
989
990
991
992
993
994
995
996
997
998
999
1000

FIGURE 1 NEAR HERE

There are two main problems in the tectonic interpretation of Ventania. The first problem is the stratigraphy of the early Paleozoic units as for some authors the Curamalal and Ventana Groups are the same unit tectonically repeated (Killmurray, 1975; Tomezzoli and Cristallini, 2004), although most of the stratigraphers agree about the original sequences proposed by Harrington (1947) where Ventana is younger than Curamalal. The second problem, and perhaps the most important, is if the Ventania fold and thrust belt was originated by collision with an allochthonous Patagonia terrane in the late Paleozoic (Ramos, 1984, 2008; Kay et al., 1989; Sellés Martínez, 1989; Von Gosen, 2003; Chernicoff and Zappettini, 2004; among others), or was an intracratonic basin inverted by contraction and strike-slip tectonics related to oblique subduction further to the south along the present continental margin (Cobbold et al., 1991; López Gamundí et al., 1994, 1995; Rossello et al., 1997;

69 Dalziel et al., 2000; Gregori et al., 2008, among others). Some authors refute the allochthony
70 of Patagonia based on paleogeographic and paleoclimatic reconstructions (López Gamundí
71 and Rossello, 1998). The provenance analyses here presented shed light to both problems and
72 provide a robust answer to previous uncertainties.

73

74 **1.1 Location**

75 The Ventania System is a 30 km wide mountain chain located in the southern part of
76 the province of Buenos Aires in central eastern Argentina. It is surrounded by plains locally
77 known as pampas, and has a length of 180 km with a W-NW trend (Fig. 2).

78 FIGURE 2 NEAR HERE

79 These mountains have a maximum height in the Cerro Tres Picos of 1,250 meters.
80 There are several ranges as the Sierras de Curamalal, Ventana and Pillahuincó (Fig. 2), which
81 expose the early and late Paleozoic sequences, tightly folded, with a constant northeast
82 vergence (Harrington, 1947; Suero, 1972).

83

84 **2. Stratigraphy**

85 **2.1 Metamorphic and igneous basement**

86 There are very scarce exposures of the basement in the southwestern slope of the
87 Sierra de Curamalal. Most of the authors recognized the igneous origin of these rocks, which
88 are highly deformed, with typical cataclastic and mylonitic textures (Kilmurray, 1968;
89 Gregori et al., 2005). There are also rhyolites exposed in different sectors further north (Figs.
90 2 and 3) and some isolated outcrops of granites exposed in Cerro Colorado and López Lecube
91 quarries further to the west.

92 FIGURE 3 NEAR HERE

93 The available geochronological data indicate an age of 607 ± 5.2 Ma for the deformed
94 granites of Cerro Corral (U-Pb SHRIMP ages in zircons, Rapela et al., 2003), that confirm old
95 Rb-Sr ages of ~ 603 -612 Ma of Varela and Cingolani (1976). New data of the Pan de Azúcar
96 Granite yielded an age of 581 ± 8 Ma (U-Pb SHRIMP ages in zircons, Tohver et al., 2012).
97 The posttectonic granites in Cerro Colorado (531.1 ± 4.1 Ma and 523.8 ± 4 Ma), San Mario
98 (524.3 ± 5.3 Ma), and Los Chilenos (533 ± 12 Ma), as well as the La Ermita Rhyolite ($509 \pm$
99 5.3 Ma and 505 ± 18 Ma), were assigned to the Cambrian (Rapela et al., 2003; Tohver et al.,
100 2012). The Agua Blanca Granite has an inheritance age of 2182 ± 18 Ma that indicates a
101 Paleoproterozoic basement in the area as part of the Río de la Plata Craton (Tohver et al.,
102 2012). The westernmost outcrops of López Lecube quarry yielded an age of 258.5 ± 1.9 Ma

103 by U-Pb SHRIMP in zircons that corresponds to posttectonic granites of the Gondwanide
104 Orogeny and it is not part of the Ventania basement (Rapela and Kostadinoff, 2005).

105 The igneous rocks have been divided in two suites based on their composition and
106 tectonic setting: a calcalkaline orogenic and collisional Neoproterozoic suite and a
107 postorogenic extensional Cambrian suite (Gregori et al., 2005). The last episode was
108 associated with a Cambrian rift by Rapela et al. (2003).

110 2.2 The Paleozoic sedimentary successions

111 The early Paleozoic sedimentary succession includes two sequences, the Curamalal
112 and Ventania Groups (Fig. 4) deposited during Ordovician and Devonian times (Harrington,
113 1947; Sellés Martínez, 2001). The late Paleozoic is represented by the Pillahuincó Group (Fig.
114 4), which is mainly Cisuralian (Early Permian). The whole Paleozoic succession is around
115 4,500 m thick, with the two lowermost sequences measuring 2,400 m thick. The upper part of
116 the succession documents a higher subsidence rate compared with the underlying part, but
117 also a contrasting paleocurrent pattern, which varies from SW to SE, with strong NE
118 prograding deltaic lobes in the uppermost part of the sedimentary section. The succession
119 contains mainly sandstones, claystones and conglomerates in the lower part. However, glacial
120 diamictites and glaciomarine deposits constitute a special type of coarse-grained deposits that
121 document the late Paleozoic glaciation (Andreis et al., 1989).

122 The Curamalal Group, which represents the beginning of the sedimentary record in the
123 basin, contains conglomerates with coarse-grained clasts in clast-supported to patchy sandy
124 matrix-supported types, with beds up to 1.5 m in thickness and erosive to sharp bases in the
125 lower part of La Lola Formation. Internally they contain well rounded quartzite clasts
126 showing normal or rarely reverse gradation. The outcrops of the source area remain unknown
127 but the almost monomict composition suggests a quartzite unit situated at a certain distance
128 that allowed the well roundness of clasts by hyperconcentrated flows or diluted debris flows.
129 Sandy deposits include different types of cross-bedding; some of them were interpreted as
130 hummocky cross stratification by Zavala et al. (2000). However, they exhibit a unidirectional
131 pattern and in all cases resemble more bidimensional subaqueous dunes. Giant cross-beds up
132 to 4 m in amplitude are common in medium grained sandstones containing clay chips, and
133 mud drapes. Thin beds show the same sedimentary structures and in cases depict clear
134 bidirectional paleocurrents that document tidal control during the sedimentation. In the
135 Ventana Group, the lower unit (Bravard Formation) has some fine conglomerates with a
136 quartzitic composition of the clasts. The overlying Napostá Formation is well known for its

137 ichnological content that includes *Skolithos*, *Arenicolites* and *Daedalus*. Abundant tidal
138 features have been observed, including **herringbone crossbeds** and mud drapes. The Lolén
139 Formation is the uppermost unit of the Ventana Group and exhibits more variability in clast
140 composition and contains brachiopods and lycophytid plant remains as *Haplostigma* that have
141 been used to date the top part in the Middle Devonian (Cingolani et al., 2002).

142 A paraconformity separates the Ventana from the overlying Pillahuincó Group,
143 deposited between the latest Carboniferous and the Cisuralian (Early Permian) indicating a
144 prolonged hiatus spanning the Upper Devonian to the middle Pennsylvanian. This group is
145 crucial to understand the evolution of the Ventana System because a thick succession was
146 deposited in a relatively short time. This fact documents a high subsidence rate related to a
147 foreland basin which contrasts with the stable depositional settings for the underlying groups
148 (Fig. 4).

FIGURE 4 NEAR HERE

149 The Sauce Grande Formation rests **unconformably** over the Ventana Group and is a
150 glaciomarine succession that documents the late Paleozoic glaciation in the Atlantic basins of
151 Argentina. The Sauce Grande Formation represents Late Carboniferous-earliest Permian
152 (Cisuralian) glacial deposits 400 m thick that are also recognized in the Claromecó Basin,
153 which correlates with the Dwyka Formation in the Karoo Basin. This correlation of glacial
154 deposits is known since the pioneer studies of Keidel (1916) and Du Toit (1927). The
155 Malvinas /Falkland Islands also record equivalent glacial deposits in the Lafonia Formation
156 (Frakes and Crowell, 1969; Bellosi and Jalfín, 1984, 1989). The pre-breakup position of the
157 Malvinas (Falkland) Islands based on the early reconstruction of Martin et al. (1981) is south
158 of the Karoo Basin and off the coast of South Africa. Recent studies of the Sauce Grande
159 tillites have found reworked limestone clasts with archeocyathids that indicate a Patagonian
160 derivation from an Antarctic source (González et al., 2011, 2013). Some paleomagnetic
161 studies support a position further to the east, but need a 180° rotation to match the data
162 (Mitchell et al., 1986). Based **on these data**, López Gamundí and Rossello (1998) conclude
163 that the paleoice flow directions of the Dwyka and the Lafonia glacial sequences were similar,
164 but different from the south-north direction of the Sauce Grande tillites.

165 The Piedra Azul Formation represents early postglacial transgressive deposits, which
166 are overlain by the marine Bonete Formation. These deposits represent the maximum flooding
167 of the basin in the Early Permian and bear the typical Gondwana fauna of *Eurydesma*
168 (Harrington, 1955). This thick-shelled bivalve *Eurydesma* was a cold-resistant and immobile,
169 epifaunal suspension feeder that dominated marine environment of Gondwana in the Early
170

171 Permian (Jones et al., 2006). Above these levels, intertidal plains deposits bear an abundant
172 *Glossopteris* flora, a widespread typical Gondwana flora also known in the Early Permian of
173 Africa, India, Antarctica and Australia (Benedetto, 2010). The upper unit of the group is the
174 Tunas Formation, represented by prodeltaic to subaerial delta plain deposits with
175 paleocurrents that indicate a source area situated to the south-southwest. Very well preserved
176 ichnofossils as *Cochlichnus* and *Gordia* have been observed in the Las Mostazas quarry and
177 cross-bedding exposures that confirm the paleocurrent pattern suggested by Andreis and
178 Cladera (1992) for the unit.

179 Recent studies on the microflora of several wells of the offshore Claromecó Basin
180 have identified on palynological bases almost the entire Permian sequence, including for the
181 first time Lopingian assemblages (Balarino, 2012).

182

183 3. Structure

184 The structure of the Ventania fold and thrust belt was a matter of discussion since the
185 early work of Harrington (1947). Based on the extraordinary ductile folding of the early
186 Paleozoic quartzites described by Keidel (1916) and Du Toit (1927), most of the authors
187 interpreted the structure as a dominant fold-type (Harrington, 1970). Detailed surveys done by
188 Varela et al. (1987), Von Gosen et al. (1990, 1991) and Tomezzoli and Cristallini (1998)
189 recognized the main thrusts and confirmed the old thrust hypothesis of Schiller (1930).
190 Seismic studies performed in the offshore depict those thrusts and their relationship with
191 lower to middle crustal deformed rocks exposed further south in the Somún Curá Massif in
192 the hinterland region (Pángaro and Ramos, 2012). These authors have shown that the
193 Ventania foreland fold and thrust belt is separated from the hinterland by an area of minimum
194 deformation interpreted as a late Paleozoic piggy-back basin. This basin is now beneath the
195 Colorado Basin, a Jurassic to Early Cretaceous aulacogenic basin developed above the suture
196 between Patagonia and Western Gondwana. This suture previously proposed by different
197 authors in land, has been depicted in the offshore by a magnetic anomaly interpreted as
198 evidence of mafic and ultramafic rocks by Max et al. (1999) and Ghidella et al. (1995).

FIGURE 5 NEAR HERE

200 The age of deformation of the Ventania fold and thrust belt is constrained in the Early
201 Permian based on the growth strata of Tunas Formation described by López Gamundí et al.
202 (1995), the paleomagnetic evidence of syndeformational magnetization of Tomezzoli and
203 Vilas (1999), and the illite recrystallization age of Buggish (1987).

204

205 4. Material and methods

206 A systematic field reconnaissance was made of the different Paleozoic units and the
207 metamorphic basement, analyzing their main sedimentological and structural characteristics.
208 A large volume of 24 samples from Curamalal, Ventana and Pillahuincó Groups with detailed
209 sampling in the uppermost tuff layers were collected. The location of the samples is indicated
210 in Figs. 2 and 4 and the sample list and the U-Pb and Lu-Hf analytical data are presented in
211 the electronic supplementary material. Petrographic and geochemistry information of
212 sedimentary and tuff samples can be found in Alessandretti et al. (2013).

213 Samples were crushed and milled using jaw crusher. Then, the zircons were separated
214 by conventional procedures using heavy liquids and an isodynamic magnetic separator after
215 concentration by hand panning. The most clear and inclusion-free zircons from the least
216 magnetic fractions were handpicked. All zircons were mounted in epoxy in 2.5-cm-diameter
217 circular grain mounts and polished until the zircons were just revealed. Images of zircons
218 were obtained using the optical microscope (Leica MZ 125) and back-scatter electron
219 microscope (Jeol JSM 5800) at the Eletron Microscope Center of the Federal University of
220 R rio Grande do Sul, but are only illustrated when necessary to support the interpretation.
221 Zircon grains were dated with laser ablation microprobe (New Wave UP213) coupled to a
222 MC-ICP-MS (Neptune) at the Geochronology Laboratory of the University of Brasilia.

223 U-Pb isotope data were acquired using static mode with spot size of 30 um in
224 diameter. Laser-induced elemental fractional and instrumental mass discrimination were
225 corrected by the reference zircon (GJ-1) (Jackson et al., 2004), following the measurement of
226 two GJ-1 analyses to every four sample zircon spots. The collector configuration used for
227 simultaneous measurements of Th, U, Pb and Hg isotopes was ^{238}U , ^{232}Th and ^{208}Pb in
228 faraday cups (H4, H2 and L4, respectively) and ^{207}Pb , ^{206}Pb , $^{204}\text{Pb}+\text{Hg}$ and ^{202}Hg in Multiplier
229 Ion Counting (MIC) channels attached to the L4 (MICs IC5, IC4, IC3 and IC2, respectively).
230 The external error is calculated after propagation error of the GJ-1 mean and the individual
231 sample zircon (or spot). A detailed description of analytical conditions and data reduction can
232 be found in Chemale et al. (2012). Isoplot 3 software (Ludwig, 2003) was used to generate the
233 concordia diagrams and histograms. For the concordia age calculations and frequency
234 histograms, only the analyses with $100 \pm 10\%$ of concordance were used. All of the calculated
235 ages are reported at the 95% confidence level.

236 Lu, Yb and Hf isotopes in single zircon crystals were acquired using static mode with
237 spot size of 50 um in diameter. The laser spot was driven to the same site or zircon phase
238 dated by the U-Pb method. To minimize aerosol deposition around the ablation pit and to

239 improve transport efficiency, He was flushed along with Ar into the ablation cell. The
240 Faraday collectors were arranged the following way: ^{171}Yb (low 4), ^{173}Yb (low 3), ^{174}Hf (low
241 2), ^{175}Lu (low 1), $^{176}(\text{Hf}+\text{Yb}+\text{Lu})$ (Center), ^{177}Hf (high 1), ^{178}Hf (high 2) and ^{179}Hf (high 3).
242 Detail of operation analytical conditions can be found in Chemale et al. (2011a). To correct
243 for isobaric interferences of Lu and Yb isotopes on mass 176, the isotopes ^{171}Yb , ^{173}Yb and
244 ^{175}Lu were simultaneously monitored during the analyses. The ^{176}Lu and ^{176}Yb concentrations
245 were calculated using a $^{176}\text{Lu}/^{175}\text{Lu}$ ratio of 0.026549 and a $^{173}\text{Yb}/^{171}\text{Yb}$ ratio of 1.123456
246 (Chu et al., 2002; Thirwall and Walder, 1995). Correction of Hf isotopic ratios for
247 instrumental mass bias was based on an exponential law and used the reference $^{179}\text{Hf}/^{177}\text{Hf}$
248 value of 0.7325 (Patchett et al., 1981). Each analytical session included determinations of the
249 βHf and βYb factors for each individual spot. The mass bias behavior of Lu was assumed to
250 follow that of Yb.

251 Lu-Hf model ages (TDM) of zircon grains were calculated based on a depleted mantle
252 source with $^{176}\text{Hf}/^{177}\text{Hf} = 0.28325$ and $^{176}\text{Lu}/^{177}\text{Hf} = 0.0388$ (Andersen et al., 2009). We also
253 calculated model ages of individual zircons for felsic and mafic sources assuming the
254 following parental magma compositions: mafic, $\text{Lu}/\text{Hf} = 0.022$; felsic, $\text{Lu}/\text{Hf} = 0.010$
255 (Pietranik et al., 2008). The values of $\varepsilon\text{Hf}(t)$ were calculated assuming the CHUR $^{176}\text{Hf}/^{177}\text{Hf}$
256 ratio of 0.282785 (Bouvier et al., 2008) and the decay constant of $\lambda^{176}\text{Lu} = 1.867 \times 10^{-11}/\text{a}$
257 (Söderlund et al., 2004).

259 5. Results

260 5.1 Pan de Azúcar mylonitic belt

261 This belt of highly deformed metamorphic rock was identified as the Pan de Azúcar
262 Formation by Cuerda et al. (1975) in the eastern slope of the Cerro Pan de Azúcar beneath the
263 contact with the La Lola Formation. Previous authors interpreted rocks similar to sample
264 SLV-VE 02 (Fig. 6a), as derived from igneous protolith, whereas others as Von Gosen et al.
265 (1990) described paragneisses from these exposures. We interpreted this sample based on the
266 internal textures seen in the back-scattering image and the Th/U ratio in each dated zircon
267 (Fig. 6) as gneiss of igneous origin; apparently deformational and metamorphic process has
268 not affected the detrital zircons. One of the main frequency peaks (Fig. 6b) coincides with the
269 ages of the Cambrian suite proposed by Gregori et al. (2005), although the major frequency
270 peak clearly indicates a Paleoproterozoic component in this rock (Fig. 6 a-b), similar to the
271 age interpreted by Tohver et al. (2012) as a basement inheritance in the granites of Agua
272 Blanca. These ages are between the main magmatic activity (2250–2120 Ma) and the

273 collisional overprint (2100–2080 Ma) recorded in the basement of Tandilia by Cingolani
274 (2011). There are also some few older and younger zircons.

275 **FIGURE 6 NEAR HERE**

276 It is possible that the orthogneiss affected by a post-540 Ma contractional deformation
277 may correlate with the main orogeny of the Saldania Belt recognized by Chemale et al.
278 (2011b) in southernmost Africa. In a Gondwana plate tectonic context, a subduction zone has
279 been proposed at the southern margin of the Kalahari plate, close to the Precambrian-
280 Cambrian boundary, as suggested by Rozendaal et al. (1999), and its extension in the Sierra
281 de la Ventana Orogen (Chemale et al., 2011b). Following Gregori et al. (2005) deformation in
282 Sierra de la Ventana should be older than 533 Ma, which is the age of the posttectonic
283 granites. **The age pattern of this orthogneiss shows different inherited zircons.**

284 However, another possible alternative would be to consider that sample a highly
285 deformed quartzite of La Lola Formation, due to the similar pattern of zircon ages in
286 comparison with other samples of this unit (see SLV-VE 05 in Fig. 8). This interpretation
287 would indicate that the main deformation of this sample could be Gondwanian in age, instead
288 of Brasiliano.

289 **5.2 Curamalal Group**

291 The base of this group is represented by La Lola Formation, which is nicely exposed
292 in the eastern slope of Cerro Pan de Azúcar (Andreis and López Gamundí, 1989). There is a
293 30 m thick orthoconglomerate dominantly formed by clasts of quartzite (SLV-VE-03). These
294 conglomerates are covered by quartzitic sandstones (SLV-VE-05). It is interesting to remark
295 that tectonically interposed with these quartzites, east of the Abra Mayer, there are some
296 lenses of mylonitic granite. One of these lenses with calcalkaline composition has a unique
297 frequency peak at 541.0 ± 8.4 Ma within the range of basement granites (Figs. 7 a,b).

298 **FIGURE 7 NEAR HERE**

299 The sedimentary facies and provenance of these conglomerates have been studied by
300 Zavala et al. (2000), who recognized a proximal shelfal environment in a flood- dominated
301 fan delta system developed from the Tandilia area. However, the good mineralogical maturity
302 almost dominated by quartzite clasts up to 25 cm in size and good roundness suggest that the
303 source area was closer, indicating that the present day quartzite outcrops of Tandilia extended
304 well into the south. The pattern of detrital zircons of both samples (see samples SLV-03 and
305 SLV-05 in Fig. 8) confirms the proposal of Zavala et al. (2000), and shows that the main peak
306 around 2050-2170 Ma corresponds with the maximum magmatic activity of the Tandilia arc

307 according with Cingolani (2011). The lower levels of La Lola Formation have minor
1 308 Cambrian peaks at 545 and 520 Ma, which indicate exhumation of the post-tectonic rocks in
2
3 309 the surrounding area.

5 310 The sample SLV-VE-09 is from the lower part of Mascota Formation from Sierra de
6
7 311 Chasicó, which is unconformably overlying the Cerro Colorado Granite (Harrington,
8
9 312 1968). The maximum age of sedimentation is 534 Ma as indicated by the highest frequency
10
11 313 peak (Fig. 8). This quartzite has been interpreted as being older than the Los Chilenos Granite
12
13 314 (533 Ma, Thover et al, 2012), but the present data may favor that the Mascota Formation is
14
15 315 younger than the granite based on field observations that coincide with criteria used in the
16
17 316 Harrington (1947) map. The sample SLV-VE-10 was collected east of Tornquist (see Fig. 2)
18
19 317 from the Mascota Formation, and presents similar age distribution pattern as sample SLV-
20
21 318 VE-09. In these samples the Paleoproterozoic sources start decreasing and some minor
22
23 319 Mesoproterozoic peaks are visible.

24 320 The analysis of the older units of the Curamalal Group shows an interesting trend in
25
26 321 their sources (Fig. 8) with a continuous decrease in the Paleoproterozoic provenance from the
27
28 322 La Lola Formation at the base of the Curamalal Group upwards, parallels the increase of the
29
30 323 Cambrian zircons towards the top of the Mascota Formation. This increase of Cambrian peaks
31
32 324 of 545 and 534 Ma may indicate a potential derivation from Eastern Sierras Pampeanas (see
33
34 325 Fig. 1) which has been exhumed at that time. The input of Grenville-age zircons around 1200
35
36 326 Ma in the Mascota Formation is somewhat older to be derived from the Namaqua belt of
37
38 327 western Kalahari craton, but similar ages recorded in the detrital zircons of the Punta Mogotes
39
40 328 basement from a borehole core, were interpreted as derived from the western Kaapval Craton
41
42 329 by Rapela et al. (2011). Similar age zircons were also recognized in the Cerro Largo
43
44 330 Formation from Tandilia by Gaucher et al. (2008). However, the most potential Grenville-age
45
46 331 source based on the rank of ages observed could be the Eastern Sierras Pampeanas where ages
47
48 332 from 1000 to 1200 Ma are common (Escayola et al., 2007).

47 333 FIGURE 8 NEAR HERE

49 334 5.3 Ventana Group

51 335 The different units of the Ventana Group are conformably deposited on the Curamalal
52
53 336 Group. The provenance analysis based on the detrital zircons shows as the most important
54
55 337 frequency peak Brasiliano ages around (564-540 Ma) (Fig. 9). The Paleoproterozoic ages of
56
57 338 Tandilia are less significant and tend to disappear. Some minor evidence of Ordovician
58
59 339 zircons (482 Ma) is seen in the Napostá Formation, as well as in the Bravard Formation,
60
61 340 which will be dominant in the upper part of the sequence. Uriz et al. (2012) analyzed a sample

341 from the Napostá Formation and detected an important frequency peak of 473 Ma, partially
342 equivalent to the Ordovician peak found by us.

343 FIGURE 9 NEAR HERE

344 The zircons of Providencia Formation follow the same trend of the lower section of
345 the Ventana Group (compare with Fig. 10), but an important change is recorded in the Lolén
346 Formation, already recognized by Uriz et al. (2011). There, an important peak of Early
347 Ordovician zircons is seen for the first time (490 Ma), as well as increasingly old Brasiliano
348 ages (641-612 Ma). The first occurrence of an Ordovician frequency peak in the Lolén
349 Formation is very similar to the one recognized by Rapela et al. (2007) further to the
350 northeast, in somewhat equivalent nearshore quartzitic sandstones of the Balcarce Formation.
351 This unit is exposed nearby the town of Balcarce (see location in Fig.1), and is
352 unconformably deposited on the metamorphic basement of the Tandilia System and pinch out
353 over the glacial diamictites of the Volcán Formation (Pazos et al., 2008).

354 There are not precise biostratigraphic constraints for its age, but it was assumed to be
355 broadly between Ordovician and Early Silurian based on its trace fossils (Borrello, 1966).
356 According to Rapela et al. (2007) who reported detrital zircon ages as young as 475–480 Ma,
357 the Balcarce Formation is not older than Early Ordovician, suggesting a Late Ordovician to
358 Early Silurian sedimentation age. Moreover, the trace fossils described by Seilacher et al.
359 (2002) from several localities, differ significantly from the familiar Arenigian suite. Rather,
360 they resemble the Lower Silurian ichnofaunas of Libya, Chad and Benin, with trilobite
361 tunnels (*Cruziana ancora*), palmate *Arthropycus alleghaniensis* and *Gyrochorte zigzag* as
362 shared elements (Seilacher et al., 2002), but also *Diplocraterion* conforming monospecific
363 suites has been observed. These authors therefore assigned an Early Silurian age to the
364 Balcarce Formation and they mentioned that the ichnofauna possibly signals an even further
365 southward extension of the Malvinocaffric Province. It is interesting to remark that the matrix
366 of the Cerro Volcán diamictites, a four meters thick level underlying typical quartzites of the
367 Balcarce Formation, has detrital zircons 485-490 Ma old and a maximum peak of 530 Ma
368 (Zimmermann and Spalletti, 2009; Van Staden et al., 2010). These data reinforce the
369 assignation to the Silurian of this unit since these glacial deposits could be interpreted as
370 representing the Hirnantian glaciation of the end of the Ordovician.

371 FIGURE 10 NEAR HERE

372 The siliciclastic deposits of the Balcarce Formation were developed in a nearshore and
373 inner shelf environment on a tide dominated platform, affected by storm events in a marine
374 system that was open to the south based on the pattern of progradational clinofolds (Poiré et

375 al., 2003). Paleocurrents indicate a north dominant sediment supply for the western and
1 376 central areas of the Balcarce Formation, while in the eastern part of the basin the main
2
3 377 transport directions are east-west oriented (Teruggi, 1964).
4

5 378 The Lolén Formation is the only unit bearing marine invertebrate fossils in the lower
6
7 379 Paleozoic sequences of the Ventania System and the occurrence of brachiopods is known
8
9 380 since the early work of Harrington (1947). Benedetto (2010) analyzed these brachiopods and
10
11 381 assigned them to *Cryptonella*, an Early Devonian genus. Based on the age of these
12
13 382 brachiopods, Newton and Cingolani (1990) correlated the Lolén Formation with the
14
15 383 Bokkeveld Group of the Cape Fold Belt, confirming the correlation of Du Toit (1937).
16

17 384 Therefore, a partial correlation between Lolén and Balcarce Formations is proposed
18
19 385 based on the detrital zircon pattern (Fig. 11), not only the Early Ordovician sources, but also
20
21 386 the range of Brasiliano ages (640-610 Ma), which are older than previous ages recorded in
22
23 387 the early Paleozoic of Ventania. The Ordovician provenance of both units should come from
24
25 388 the northwest, derived from the Western Sierras Pampeanas Orogen, the only sector that
26
27 389 records plutonic and volcanic rocks of Famatinian age at these latitudes (Ramos et al., 2010).
28

29 390 FIGURE 11 NEAR HERE

30 391 **5.4 Comparison between the Curamalal and the Ventana Groups**

31 392 Kilmurray (1975) proposed that both groups were result of a tectonic repetition based
32
33 393 on an apparent similarity between the quartzitic sandstones. Tomezzoli and Cristallini (2004)
34
35 394 formalized Kilmurray' hypothesis in their study of the structure of Sierras de la Ventana and
36
37 395 Curamalal through a viable structural section of these ranges, which shows both groups as a
38
39 396 single sequence tectonically repeated. However, our present results indicate a striking
40
41 397 difference between the detrital zircon patterns of both groups. When the pattern of La Lola
42
43 398 Formation (Fig. 8) is compared with the lower part of the Ventana Group, in particular the
44
45 399 Bravard and Napostá Formations (Fig. 9), it is clear the absence of Paleoproterozoic
46
47 400 population in these units (Fig. 12).
48

49 401 FIGURE 12 NEAR HERE

50 402 The Curamalal Group begins with a high frequency peak of Paleoproterozoic ages
51
52 403 with a minor peak in the Brasiliano ages, showing exhumation of the Tandilia rocks at that
53
54 404 time. An irregular exposed topography extended to the south of the present ranges that
55
56 405 explains the zircon detrital pattern and facies of the conglomerates of La Lola Formation. The
57
58 406 absence of carbonate clasts contrasts with the abundance of carbonates in the Neoproterozoic
59
60 407 sedimentary cover of Tandilia. This could be explained by a combination of climate and
61
62 408 transport that favored resistant lithologies over carbonates.
63
64
65

409 The maximum frequency in the base of Ventana Group shows exhumation of the
410 Brasiliano rocks and almost no existence of Paleoproterozoic ages, contrasting with the
411 Curamalal Group pattern. These different patterns also characterize the upper part of the
412 Curamalal and Ventana Groups (see Figs. 8 and 10). The major difference is the first
413 occurrence of Ordovician zircons which is exclusive of the Ventana Group and Balcarce
414 Formation (Fig. 12). The Cerro Largo Formation in the Tandilia System has been considered
415 correlatable with the Balcarce Formation, but Pazos and Rapalini (2011) kept the unit in the
416 Precambrian as traditionally suggested in agreement with the detrital pattern of this unit.

417 These evidences permit to discard the correlation of both groups and reevaluate the
418 early proposed stratigraphy of Harrington (1947) which, at the present level of knowledge, is
419 the one that best explains the data.

421 **5.5 Pillahuincó Group**

422 The late Paleozoic deposits of this group indicate the inception of a foreland basin
423 stage in the evolution of the Ventania System (Ramos, 1984; López Gamundí and Rossello,
424 1992, among others). The unconformity that separates the Ventana and Pillahuincó Group,
425 although quite elusive in the structural evidence (López Gamundí and Rossello, 1993),
426 coincides with an important change in the petrography of the sandstones (Andreis and
427 Cladera, 1992). Compositionally, the initial passive margin phase of the continental platform
428 was characterized by quartz-rich, craton-derived detritus, but was followed by a foreland
429 phase that shows a paleocurrent reversal and dominance of arc/foldbelt-derived material
430 (López Gamundí and Rossello, 1998).

431 The recent finding of subrounded clasts with archeocyathids in the glaciomarine Sauce
432 Grande Formation in Ventania derived from Antarctica (González et al., 2013) as well as in
433 the Lafonia (Fitzroy) tillites in the Malvinas (Falkland) Islands, and in the Dwyka tillites
434 (South Africa) support the correlation of these glacial deposits (Veevers and Saeed, 2013).

435 The analysis of the detrital zircon provenance of the late Paleozoic deposits (Fig. 13)
436 shows several differences regarding the early Paleozoic sequences. The first important
437 difference is that in the Sauce Grande Formation there are Archean zircons with conspicuous
438 ages of 2729, 2990 and 3200 Ma, not seen in the lower Paleozoic sequence of Ventania. As
439 the Tandil area shows strong evidence supporting the derivation from a Neoproterozoic crust
440 (less than 2.65 Ga) as inferred by Cingolani (2011) based on the positive ϵ_{Hf} data, those
441 zircons together with the reversal of the paleocurrents indicate a different old cratonic source
442 south of the study area. The second striking difference is the frequency peaks of 319-322 Ma

443 in the Piedra Azul, Bonete, and Tunas formations that are characteristic from northern
1 444 Patagonia, as well as the Silurian 432-417 Ma peaks, similar to the age recorded in Los
2 445 Pájaros Island in northeastern Patagonia granites (Nuñez et al., 1975). The Piedra Azul
3 446 Formation represents early postglacial transgressive deposits, which are overlain by the
4 447 marine deposits of the Bonete Formation bearing the typical *Eurydesma* Gondwana fauna
5 448 (Harrington, 1955), which represent the maximum flooding of the basins in the Early
6 449 Permian. Above this fauna, some intertidal plain deposits bear an abundant *Glossopteris* flora,
7 450 a typical Gondwana flora also known in the Early Permian of Africa, India, Antarctica and
8 451 Australia (Benedetto, 2010).

16 452 FIGURE 13 NEAR HERE

18 453 The other frequency peaks (Fig. 13) are common ages in the crystalline basement of
19 454 northern Somún Cura Massif. Zircons ages of Grenvillian (1100-1000 Ma), Brasiliano (584-
20 455 532 Ma), and Ordovician (491-450) have been widely reported by Pankhurst et al. (2001,
21 456 2006); Ramos (2008), and Naipauer et al. (2010). This spectrum of frequency peaks is
22 457 duplicated by the detrital zircons of the Sierra Grande Formation (Fig. 14), a Siluro-Devonian
23 458 sedimentary cover unconformably deposited over the crystalline basement (Uriz et al., 2011).

29 459 FIGURE 14 NEAR HERE

31 460 There are some minor outcrops of sandstones near González Chaves, 113 km east of
32 461 the Coronel Pringles in the middle of the Claromecó Basin (Figs. 1 and 2) (Llambías and
33 462 Prozzi, 1975). Monteverde (1937) correlated these sandstones with the quartzites of Las
34 463 Mostazas in the southeastern part of the Sierra de Pillahuincó (Tunas Formation). Furque
35 464 (1965) described similar quartzites with rest of lepidophytes in a similar setting 50 km further
36 465 east of González Chaves. A representative sample of these outcrops near González Chaves
37 466 was dated (SLV-VE 24, Fig. 15).

44 467 FIGURE 15 NEAR HERE

45 468 The detrital zircon ages show two important frequency peaks, one in the Late
46 469 Carboniferous (316 Ma), and another in the Early Devonian (406 Ma), a pattern characteristic
47 470 of other Pillahuincó Group rocks (Fig. 13). It is important to note that the youngest
48 471 sedimentary deposits exposed in the Claromecó Basin belong to this group, although
49 472 Tomezzoli and Vilas (1997) and Tomezzoli (2009) indicated that these exposures are
50 473 consistent with an Early to Late Permian age based on paleomagnetic grounds. This has been
51 474 challenged by Domeier et al. (2011), who supported younger ages based on recent dating in
52 475 Sierra Chica.

60 476

477 5.6 The Permian ash-fall tuffs of Tunas Formation

1 478 The occurrence of pyroclastic levels in the Tunas Formation first described by Iñiguez
2
3 479 et al. (1988) is one of the best time-lines to constrain the age of the late Paleozoic sequences.
4
5 480 The age of this unit was based on the *Eurydesma* Fauna and the *Glossopteris* Flora in the
6
7 481 deposits underlying the Tunas Formation, both of Early Permian age (Harrington 1947, 1955;
8
9 482 Benedetto, 2010). The upper part of the Tunas Formation bears the *Gangamopteris* Flora of
10
11 483 latest Early Permian age according to Archangelsky and Cúneo (1984).

12 484 Several ash-fall tuffs levels were sampled in the Abra del Despeñadero, in the
13
14 485 southeastern sector of Sierra de Pillahuincó. There, thin beds of smectite-rich claystones have
15
16 486 been identified in the predominantly sandy upper half of the Tunas Formation and are
17
18 487 characterized by abundant vitroclasts and fragments of vitric tuffs (Iñiguez et al., 1988; López
19
20 488 Gamundí, 2006). The dated zircons of three beds yielded an average $^{206}\text{Pb}/^{238}\text{U}$ age of 304
21
22 489 Ma, that corresponds to some sort of mixing of zircons formed between 280 and 288 Ma
23
24 490 (interpreted as juvenile zircons based on ϵHf data) and zircons formed between 290 to 315
25
26 491 Ma. Alessandreti et al. (2013) presented for the same SLV-VE-19 sample an U-Pb in situ LA-
27
28 492 MC-ICPMS age of 284 ± 15 Ma.

29 493 One tuff layer of the same outcrop as the samples SLV-VE-19, 20 and 21 has been
30
31 494 dated by Tohver et al. (2008) and yielded an age of 282.4 ± 2.8 Ma (U-Pb-SHRIMP). A
32
33 495 similar age of 280.9 ± 1.9 Ma (U-Pb SHRIMP) was recently reported by López-Gamundí et
34
35 496 al. (2013) on volcanic zircons from a tuff layer in the uppermost section of the Tunas
36
37 497 Formation. Both SHRIMP U-Pb ages are more reliable.

38 498 Based on these data, it is assumed that the tuff layers with the younger frequency
39
40 499 peaks, have crystallization ages close to 280 and 288 Ma (see Fig. 13), indicating a middle
41
42 500 Early Permian age, consistent with SHRIMP recent ages and the biochron of the fossil fauna
43
44 501 and flora.

45 502 The intimate relationship between volcanic activity inboard of the paleo-Pacific
46
47 503 margin, deformation in the adjacent orogenic belt, and subsidence and sedimentation in the
48
49 504 contiguous foreland basin led López Gamundí and Rossello (1998) to interpret the magmatic
50
51 505 belt as an Andean-type margin related to the paleo-Pacific margin. This proposal was
52
53 506 followed by Turner (1999) and Dalziel et al. (2000), among others. The main problem of this
54
55 507 interpretation is that the magmatic arc, as pointed out by Turner (1999) was located over
56
57 508 1,000 km away from the continental margin. No subduction related magmatism can exist that
58
59 509 far from the margin, even if a flat-subduction is proposed. A magmatic arc belt cannot be
60
61 510 developed further than 300-400 km away of the trench. Some authors proposed an
62
63
64
65

511 intermediate location (Pankhurst et al., 2006), but still inconsistent with a magmatic arc along
512 northern Patagonia in the Somún Cura Massif. Recent work of Chernicoff et al. (2012 a)
513 demonstrates that a series of calc-alkaline orthogneisses are Permian in age and represent the
514 relicts of the late Paleozoic magmatic arc developed in the northern Patagonia as proposed by
515 different authors (Ramos, 2008, and cites therein).

516 Although, the classic interpretation to explain the pyroclastic levels in the Las Tunas
517 Formation and in the Paraná Basin in southern Brazil is a source in the Choiyoi volcanic rocks
518 (Kay et al., 1989), we favor a more proximal origin. Based on U-Pb SHRIMP ages around
519 281.4 ± 2.5 Ma from Los Reyunos Formation, lower section of the Choiyoi volcanic rocks,
520 Rocha Campos et al. (2011) correlated these rocks with the older tuffs of the Paraná Basin.
521 This correlation is supported by the northeast paleocurrent directions measured in the aeolian
522 sandstones of Los Reyunos Formation by Pazos et al. (2011). However, if we want to use the
523 same Choiyoi source for the pyroclastic deposits of Las Tunas Formation, even with similar
524 ages, the dominant winds should be to the southeast, different from what was measured in the
525 Choiyoi intercalated aeolian sandstones. The distance is closer from Somún Cura, the ages are
526 similar, and the required paleowind direction is also to the northeast. Therefore, we prefer as a
527 potential source the Early Permian widespread calderas and rhyolites of the same age found in
528 the Somún Cura Massif. This interpretation also explains the source of the large amount of
529 volcanic debris and igneous Carboniferous detrital zircons found in Las Tunas Formation.

530

531 6. Lu-Hf-Isotope analyses

532 Hf isotopes have been analyzed in 65 detrital zircons of samples from the Cambrian
533 paragneiss (SLV-VE-02), and from the Lolén (SLVE-01) and Tunas (SLV-VE 20/21)
534 Formations, in order to understand the characteristics of the source region (Fig. 16).

535 Several zircons from different representative sources have been analyzed in the sample
536 of metamorphic basement (SLV-VE-02). Two Neoarchean zircons yielded negative values of
537 $\epsilon\text{Hf}(t)$ of -7.06 and -5.11 and TDM ages 2.98 and 3.22 Ga; one Mesoarchean zircon has an
538 $\epsilon\text{Hf}(t)$ of +1.73 with a TDM age of 3.06 Ga. The Paleoproterozoic source was analyzed in
539 eight zircons, which yielded values of $\epsilon\text{Hf}(t)$ between + 2.19 and -1.8. These values are
540 typical of the juvenile arc granitoids of Tandilia (Fig. 16). The younger zircon of 1,782 Ma
541 gave a quite negative value of -5.57 far from the previous ones; the TDM ages yielded
542 between 2.57 and 2.19 Ga. This 1.78 Ga corresponds to the age of post-collisional granites in
543 the Tandilia area (Cingolani, 2011), which clearly shows important crustal recycling (Fig. 16).

544 A few Mesoproterozoic zircons analyzed have disperse $\epsilon\text{Hf}(t)$ values from -14.8 and an TDM
545 age of 2.05 Ga, to $\epsilon\text{Hf}(t)$ positives and TDM ages 1.87 and 1.62 Ga. The other well
546 represented fraction is the Neoproterozoic (ca. 552 Ma) with $\epsilon\text{Hf}(t)$ values between -5.4 and -
547 3.08 with similar TDM Mesoproterozoic ages between 1.34 and 1.26 Ga within the range
548 described for the Sierras Pampeanas by Dahlquist et al. (2013).

FIGURE 16 NEAR HERE

550 In the Lolén Formation 35 zircons have been analyzed from sample (SL-VE-01)
551 representing different sources (Fig. 16). The Paleoproterozoic source yielded values of $\epsilon\text{Hf}(t)$
552 of +2.86 and -1.57 and TDM ages between 2.49 and 2.31 Ga; however, a few zircons yielded
553 $\epsilon\text{Hf}(t)$ values more negatives between -4.04 and -20.68 and older TDM ages between 2.81 and
554 2.59 Ga. Grenville-age zircons yielded similar $\epsilon\text{Hf}(t)$ values, but highly positive, between
555 +12.75 and +7.22, and model ages close to the crystallization ages, between 1.27 and 1.50 Ga,
556 showing their juvenile nature (Fig. 16). The Neoproterozoic zircons have variable
557 characteristics with a group of highly negative $\epsilon\text{Hf}(t)$ values between -35.17 and -18.22 and
558 model ages between 2.52 and 1.80 Ga; a second group has less negative $\epsilon\text{Hf}(t)$ values
559 between -5.64 and -0.73 and younger TDM ages between 1.16 and 1.35 Ga. The Paleozoic
560 sources can also be grouped in two sets, a group of Cambrian, Ordovician, and Devonian
561 zircons with very negative $\epsilon\text{Hf}(t)$ values (-43.93 and -11.09) and TDM ages between 2.61 and
562 1.47 Ga; the other group has more positive $\epsilon\text{Hf}(t)$ values (+28.71 and -5.01) and younger
563 TDM ages (1.26 and 1.03 Ga).

564 The last samples from the Tunas Formation (SLV-VE 20/21), which have late
565 Paleozoic zircons (290-340 Ma) yielded $\epsilon\text{Hf}(t)$ values between +10.51 and -1.87, with TDM
566 ages restricted between 0.98 and 0.80 Ga. These zircons probably belong to the juvenile
567 magmatic arc of northern Patagonia (see Ramos, 2008). There is also a crystal with highly
568 negative $\epsilon\text{Hf}(t)$ value (-30.82) and a model age of 1.82 Ga, very distinct of the rest of the
569 group (Fig. 16). Those highly negative values were also recorded by Chernicoff et al. (2012
570 a).

7. Analyses of the provenance

573 Based on the previous detrital zircon analyses, together with conventional
574 petrographic and paleocurrents studies performed by Reinoso (1968), Andreis and Cladera
575 (1992) and López Gamundí and Rossello (1998), among others, a tentative paleogeography
576 can be reconstructed along a series of stages.

577

7.1 Cambrian-Ordovician

The provenance at this stage looks simple and conditioned by the basement exposed at that time. The Paleoproterozoic of Tandilia is the main source, a clear indication that these mountains were conspicuous at that time. Through time, the Pampean basement of Ventania starts being exhumed and Cambrian and Neoproterozoic granitoids became the main source (Fig. 17).

FIGURE 17 NEAR HERE

The proposed paleogeography shows an old mountain system being exhumed, represented by the Tandilia mountains, surrounded to the west (present coordinates) by the Pampean orogenic belt of Eastern Sierras Pampeanas. The exhumation of this belt produced an increased participation of this source through time. At the eastern side the Punta Mogotes Belt, a Brasiliano orogen related to the final closure of Adamastor Ocean at Early Cambrian times (Gaucher et al., 2005), was one of the last events related to the amalgamation of Gondwana. However, this orogen was not source of the analyzed samples of Ventania. The comparison of the different units of the Curamalal Group (Figs. 7 and 8) with the Mogotes Formation detrital zircon patterns shows striking differences (Fig.18).

FIGURE 18 NEAR HERE

The Cambrian-Ordovician paleogeography is illustrated in Fig. 19. The drainage should have an important component from the west or northwest to explain the lack of zircons from the Punta Mogotes Belt seen in the frequency peaks of Fig. 18. Note that these peaks are partially recognized in the younger Balcarce Formation (Fig. 11).

FIGURE 19 NEAR HERE

7.2 Silurian-Devonian

At this time the main dominant provenance was from the west and northwest. The Pampean basement of Eastern Sierras Pampeanas as described by Rapela et al. (1998), Ramos et al. (2010) and Chernicoff et al. (2009, 2012 b), was the main source of the lower Ventana Group (Fig. 17). The angular unconformity between the Balcarce Formation and the Neoproterozoic and Early Cambrian sedimentary cover of Tandilia (Cingolani, 2011) may be either the result of the collision of Pampia with the Río de la Plata Craton (Early Cambrian), or the Famatinian collision (Middle Ordovician). The sedimentary record of Balcarce Formation indicates a post Hirnantian glaciation age (Late Ordovician). The Pampean unconformity is seen in different places of Eastern Sierras Pampeanas and was dated in 530 Ma by Escayola et al. (2007) and Ianizzotto et al. (2013). But, as the main source is coming

611 from Eastern Sierras Pampeanas which is closer to Tandilia, it is more probable that
1 612 deformation is related to the Pampean orogen (see further details in Pazos and Rapalini,
2 613 2011).

3 614 Through time, the Pampean Belt had the relief partially eroded, and during Silurian
4 615 times the first Ordovician zircons were recorded, indicating that either the Famatinian Belt
5 616 was supplying zircons to the area, or some scarce Ordovician granitoids in the Eastern
6 617 Pampean Belt were exhumed. Also, Grenvillian-age zircons began to appear in the pattern of
7 618 provenance, suggesting that the Mesoproterozoic basement of Cuyania and/or Pampia was
8 619 also exhumed (Sato et al., 2000). The relief of Tandilia was almost non-existent as a source.
9 620 At this time, an important source from Punta Mogotes Belt is recorded in the Balcarce
10 621 Formation, indicating that this belt was actively exhumed. In Silurian times the
11 622 paleogeography was characterized by higher mountains in the Famatinian Belt in the west, a
12 623 partially eroded Pampean Belt, almost non-existent Tandilia Mountains, and an important
13 624 relief in the Punta Mogotes Belt. Some sort of by-pass existed through the Pampean Belt in
14 625 order to register Ordovician zircons in the Balcarce and Lolén Formations. The continental
15 626 margin was opened to the present south (Fig. 19).

30 627

31 628 **7.3 Late Paleozoic**

32 629 A drastic change in paleogeography was produced at this time. A volcanic relief
33 630 associated with a magmatic arc was located to the south, in present northern Patagonia.
34 631 Volcanic debris (Andreis and Cladera, 1992) together with magmatic zircons were recorded in
35 632 Ventania from 320 to 270 Ma. Classic petrographic provenance studies in Ventania and Cape
36 633 Fold Belt of South Africa indicate a dissected arc source for these rocks (López Gamundí and
37 634 Rossello, 1998). The older data of Late Carboniferous age observed as detrital zircons are in
38 635 agreement with their derivation from the northern late Paleozoic magmatic arc proposed by
39 636 Ramos (2008) in northern Patagonian along the Somún Cura Massif. Recent studies of
40 637 Chernicoff et al. (2012 a) in the Yaminué region in the Somún Cura Massif show that a biotite
41 638 paraschist has a maximum U/Pb SHRIMP age of 318 ± 5 Ma coherent with the frequency
42 639 peaks of several units of the Pillahuincó Group of the Ventania System. On the other hand,
43 640 the tonalitic orthogneiss has a crystallization age of 261.3 ± 2.7 Ma, which is broadly coeval
44 641 with deformation, and Neoproterozoic inheritance, indicating the occurrence of
45 642 Archean crust in this sector of Patagonia. Hf TDM ages of Permian zircons are mainly Meso-
46 643 Paleoproterozoic (2.97–3.35 Ga) with highly negative $\epsilon(\text{Hf})$ values (ca. -33) according to
47 644 Chernicoff et al. (2012 a). It is interesting to remark that the first Archean zircons observed in
48
49
50
51
52
53
54
55
56
57
58
59
60
61
62
63
64
65

645 Ventania are the 2729, 2990 and 3200 Ma frequency peaks of Sauce Grande Formation,
646 within the range of inherited Archean zircons of the Yaminué region described by these
647 authors.

648 The obtained zircon dates of the ash-fall tuffs of the Tunas Formation indicate an
649 Early Permian age, close to the depositional age of this unit (López Gamundí et al., 1995),
650 which was interpreted as synorogenic deposits based on the occurrence of growth strata. The
651 age of deformation is consistent with the deformation ages of the orthogneisses in north
652 Patagonia in the adjacent Somún Cura Massif (Chernicoff et al., 2012a).

653 A Permian very juvenile poorly dissected relief dominated the Somún Cura Massif and
654 the uplifted Ventania fold belt providing immature detritus to the Claromecó Basin. The
655 Ventania fold and thrust belt continues in the offshore in the Colorado syntaxis (Pángaro and
656 Ramos, 2012), a mirror image of the Cape Syntaxis (Fig. 20).

657

658 **8. Correlation with the Cape Fold Belt in South Africa**

659 It is important to note that in South Africa, the Cape Fold Belt was developed at the
660 same time that the Ventania Belt (Fig. 20) as parts of the Gondwanides Orogen (Keidel, 1916,
661 1921). There is consensus in the correlation of the different units of the Neoproterozoic-
662 Cambrian basement and the Paleozoic sedimentary sequences since the early work of Keidel
663 (1916) and DuToit (1927) followed by Harrington (1947). This correlation was based on the
664 rock types and age of the basement as proposed by Rapela et al. (2003), Milani and DeWitt
665 (2008), and Chemale et al. (2011b). On fossiliferous grounds the correlation was based on the
666 *Eurydesma* fauna and the *Glossopteris* flora, as well as in the Devonian marine fossils
667 (Harrington, 1955; Benedetto, 2010). Another piercing point is the correlation of the glacial
668 deposits of Sauce Grande and the Dwyka Tillite, which has been identified since the early
669 work of Keidel (1913), and corroborated several times by more recent works (López Gamundi
670 and Rossello, 1998).

671

FIGURE 20 NEAR HERE

672 A recent study on the detrital zircons of several pre-Carboniferous units of the Cape
673 Supergroup shows striking differences and similarities with the Ventania System (Fourie et
674 al., 2011). The main difference is the dominant Mesoproterozoic (1.0-1.2 Ga) provenance of
675 the Cape Supergroup that points out to the Namaqua Belt as the source area. The Curamalal
676 and Ventana Groups have the Paleoproterozoic ages from Tandilia Belt (2.2-2.0 Ga) as the
677 main Precambrian source. The similarities are the Neoproterozoic-Cambrian ages derived in
678 the present study from the Eastern Sierras Pampeanas, and from the pan-African belts and the

61
62
63
64
65

679 Cape Granites for Fourie et al. (2011). Both studies have also a striking coincidence in the
1 680 Ordovician ages. The analyses performed in the pre-Carboniferous rocks of the Cape Fold
2 681 Belt have a noticeable frequency peak at 469 Ma, similar to the frequency peak of 475 Ma of
3 682 Lolén Formation in the Ventania Belt that in the present study is straight forward derived
4 683 from the Famatinian Belt of Western Sierras Pampeanas. A similar Ordovician peak (478 Ma,
5 684 see Fig. 11) was identified in the Balcarce Formation by Rapela et al. (2011). Nonetheless,
6 685 Fourie et al. (2011) assumed that the source area could be either the Ross Orogen in
7 686 Antarctica or the Patagonian Deseado Massif of Argentina. As we noticed, the abrupt change
8 687 in provenance occurred after the collision of Patagonia, where a very different provenance is
9 688 recorded for the first time.

10 689 Based on the evaluation of both detrital zircon data bases we consider the Ordovician
11 690 (480-460 Ma) provenances in both Ventania and Cape belts, as derived from Western Sierras
12 691 Pampeanas, while the Neoproterozoic-Cambrian (560-530 Ma) zircons have local sources.
13 692 Zircons are derived in the Ventania Belt from Eastern Sierra Pampeanas, but in the Cape Fold
14 693 Belt come from local pan-African belts.

15 694

16 695 **9. Concluding remarks**

17 696 The obtained data permit to confirm some hypotheses and discard some previous
18 697 interpretations. The comparison of the provenance between the Curamalal and Ventana
19 698 Groups allows once more to confirm the stratigraphy of Harrington (1947), and to reject some
20 699 hypotheses that interpreted these units as tectonic repetitions of the same succession. These
21 700 pre-Carboniferous sequences of the Ventania Belt have a pattern derived from the Tandilia
22 701 Belt, as well as from Eastern and Western Sierras Pampeanas. These characteristics can be
23 702 compared with the detrital zircon pattern of the pre-Carboniferous Cape Fold Belt sequences.
24 703 Differences and similarities can be explained with common and local sources; both belts share
25 704 a similar Early to Middle Ordovician age zircons, which seem to be derived from the Sierras
26 705 Pampeanas Belt.

27 706 The change in provenance between the early Paleozoic deposits of the Ventana Group
28 707 and the late Paleozoic foreland sequences of the Pillahuincó Group indicates a different
29 708 source region from these deposits. A series of Carboniferous to Permian zircons, absent in the
30 709 previous units, together with the drastic change in paleocurrents indicate their derivation from
31 710 northern Patagonia as part of the Gondwanides Belt. The source area for the Pillahuincó
32 711 Group matches one to one the lithological characteristics of the Somún Cura Massif (see
33 712 location in Fig. 1), and the U-Pb ages of the main igneous and metamorphic rocks.

34
35
36
37
38
39
40
41
42
43
44
45
46
47
48
49
50
51
52
53
54
55
56
57
58
59
60
61
62
63
64
65

713 The occurrence of clasts with archeocyathids in the Somún Cura Massif sequences,
714 together with the detrital zircon patterns, are compatible with a source in Eastern Antarctica
715 (González et al., 2011; Naipauer et al., 2011; Ramos and Naipauer, 2012; Veevers and Saeed,
716 2013). The recent finding of archeocyathids in clasts of the Sauce Grande tillites (González et
717 al., 2013), reinforces this provenance. This match indicates that Patagonia should have
718 originated in Eastern Gondwana, and that it was transferred to Western Gondwana during the
719 Gondwanan orogeny. For further details see the recent analysis of Ramos and Naipauer
720 (2013 and cites there in). Although some recent papers proposed a continuation of the
721 magmatic activity in the early Paleozoic from the Sierras Pampeanas to the Somún Cura area
722 (Rapalini et al., 2013), a classic proposal advanced by Braccini (1960), it is not able to
723 elucidate the presence of archeocyathids (see discussion in Ramos and Naipauer, 2013).
724 Rapalini et al. (2013) follow the arguments of Dalziel et al. (2013) who propose a continuous
725 archeocyathid reef along the margin of Antarctica. However, this argument needs a magmatic
726 arc located in the Somún Cura arc more than thousand kilometers away from the Pacific
727 margin (see discussion in Ramos, 2008).

728 The integrated evolution of the Gondwanides in this sector of the southwestern
729 Gondwana margin with the general evolution of the Terra Australis Orogen as defined by
730 Cawood (2005) and modified by Ramos (2009), shows some interesting features. The early
731 Paleozoic continental margin of Ventania interrupts the almost continuous Famatinian-Ross
732 orogens. The Famatinian Orogen characterizes an active continental margin with a
733 voluminous magmatic arc developed along the proto-Andean margin of Western Gondwana
734 from Venezuela and Colombia through most of Argentina down to Ventania, during latest
735 Cambrian and Middle Ordovician times. The Ross Orogen (Stump, 1995; Myrow et al., 2001)
736 continues to the present east from Patagonia all along the Transantarctic Mountains and
737 Australia, and has a latest Cambrian to Early Ordovician magmatic arc. The Ventania early
738 Paleozoic basin is devoid of any magmatic activity in these intervals, representing a passive
739 continental margin. The tectonic causes of such differences are beyond the present research.

741 **Acknowledgements**

742 The authors want to thank Dr. Silvia Japas and Dr. Claudia Marsicano from the
743 Universidad de Buenos Aires for their help in the field work as well as to grants to VAR and
744 FC. We want to express our recognition to Dr. Eric Thover and an anonymous reviewer for
745 their critical and positive comments. This is the contribution R-90 of the Instituto de Estudios
746 Andinos “Don Pablo Groeber” (IDEAN).

References

749

750 Alessandreti, L, Philipp, R.P., Chemale Jr., F., Brückmann, M.P., Zvirtes, G., Matté, V., Ramos, V.A.,
751 2013. Geochemistry, provenance, and tectonic setting of the Paleozoic Ventania Fold Belt and the
752 Claromecó Foreland Basin: implications on sedimentation and volcanism along the southwestern
753 Gondwana margin. *Journal South American Earth Sciences* (in press).

754

755 Andersen, T., Graham, S., Aberg, G, Simonsen, S.L., 2009. Granitic magmatism by melting of
756 juvenile continental crust: new constraints on the source of Palaeoproterozoic granitoids in
757 Fennoscandia from Hf isotopes in zircon. *Journal of the Geological Society* 166, 233–247.

758

759 Andreis, R.R., Cladera, G., 1992. Las epiclastitas pérmicas de la cuenca Sauce Grande (Sierras
760 Australes, Buenos Aires, Argentina). Parte I: composición y procedencia de detritos. 4° Reunión
761 Argentina de Sedimentología (La Plata), Actas, p. 127–134.

762

763 Andreis, R., López Gamundi, O., 1989. Interpretación paleoambiental de la secuencia paleozoica del
764 Cerro Pan de Azúcar, Sierras Australes, Prov. de Buenos Aires. 1° Jornadas Geológicas Bonaerenses
765 (Tandil), Actas, p. 953–966, Bahía Blanca.

766

767 Andreis, R.R., Iñiguez, A.M., Lluch, J.J., Rodriguez, S., 1989. Cuenca Paleozoica de Ventania, Sierras
768 Australes, Buenos Aires. In: Chebli, G., Spalletti, L. (Eds.), *Cuencas Sedimentarias Argentinas:*
769 *Universidad Nacional de Tucumán, Correlación Geológica Serie 6*, p. 265–298.

770

771 Archangelsky, S., Cúneo, R., 1984. Zonación del Pérmico continental argentino sobre la base de sus
772 plantas fósiles. 3° Congreso Latinoamericano de Paleontología (México), *Memorias*, p. 143–153.

773

774 Balarino, M.L., 2012. Palinología del Pérmico de la cuenca de Claromecó-Colorado, Argentina.
775 *Ameghiniana* 49, 343–364.

776

777 Bellosi, E.S., Jalfin, G.A., 1984. Litoestratigrafía y evolución paleoambiental neopaleozoica de las
778 islas Malvinas, Argentina. 9° Congreso Geológico Argentino (Bariloche), *Actas* 5, p. 66–86.

779

780 Bellosi, E.S., Jalfin, G.A., 1989. Cuencas neopaleozoicas de la Patagonia extraandina e Islas Malvinas.
781 In: Chebli, G., Spalletti, L. (Eds.), *Cuencas Sedimentarias Argentinas: Universidad Nacional de*
782 *Tucumán, Correlación Geológica Serie, 6*, p. 379–394.

60

61

62

63

64

65

783

- 1 784 Benedetto, J.L., 2010. El continente de Gondwana a través del tiempo. Una introducción a la Geología
2 Histórica. Academia Nacional de Ciencias, Córdoba, 384 p.
- 3 785
4
5 786
- 6 787 Borrello, A.V., 1966. Trazas, restos tubiformes y cuerpos fósiles problemáticos de la Formación La
7 Tinta, Sierras Septentrionales de la Provincia de Buenos Aires. Comisión de Investigaciones
8 Científicas de la Provincia de Buenos Aires. *Paleontografía Bonaerense* 5, 1–42.
- 9 789
10
11 790
- 12
13 791 Bouvier, A., Vervoort, J.D., Patchett, P.J., 2008. The Lu–Hf and Sm–Nd isotopic composition of
14 CHUR: Constraints from unequilibrated chondrites and implications for the bulk composition of
15 terrestrial planets. *Earth and Planetary Science Letters* 273, 48–57.
- 16 793
17
18 794
- 19 795 Braccacini, O., 1960. Lineamientos principales de la evolución estructural de la Argentina.
20 *Petrotecnica, Revista del Instituto Argentino del Petróleo* 10(6), 57–69.
- 21 796
22
23 797
- 24 798 Buggisch, W., 1987. Stratigraphy and very low grade metamorphism of the Sierras Australes of the
25 Province of Buenos Aires, Argentina and implications in Gondwana correlations. *Zentralblatt*
26 *Mineralogie Geologie Paläontologie* 1, 819–837.
- 27 799
28 800
29
30 801
- 31 802 Cawood, P.A., 2005. Terra Australis orogen: Rodinia breakup and development of the Pacific and
32 Iapetus margins of Gondwana during the Neoproterozoic and Paleozoic. *Earth-Science Reviews* 69,
33 249–279.
- 34 803
35 804
36 805
- 37 806 Chemale Jr., F., Philipp, R.P., Dussin, I.A., Formoso, M.L.L., Kawashita, K., Bertotti, A.L., 2011a.
38 Lu-Hf and U-Pb age determinations of Capivarita Anorthosite in the Dom Feliciano Belt, Brazil.
39 *Precambrian Research* 186, 117–126.
- 40 807
41 808
42
43 809
- 44 810 Chemale Jr., F., Scheepers, R., Gresse, P.G., Van Schmus, W.R., 2011b. Geochronology and sources
45 of late Neoproterozoic to Cambrian granites of the Saldania Belt. *International Journal of Earth*
46 *Sciences (Geologische Rundschau)* 100, 431–444.
- 47 811
48 812
49
50 813
- 51 814 Chemale Jr., F., Kawashita, K., Dussin, I. A., Ávila, J. N., Justino, D., Bertotti, Anelise L., 2012. U-Pb
52 zircon in situ dating with LA-MC-ICP-MS using a mixed detector configuration. *Anais da Academia*
53 *Brasileira de Ciências* 84, 275–295.
- 54 815
55 816
56 817
- 57 818 Chernicoff, J., Zapettini, E., 2004. Geophysical evidence for terrane boundaries in South-Central
58 Argentina. *Gondwana Research* 7, 1105–1117.
- 59 819
60
61
62
63
64
65

- 1 821 Chernicoff, C.J., Zappettini, E.O., Villar, L.M., Chemale Jr., F., Hernández, L., 2009. The belt of
2 metagabros of La Pampa: Lower Paleozoic back-arc magmatism in south-central Argentina. *Journal of*
3 822 *South American Earth Sciences* 28, 383–397.
- 4
5 823
6 824
- 7
8 825 Chernicoff, C.J., Zappettini, E.O., Santos, J.O.S., Godeas, M.C, Belousova, E., McNaughton, N.K.,
9
10 826 2012 a. Identification and isotopic studies of early Cambrian magmatism (El Carancho Igneous
11 827 Complex) at the boundary between Pampia terrane and the Río de la Plata craton, La Pampa province,
12 Argentina. *Gondwana Research* 21, 378–393.
- 13 828
14
15 829
- 16 830 Chernicoff, C.J., Zappettini, E.O., Santos, J.O.S., McNaughton, N.J., Belousova, E., 2012 b.
17 831 Combined U-Pb SHRIMP and Hf isotope study of the Late Paleozoic Yaminué Complex, Rio Negro
18 832 Province, Argentina: Implications for the origin and evolution of the Patagonia Composite Terrane.
19
20 833 *Geoscience Frontiers*, doi: 10.1016/j.gsf.2012.06.003.
- 21 834
22
23 835
- 24 836 Chu, N.C., Taylor, R.N., Chavagnac, V., Nesbitt, R.W., Boella, M., Milton, J.A., 2002. Hf isotope
25 837 ratio analysis using multi-collector inductively coupled plasma mass spectrometry: an evaluation of
26 isobaric interference corrections. *Journal Analytic Atmospheric Spectrom* 17, 1567–1574.
- 27 838
28
29 839
- 30 840 Cingolani, C., 2005. Unidades morfoestructurales (y estructuras menores) de la provincia de Buenos
31 841 Aires. In: de Barrio, R.E., Etcheverry, R.O., Caballé, M.F., Llambías, E. (Eds.) *Geología y recursos*
32 minerales de la Provincia de Buenos Aires. 16° Congreso Geológico Argentino, Relatorio, p. 21–30,
33 La Plata.
- 34 842
35 843
36
37 844
- 38 845 Cingolani, C., 2011. The Tandilia System of Argentina as a southern extension of the Río de la Plata
39 846 craton: an overview. *International Journal of Earth Sciences (Geologische Rundschau)* 100, 221–242.
- 40 847
41 848
- 42 849 Cingolani, C., Berry, C.M., Morel, E., Tomezzoli, R., 2002. Middle Devonian lycosids from high
43 850 southern palaeolatitudes of Gondwana (Argentina). *Geological Magazine* 139, 641–649.
- 44 851
45 852
46 853
- 47 854 Cobbold, P.R., Gapais, D., Rossello, E.A., 1991. Partitioning of transpressive motions within a
48 855 sigmoidal foldbelt: the Variscan Sierras Australes, Argentina. *Journal of Structural Geology* 13, 743–
49 758.
- 50 856
51 857
- 52 858 Cuerda, A., Cingolani, C., Barranquero, H., 1975. Estratigrafía del basamento Precámbrico en la
53 859 comarca de los cerros Pan de Azúcar del Coral, Sierras Australes, prov. de Buenos Aires, Rep.
- 54
55
56
57
58
59
60
61
62
63
64
65

856 Argentina. 2° Congreso Iberoamericano de Geología Económica (Buenos Aires), Actas 1, p. 57–64,
1 857 Buenos Aires.
2
3 858
4
5 859 Dahlquist, J.A., Pankhurst, R.J., Gaschnig, R.M., Rapela, C.W., Casquet, C., Alasino, P.H., Galindo,
6 860 C., Baldo, E.G., 2013. Hf and Nd isotopes in Early Ordovician to Early Carboniferous granites as
7 861 monitors of crustal growth in the Proto-Andean margin of Gondwana. *Gondwana Research* 23, 1617–
8 862 1630.
9
10
11 863
12
13 864 Dalziel, I.W.D., Lawver, L.A., Murphy, J.B., 2000. Plumes, orogenesis, and supercontinental
14 865 fragmentation. *Earth and Planetary Science Letters* 178, 1–11.
15
16 866
17
18 867 Dalziel, I.W.D., Lawver, L.A., Norton, I.O., Gahagan, L.M., 2013. The Scotia Arc: Genesis,
19 868 Evolution, Global Significance. *Annual Reviews in Earth and Planetary Sciences* 41, 1–27.
20
21 869
22
23 870 de Beer, C.H., 1995. Fold interference from simultaneous shortening in different directions: the Cape
24 871 Fold Belt syntaxis. *Journal of African Earth Sciences* 21, 157–169.
25
26 872
27
28 873 Domeier, M., Van der Voo, R., Tohver, E., Tomezzoli, R.N., Vizan, H., Torsvik, T.H., Kirshner, J.,
29 874 2011. New Late Permian Constraints on the Apparent Polar Wander Path and Paleo-Marginal
30 875 Deformation of Gondwana. *Geochemistry, Geophysics, Geosystems*, 12, Q07002.
31
32 876
33
34 877 Dimieri, L., Delpino, S., Turienzo, M., 2005. Estructura de las Sierras Australes de Buenos Aires. In:
35 878 de Barrio, R., Etcheverry, O., Caballé, M.F., Llambías E. (Eds.), *Geología y recursos minerales de la*
36 879 *Provincia de Buenos Aires. 16° Congreso Geológico Argentino, Relatorio*, p. 101–118, La Plata.
37
38 880
39
40 881 Du Toit, A.L., 1927. A geological comparison of South America with South Africa. *Publications*
41 882 *Carnegie Institute* 381, 1–157.
42
43 883
44
45 884 Du Toit, A.L., 1937. Our wandering continents. An hypothesis of continental drifting. Oliver & Boyd,
46 885 London, 366 p.
47
48 886
49
50 887 Escayola, M., Pimentel, M., Armstrong, R., 2007. Neoproterozoic backarc basin: Sensitive high-
51 888 resolution ion microprobe U-Pb and Sm-Nd isotopic evidence from the Eastern Pampean Ranges,
52 889 Argentina. *Geology* 36, 495–498.
53
54 890
55
56 891 Fourie, P.H., Zimmermann, U., Beukes, N.J., Naidoo, T., Kobayashi, K., Kosler, J., Nakamura, E.,
57 892 Tait, J., Theron, J.N., 2011. Provenance and reconnaissance study of detrital zircons of the Palaeozoic
58
59
60
61
62
63
64
65

893 Cape Supergroup in South Africa: revealing the interaction of the Kalahari and Rio de la Plata cratons.
1 894 International Journal of Earth Sciences 100, 527–541.
2
3 895
4
5 896 Frakes, L.A., Crowell, J.C., 1969. Late Paleozoic glaciation. Part I. South America. Geological
6 897 Society America, Bulletin 80, 1007–1042.
7
8 898
9
10 899 Furque, G., 1965. Nuevos afloramientos del Paleozoico en la provincia de Buenos Aires. Revista del
11 900 Museo de la Plata, n.s. 5 (Geología 25), 239–243.
12
13 901
14 902 Gaucher, C., Poiré, D.G., Gómez Peral, L., Chiglino, L., 2005. Litoestratigrafía, bioestratigrafía y
15 903 correlaciones de las sucesiones sedimentarias del Neoproterozoico-Cámbrico del Cratón del Río de la
16 904 Plata (Uruguay y Argentina). Latinamerican Journal of Sedimentology and Basin Analysis 12, 145–
17 905 160.
18
19 906
20
21 907 Gaucher, C., Finney, S.C., Poiré, D.G., Valencia, V.A., Grove, M., Blanco, G., Pamoukaghlián, K.,
22 908 Gómez Peral, L., 2008. Detrital zircon ages of Neoproterozoic sedimentary successions in Uruguay
23 909 and Argentina: insights into the geological evolution of the Río de la Plata Craton. Precambrian
24 910 Research 167, 150–170.
25
26 911
27
28 912 Ghidella, M.E., Paterlini, C.M., Kovacs, L.C., Rodríguez, G.A., 1995. Magnetic anomalies on the
29 913 Argentina Continental Shelf. Fourth International Congress of the Brazilian Geophysical Society and
30 914 First Latin American Geophysical Conference (Río de Janeiro), Expanded Abstracts 1, 269–272.
31
32 915
33
34 916 Goodge, J.W., Vervoort, J.D., 2006. Origin of Mesoproterozoic A-type granites in Laurentia: Hf
35 917 isotope evidence. Earth and Planetary Science Letters 243, 711–731.
36
37 918
38
39 919 González, P.D., Tortello, M.F., Damborenea, S.E., 2011. Early Cambrian archaeocyathan limestone
40 920 blocks in low-grade meta-conglomerate from El Jagüelito Formation (Sierra Grande, Río Negro,
41 921 Argentina). Geologica Acta 9, 159–174.
42
43 922
44
45 923 González, P.D., Tortello, M.F., Damborenea, S.E., Naipauer, M. Sato, A.M., Varela, R., 2013.
46 924 Archaeocyaths from South America: review and a new record. Geological Journal 48, 114–125.
47
48 925
49
50 926 Gregori, D.A., López, V.L., Grecco, L.E., 2005. A Late Proterozoic–Early Paleozoic magmatic cycle
51 927 in Sierra de la Ventana, Argentina. Journal of South American Earth Sciences 19, 155–171.
52
53 928
54
55
56
57
58
59
60
61
62
63
64
65

929 Gregori, D.A., Kostadinoff, J., Strazzere, L., Raniolo, A., 2008. Tectonic significance and
1 930 consequences of the Gondwanide orogeny in northern Patagonia, Argentina. *Gondwana Research* 14,
2 429–450.
3 931
4
5 932
6 933 Griffin, W.L., Pearson, N.J., Belousova, E., Jackson, S.E., van Achterbergh, E., O'Reilly, S.Y., Shee,
7 S.R., 2000. The Hf isotope composition of cratonic mantle: LAM-MC-ICPMS analysis of zircon
8 934 megacrysts in kimberlites. *Geochimica et Cosmochimica Acta* 64, 133–147.
9 935
10 936
11 937 Harrington, H.J., 1942. Algunas consideraciones sobre el sector argentino del geosinclinal de
12 SAMFRAU. Primer Congreso Panamericano de Ingeniería, Minería y Geología (Santiago), *Anales* 2,
13 938 319–339.
14
15 939
16 940
17 941 Harrington, H.J., 1947. Explicación de las Hojas 33m y 34m, Sierras de Curamalal y de la Ventana,
18 942 provincia de Buenos Aires. *Boletín Dirección Nacional de Geología y Minería* 6, 1-56, Buenos Aires.
19 943
20 944 Harrington, H.J., 1955. The Permian *Eurydesma* fauna of eastern Argentina. *Journal of Paleontology*
21 945 29, 112–128.
22 946
23 947 Harrington, H.J., 1968. Desarrollo paleogeográfico de Sudamérica. Universidad Nacional de
24 948 Tucumán, Instituto Miguel Lillo, *Miscelánea* 26, 1–74.
25 949
26 950 Harrington, H.J., 1970. Las Sierras Australes de Buenos Aires, República Argentina: cadena
27 951 aulacogénica. *Revista de la Asociación Geológica Argentina* 25, 151–181.
28 952
29 953 Iannizzotto, N.F., Rapela, C.W., Baldo, E., Galindo, C., Fanning, C.M., Pankhurst, R., 2013. The
30 954 Sierra Norte-Ambargasta batholith: Late Ediacaran–Early Cambrian magmatism associated with
31 955 Pampean transpressional tectonics. *Journal of South American Earth Sciences* 42, 127–143.
32 956
33 957 Iñíguez, A.M., Andreis, R.R., Zalba, P.E., 1988. Eventos piroclásticos en la Formación Tunas
34 958 (Pérmico), Sierras Australes, provincia de Buenos Aires, República Argentina. 2° Jornadas Geológicas
35 959 Bonaerenses (Bahía Blanca), *Actas*, p. 383–395.
36 960
37 961 Jackson, S.E., Pearson, N.J., Griffin, W.L., Belousov, E.A., 2004. The application of laser ablation-
38 962 inductively coupled plasma-mass spectrometry to in situ U–Pb zircon geochronology. *Chemical*
39 963 *Geology* 211, 47–69.
40 964
41
42
43
44
45
46
47
48
49
50
51
52
53
54
55
56
57
58
59
60
61
62
63
64
65

- 965 Johnston, S.T., 2000. The Cape Fold Belt and syntaxis and the rotated Falkland Islands: dextral
1 966 transpressional tectonics along the southwest margin of Gondwana. *Journal of African Earth Sciences*
2 31, 4–13.
3
4
5 968
6 969 Jones, A.T., Franck, T.D., Fielding, C.R., 2006. Cold climate in the eastern Australian mid to late
7 Permian may reflect cold upwelling waters. *Palaeogeography, Palaeoclimatology, Palaeoecology* 237,
8 970 370–377.
9 370–377.
10
11 972
12
13 973 Kay, S.M., Ramos, V.A., Mpodozis, C., Sruoga, P., 1989. Late Paleozoic to Jurassic silicic
14 974 magmatism at the Gondwana margin: analogy to the Middle Proterozoic in North America? *Geology*
15 17, 324–328.
16 975
17
18 976
19
20 977 Keidel, J., 1913. Über das Alter, die Verbreitung und die gegenseitigen Beziehungen der
21 978 verschiedenen tektonischen strukturen in den argentinischen Gebirgen. 12° Session du Congrès
22 Géologique International (Toronto), *Compte Rendus*, p. 671–687.
23 979
24
25 980
26 981 Keidel, J., 1916. La geología de las Sierras de la Provincia de Buenos Aires y sus relaciones con las
27 982 montañas de Sudáfrica y Los Andes. Ministerio de Agricultura de la Nación, Sección Geología,
28 983 Mineralogía y Minería, *Anales* 11, 1–78, Buenos Aires.
29
30
31 984
32
33 985 Keidel, J., 1921. Sobre la distribución de los depósitos glaciares del Pérmico conocidos en la
34 986 Argentina y su significación para la estratigrafía de la serie del Gondwana y la paleogeografía del
35 987 Hemisferio Austral. *Academia Nacional de Ciencias, Boletín* 25, 239–368.
36
37
38 988
39
40 989 Kilmurray, J.O., 1968. Petrología de las rocas cataclásticas y el skarn del anticlinal del cerro Pan de
41 990 Azúcar, partido de Saavedra, provincia de Buenos Aires. 3° Jornadas Geológicas Argentinas
42 (Comodoro Rivadavia), *Actas* 3, p. 217–239.
43 991
44
45 992
46 993 Kilmurray, J.O., 1975. Las Sierras Australes de la provincia de Buenos Aires. Las fases de
47 994 deformación y nueva interpretación estratigráfica. *Revista de la Asociación Geológica Argentina* 30,
48 995 331–348.
49 331–348.
50
51 996
52
53 997 Llambías, E., Prozzi, C.R., 1975. Ventania. In: *Geología de la Provincia de Buenos Aires, 6° Congreso*
54 998 *Geológico Argentino, Relatorio*, p. 79–101, Buenos Aires.
55 999
56
57
58
59
60
61
62
63
64
65

- 1000 López Gamundí, O., 2006. Permian plate margin volcanism and tuffs in adjacent basins of west
1 1001 Gondwana: Age constraints and common characteristics. *Journal of South American Earth Sciences*
2 22, 227–238.
3 1002
4
5 1003
6 1004 López Gamundí, O.R., Rossello, E.A., 1992. La Cuenca interserrana (Claromecó) de Buenos Aires,
7 Argentina: un ejemplo de cuenca hercínica de antepais. 3° Congreso Geológico de España y 8°
8 1005 Congreso Latinoamericano de Geología (Salamanca), Actas 4, p. 55–59.
9 1006
10 1007
11 1008 López Gamundí, O.R., Rossello, E.A., 1993. The Devonian-Carboniferous unconformity in Argentina
12 and its relation to the Eo-Hercynian orogeny in southern South America. *Geologische Rundschau* 82,
13 1009 136–147.
14
15 1010
16 1011
17 1012 López Gamundí, O.R., Rossello, E.A., 1998. Basin fill evolution and paleotectonic patterns along the
18 Samfrau geosyncline: the Sauce Grande basin–Ventana foldbelt (Argentina) and Karoo basin-Cape
19 1013 foldbelt (South Africa) revisited. *Geologische Rundschau* 86, 819–834.
20
21 1014
22 1015 López Gamundí, O.R., Espejo, I.S., Conaghan, P.J, Powell, C., 1994. Southern South America.
23 1016 *Geological Society of America, Memoir* 184, 281–330.
24
25 1017
26 1018 López Gamundí, O.R., Conaghan, P.C., Rossello, E.A., Cobbold, P.R., 1995. The Tunas Formation
27 1019 (Permian) in the Sierras Australes foldbelt, East Central Argentina: evidence for syntectonic
28 1020 sedimentation in a foreland basin. *Journal of South American Earth Sciences* 8, 129–142.
29
30 1021
31 1022 López Gamundí, O., Fildani, A., Weislogel, A., Rossello, E.A., 2013. The age of the Tunas Formation
32 1023 in the Sauce Grande basin-Ventana foldbelt (Argentina): implications for the Permian evolution of the
33 1024 southwestern margin of Gondwana. *Journal of South American Earth Sciences* (in press).
34
35 1025
36 1026 Ludwig, K.R., 2003. *Isoplot 3.00: A geochronological toolkit for Microsoft Excel*. Berkeley
37 1027 Geochronological Center, Special Publication 4, 70p.
38
39 1028
40 1029 Martin, A.K., C.J.H., Hartnady, Goodland, S.W., 1981. A revised fit of South America and South
41 1030 Central Africa. *Earth and Planetary Science Letters* 54, 293–305.
42
43 1031
44 1032 Max, M.D., Ghidella, M., Kovacs, L., Paterlini, M., Valladares, J.A., 1999. Geology of the Argentine
45 1033 continental shelf and margin from aeromagnetic survey. *Marine and Petroleum Geology* 16, 41–64.
46
47 1034
48 1035
49
50
51
52
53
54
55
56
57
58
59
60
61
62
63
64
65

- 1036 Milani, E.J., DeWitt, M.J., 2008. Correlations between the classic Paraná and Cape–Karoo sequences
1 of South America and southern Africa and their basin infills flanking the Gondwanides: du Toit
2 1037 revisited. In: Pankhurst, R.J., Trouw, R.A.J., Brito Neves, B.B., De Wit, M.J. (Eds.), West Gondwana:
3 1038 Pre-Cenozoic Correlations Across the South Atlantic Region. Geological Society, Special Publications
4 1039 294, p. 319–342.
5 1040
6 1041
7 1042 Monteverde, A., 1937. Nuevo yacimiento de material pétreo en González Chaves. *Revista Minera* 8,
8 1043 116–124.
9 1044
10 1045 Myrow, P.M., Pope, M.C., Goodge, J.W., Fischer, W., Palmer, A.R., 2001. Depositional history of
11 1046 pre-Devonian strata and timing of Ross orogenic tectonism in the central Transantarctic Mountains,
12 1047 Antarctica. *Geological Society of America, Bulletin* 114, 1070–1088.
13 1048
14 1049 Mitchell, C., Taylor, G.K., Cox, K.G., Shaw, J., 1986. Are the Falkland Islands a rotated microplate?
15 1050 *Nature* 319, 131–134.
16 1051
17 1052 Naipauer, M., Sato, A.M., González, P.D., Chemale Jr. F., Varela, R., Llambías, E.J., Greco, G.A.,
18 1053 Dantas, E., 2010. Eopaleozoic Patagonia–East Antarctica connection: fossil and U-Pb evidence from
19 1054 El Jagüelito Formation. 7° South American Symposium on Isotope Geology (Brasilia), Extended
20 1055 Abstracts, 602–605.
21 1056
22 1057 Naipauer, M., González, P.D., Varela, R., Sato, A.M., Chemale Jr., F., Llambías, E., Greco, G., 2011.
23 1058 Edades U-Pb (LA-ICP-MS) en circones detríticos del Miembro Polke, Formación Sierra Grande, Río
24 1059 Negro: ¿Una nueva unidad cambro-ordovícica? 18° Congreso Geológico Argentino (Neuquén), Actas
25 1060 in CD, 113.
26 1061
27 1062 Newton, A.A., Cingolani, C.A., 1990. Aspectos estratigráficos y estructurales comparativos entre las
28 1063 secuencias siluro-devónicas de la Sierra de la Ventana (Argentina) y el Cinturón Plegado del Cabo
29 1064 (Sudáfrica). *Revista Técnica de YPF* 11, 59–63.
30 1065
31 1066 Nuñez, E., Bachmann, E.W. de, Ravazzoli, I., Britos, A., Franchi, M., Lizuaín, A., Sepúlveda, E.,
32 1067 1975. Rasgos geológicos del sector oriental del Macizo Somuncurá, provincia de Río Negro,
33 1068 República Argentina. 2° Congreso Iberoamericano Geología Económica (Buenos Aires), Actas 4, p.
34 1069 247–266.
35 1070
36 1071 Pángaro, F., Ramos, V.A., 2012. Paleozoic crustal blocks of onshore and offshore central Argentina:
37 1072 new pieces of the southwestern Gondwana collage and their role in the accretion of Patagonia and the
38
39
40
41
42
43
44
45
46
47
48
49
50
51
52
53
54
55
56
57
58
59
60
61
62
63
64
65

- 1073 evolution of Mesozoic south Atlantic sedimentary basins. *Marine and Petroleum Geology* 37, 162–
1074 183.
- 1075
- 1076 Pankhurst, R.J., Rapela, C.W., Fanning, C.M., 2001. The Mina Gonzalito Gneiss: Early Ordovician
1077 Metamorphism in Northern Patagonia. 3° South American Symposium on Isotope Geology (Pucón),
1078 Actas electrónicas Session 6(4), 1–4.
- 1079
- 1080 Pankhurst, R.J., Rapela, C.W., Fanning, C.M., Márquez, M., 2006. Gondwanide continental collision
1081 and the origin of Patagonia. *Earth Science Reviews* 76, 235–257.
- 1082
- 1083 Patchett, P.J., Kuovo, O., Hedge, C.E., Tatsumoto, M., 1981. Evolution of continental crust and
1084 mantle heterogeneity: evidence from Hf isotopes. *Contribution to Mineralogy and Petrology* 78, 279–
1085 297.
- 1086
- 1087 Pazos, P.J., Rapalini, A., 2011. The controversial stratigraphy of the glacial deposits in the Tandilia
1088 System, Argentina. In: Arnaud, E., Halverson, G.P., Shields-Zou, G. (Eds.), *The Geological Record of*
1089 *Neoproterozoic Glaciations*, Geological Society, Memoirs 36, 565–569.
- 1090
- 1091 Pazos, P.J., Bettucci, L.S., Loureiro, J., 2008. The Neoproterozoic glacial record in the Río de la Plata
1092 Craton: a critical reappraisal. In: Pankhurst, R.J., Trouw, R.A.J., Brito Neves, B.B., De Wit, M.J.
1093 (Eds.), *West Gondwana: Pre-Cenozoic Correlations Across the South Atlantic Region*. Geological
1094 Society, Special Publications 294, p. 343–364.
- 1095
- 1096 Pazos, P.J., Rey, F., Marsicano, C., Ottone, G., de la Fuente, M., 2011. Permian unroofing,
1097 palaeoenvironmental and palaeoclimate evolution in the San Rafael foreland basin, Mendoza,
1098 Argentina. *Gondwana 14, Reuniting Gondwana: East meets West (Buzios)*, Abstracts , p. 149.
- 1099
- 1100 Pietranik, A.B., Hawkesworth, C.J., Storey, C.D., Kemp, T.I., Sircombe, K.N., Whitehouse, M.J.,
1101 Bleeker, W., 2008. Episodic, mafic crust formation from 4.5 to 2.8 Ga: New evidence from detrital
1102 zircons, Slave craton, Canada. *Geology* 36, 875–878.
- 1103
- 1104 Ploszkiewicz, J.V., 1999. ¿Será Buenos Aires una nueva provincia petrolera? Antecedentes, hipótesis
1105 y certezas. *Boletín de Informaciones Petroleras* 58, 56–45.
- 1106
- 1107 Poiré, D.G., Spalletti, L.A., del Valle, A., 2003. The Cambrian-Ordovician siliciclastic platform of the
1108 Balcarce Formation (Tandilia System, Argentina): Facies, trace fossils, palaeoenvironments and
1109 sequence stratigraphy. *Geologica Acta* 1, 41–60.

- 1110
- ¹1111 Ramos, V.A., 1984. Patagonia: un continente a la deriva? 9º Congreso Geológico Argentino
²
³1112 (Bariloche), Actas 2, p. 311–328.
⁴
⁵1113
- ⁶1114 Ramos, V.A., 1986. Tectonostratigraphy, as applied to analysis of South African Phanerozoic Basins
⁷
⁸1115 by H. de la R. Winter, discussion. Transactions Geological Society South Africa 87, 169–179.
⁹
¹⁰1116
- ¹¹1117 Ramos, V.A., 1988. Tectonic of the Late Proterozoic-Early Paleozoic: a collisional history of the
¹²
¹³1118 southern South American. Episodes 12, 168–174.
¹⁴
¹⁵1119
- ¹⁶1120 Ramos, V.A., 2008. The basement of the Central Andes: the Arequipa and related terranes. Annual
¹⁷
¹⁸1121 Review on Earth and Planetary Sciences 36, 289–324.
¹⁹
²⁰1122
- ²¹1123 Ramos, V.A., 2009. Anatomy and global context of the Andes: Main geologic features and the Andean
²²
²³1124 orogenic cycle. In: Kay, S.M., Ramos, V.A., Dickinson, W. (Eds.), Backbone of the Americas:
²⁴
²⁵1125 Shallow Subduction, Plateau Uplift, and Ridge and Terrane Collision, Geological Society of America,
²⁶
²⁷1126 Memoir 204, p. 31–65.
²⁸1127
²⁹
- ³⁰1128 Ramos, V.A., Kostadinoff, J., 2005. La cuenca de Claromecó. In: de Barrio, R.E., Etcheverry, R.O.,
³¹
³²1129 Caballé, M.F., Llambías, E. (Eds.), Geología y recursos minerales de la Provincia de Buenos Aires.
³³1130 16º Congreso Geológico Argentino, Relatorio, p. 473–480.
³⁴
³⁵1131
- ³⁶1132 Ramos, V.A., Naipauer, M., 2012. Patagonia: an allochthonous terrane accreted to the Western
³⁷
³⁸1133 Gondwana and its contribution to the formation of the paleo-Andes in the late Paleozoic. In: Heredia
³⁹
⁴⁰1134 Carballo, N., Colombo Piñol, F., García Sansegundo, J. (Eds.) Geology of the Andean Cordillera and
⁴¹
⁴²1135 its foreland, Geo-Temas 13, 1903–1906.
⁴³1136
⁴⁴
- ⁴⁵1137 Ramos, V.A., Naipauer, M., 2013. Patagonia: Where does it come from? Journal of Iberian Geology
⁴⁶
⁴⁷1138 (in press).
⁴⁸1139
⁴⁹
- ⁵⁰1140 Ramos, V.A., Vujovich, G., Martino, R., Otamendi, J., 2010. Pampia: a large cratonic block missing in
⁵¹
⁵²1141 the Rodinia supercontinent. Journal of Geodynamics 50, 243–255.
⁵³1142
⁵⁴
- ⁵⁵1143 Rapalini, A., López de Luchi, M., Tohver, E., Cawood, P.A., 2013. The South American ancestry of
⁵⁶
⁵⁷1144 the North Patagonian Massif: geochronological evidence for an autochthonous origin? Terra Nova doi:
⁵⁸1145 10.1111/ter.12043.
⁵⁹
⁶⁰1146
⁶¹
⁶²
⁶³
⁶⁴
⁶⁵

- 1147 Rapela, C.W., Kostadinoff, J., 2005. El basamento de Sierra de la Ventana: historia tectonomagmática.
1
2 1148 In: de Barrio, R.E., Etcheverry, R.O., Caballé, M.F., Llambías, E. (Eds.), Geología y recursos
3 1149 minerales de la Provincia de Buenos Aires. 16° Congreso Geológico Argentino, Relatorio, p. 69–84.
4
5 1150
- 6 1151 Rapela, C.W., Pankhurst, R.J., Casquet, C., Baldo, E., Saavedra, J., Galindo, C., Fanning, C.M., 1998.
7
8 1152 The Pampean orogeny of the southern proto-Andes: Cambrian continental collision in the Sierras de
9
10 1153 Córdoba. In: Pankhurst, R.J., Rapela, C.W. (Eds.), The Proto-Andean Margin of Gondwana.
11
12 1154 Geological Society, Special Publication 142, p. 181–217.
13
14 1155
- 15 1156 Rapela, C.W., Pankhurst, R.J., Fanning, C.M., Grecco, L.E., 2003. Basement evolution of the Sierra
16
17 1157 de la Ventana Fold Belt: new evidence for Cambrian continental rifting along the southern margin of
18 1158 Gondwana. *Journal of the Geological Society* 160, 613–628.
19
20 1159
- 21 1160 Rapela, C.W., Pankhurst, R.J., Casquet, C., Fanning, C.M., Baldo, E.G., González-Casado, J.M.,
22
23 1161 Galindo, C., Dahlquist, J., 2007. The Río de la Plata craton and the assembly of SW Gondwana. *Earth-*
24
25 1162 *Science Reviews* 83, 49–82.
26
27 1163
- 28 1164 Rapela, C.W., Fanning, C.M., Casquet, C., Pankhurst, R.J., Spalletti, L., Poiré, D., Baldo, E.G., 2011.
29
30 1165 The Río de la Plata craton and the adjoining Pan-African/brasiliano terranes: Their origins and
31
32 1166 incorporation into south-west Gondwana. *Gondwana Research* 20, 673–690.
33
34 1167
- 35 1168 Reinoso, M., 1968. Paleocorrientes en la Formación Providencia. Devónico, Sierras Australes de la
36
37 1169 provincia de Buenos Aires. *Revista de la Asociación Geológica Argentina* 23, 287–296.
38
39 1170
- 40 1171 Rocha Campos, A.C., Basei, M.A., Nutman, A.P., Kleiman, L.E., Varela, R., Llambias, E., Canile,
41
42 1172 F.M., da Rosa, O. de C.R., 2011. 30 million years of Permian volcanism recorded in the Choiyoi
43 1173 igneous province (W Argentina) and their source for younger ash fall deposits in the Paraná Basin:
44
45 1174 SHRIMP U–Pb zircon geochronology evidence. *Gondwana Research* 19, 509–523.
46
47 1175
- 48 1176 Rossello, E., Massabie, A.C., López Gamundí, O.R., Cobbold, P.R., Gapais, D., 1997. Late Paleozoic
49
50 1177 transpression in Buenos Aires and Northeast Patagonian ranges, Argentina. *Journal of South American*
51
52 1178 *Earth Sciences* 10, 389–402.
53
54 1179
- 55 1180 Rozendaal, A., Gresse, P.G., Scheepers, R., Le Roux, J.P., 1999. Neoproterozoic to Early Cambrian
56
57 1181 Crustal Evolution of the Pan-African Saldania Belt, South Africa. *Precambrian Research* 97, 303–323.
58
59 1182
60
61
62
63
64
65

- 1183 Sato, A.M., Tickyj, H., Llambías, E.J., Sato, K., 2000. The Las Matras tonalitic-trondhjemitic pluton,
1184 central Argentina: Grenvillian-age constraints, geochemical characteristics, and regional implications.
1185 Journal of South American Earth Sciences 13, 587–610.
1186
- 1187 Schiller, W., 1930. Investigaciones geológicas en las montañas del sudoeste de la Provincia de Buenos
1188 Aires. Anales del Museo de La Plata 4 (2a. Serie), 9–84.
1189
- 1190 Seilacher, A., Cingolani, C.A., Varela, R., 2002. Ichnostratigraphic correlation of Early Paleozoic
1191 sandstones in North Africa and Central Argentina. In: Salem, M., Oun, K. (Eds.), Geology of
1192 Northwest Libya, Earth Sci Soc Lybia, 1, 275–292.
1193
- 1194 Sellés Martínez, J., 1989. The structure of the Sierras Australes (Buenos Aires province, Argentina): an
1195 example of folding in a transpressive environment. Journal of South American Earth Sciences 3, 317–
1196 329.
1197
- 1198 Sellés Martínez, J., 2001. Geología de la Ventania (Provincia de Buenos Aires (Argentina)). Journal of
1199 Iberian Geology 27, 43–69.
1200
- 1201 Söderlund, U., Patchett, P.J., Vervoort, J.D., Isachsen, C.E., 2004. The ^{176}Lu decay constant
1202 determined by Lu–Hf and U–Pb isotope systematics of Precambrian mafic intrusions. Earth Planetary
1203 Science Letters 219, 311–324.
1204
- 1205 Stacey, J.S., Kramers, J.D., 1975. Approximation of terrestrial lead isotope evolution by a two-stage
1206 model. Earth and Planetary Science Letters 26, 207–221.
1207
- 1208 Stump, E., 1995. The Ross Orogeny of the Transantarctic Mountains. Cambridge University Press,
1209 Cambridge, 284 p.
1210
- 1211 Suero, T., 1972. Compilación geológica de las Sierras Australes de la provincia de Buenos Aires.
1212 LEMIT (La Plata), Anales 3, 135–147.
1213
- 1214 Teruggi, M.E., 1964. Paleocorrientes y paleogeografía de las ortocuarcitas de la Serie de La Tinta
1215 (provincia de Buenos Aires). Comisión de Investigaciones Científicas de la provincia de Buenos
1216 Aires, Anales 5, 1–27.
1217
- 1218
1219
1220
1221
1222
1223
1224
1225
1226
1227
1228
1229
1230
1231
1232
1233
1234
1235

- 1218 Teruggi, M.E., Leguizamón, M.A., Ramos, V.A., 1988. Metamorfitas de bajo grado con afinidades
1 1219 oceánicas en el basamento de Tandil: sus implicaciones geotectónicas, provincia de Buenos Aires.
2
3 1220 Revista de la Asociación Geológica Argentina 43, 366–374.
4
5 1221
6 1222 Thirwall, M.F., Walder, A.J., 1995. In situ hafnium isotope ratio analyses of zircon by inductively
7
8 1223 coupled plasma mass spectrometry. *Chemical Geology* 122, 241–247.
9
10 1224
11 1225 Tohver, E., Cawood, P.A., Rossello, E., López de Luchi, M.G., Rapalini, A., Jourdan, F., 2008. New
12
13 1226 SHRIMP U-Pb and ⁴⁰Ar/³⁹Ar constraints on the crustal stabilization of southern South America,
14
15 1227 from the margin of the Rio de Plata (Sierra de Ventana) craton to northern Patagonia. American
16
17 1228 Geophysical Union, Fall Meeting, EOS (Abstract), T23C-2052.
18
19 1229
20 1230 Tohver, E., Cawood, P.A., Rossello, E.A., Jourdan, F., 2012. Closure of the Clymene Ocean and
21
22 1231 formation of West Gondwana in the Cambrian: Evidence from the Sierras Australes of the
23
24 1232 southernmost Rio de la Plata craton, Argentina. *Gondwana Research* 21, 394–405.
25
26 1233
27 1234 Tomezzoli, R.N., 2009. The apparent polar wander path for South America during the
28
29 1235 Permian-Triassic. *Gondwana Research* 15, 209–215.
30
31 1236
32 1237 Tomezzoli, R.N., Cristallini, E.O., 1998. Nuevas evidencias sobre la importancia del fallamiento en la
33
34 1238 estructura de las Sierras Australes de la Provincia de Buenos Aires. *Revista de la Asociación*
35
36 1239 *Geológica Argentina* 53, 117–129.
37
38 1240
39 1241 Tomezzoli, R.N., Cristallini, E.O., 2004. Secciones estructurales de las Sierras Australes de la
40
41 1242 provincia de Buenos Aires: Repetición de la secuencia estratigráfica a partir de fallas inversas? *Revista*
42
43 1243 *de la Asociación Geológica Argentina* 59, 330–340.
44
45 1244
46 1245 Tomezzoli, R.N., Vilas, J.F., 1997. Estudios paleomagnéticos preliminares y de fábrica magnética en
47
48 1246 afloramientos de López Lecube (38° lat S, 62° long. O) y González Chaves (38° lat. S, 60° long. O), en
49
50 1247 las cercanías de las Sierras Australes de la provincia de Buenos Aires, Argentina. *Revista de la*
51
52 1248 *Asociación Geológica Argentina* 52, 419–432.
53
54 1249
55 1250 Tomezzoli, R.N., Vilas, J.F., 1999. Paleomagnetic constraints on the age of deformation of the Sierras
56
57 1251 Australes thrust and fold belt, Argentina. *Geophysical Journal Interior* 138, 857–870.
58
59 1252
60 1253 Turner, B.R., 1999. Tectonostratigraphical development of the Upper Karoo foreland basin: orogenic
61
62 1254 unloading versus thermally-induced Gondwana rifting. *Journal of African Earth Sciences* 28, 215–238.
63
64
65

1255

¹1256 Uriz, N.J., Cingolani, C.A., Chemale Jr, F., Macambira, M.B., Armstrong, R., 2011. Isotopic studies
²
³1257 on detrital zircons of Silurian–Devonian siliciclastic sequences from Argentinean North Patagonia and
⁴
⁵1258 Sierra de la Ventana regions: comparative provenance. *International Journal of Earth Sciences*
⁶
⁷1259 (Geologische Rundschau) 100, 571–589.

⁸1260

⁹
¹⁰1261 Uriz, N.J., Cingolani, C.A., Marques, J., 2012. Procedencia sedimentaria del Paleozoico inferior –
¹¹
¹²1262 medio del Grupo Ventana y de la Formación Sierra Grande. *Nuevas edades U-Pb (LA-ICP.MS) en*
¹³1263 *circones detríticos. 13° Reunión Argentina de Sedimentología (Salta), Actas, 215–216.*

¹⁴1264

¹⁵
¹⁶1265 Van Staden, A., Zimmermann, U., Gutzmer, J., Chemale, F. Jr, Germs, G., 2010. Correlation of
¹⁷
¹⁸1266 Ordovician diamictites from Argentina and South Africa using detrital zircon dating. *Journal of the*
¹⁹
²⁰1267 *Geological Society* 167, 217–220.

²¹1268

²²
²³1269 Varela, R., Cingolani, C.A., 1976. Nuevas edades radimétricas del basamento aflorante en el perfil del
²⁴
²⁵1270 cerro Pan de Azúcar - Cerro del Corral y consideraciones sobre la evolución geocronológica de las
²⁶
²⁷1271 rocas ígneas de las Sierras Australes, Buenos Aires. 6° Congreso Geológico Argentino (Bahía Blanca),
²⁸1272 *Actas 1, 543–556.*

²⁹1273

³⁰
³¹1274 Varela, R., Leone, E.M., Manceda, R., 1987. Estructura tectónica en la zona del cerro del Corral,
³²
³³1275 Sierras Australes de Buenos Aires. *Revista de la Asociación Geológica Argentina* 41, 256–261.

³⁴1276

³⁵
³⁶1277 Veevers, J.J., 2003. Pan-African is Pan-Gondwanaland: oblique convergence drives rotation during
³⁷
³⁸1278 650– 500 Ma assembly. *Geology* 31, 501–504.

³⁹1279

⁴⁰
⁴¹1280 Veevers, J.J., 2004. Gondwanaland from 650– 500 Ma assembly through 320 Ma merger in Pangea to
⁴²
⁴³1281 185– 100 Ma breakup: supercontinental tectonics via stratigraphy and radiometric dating. *Earth-*
⁴⁴
⁴⁵1282 *Science Reviews* 68, 1–132.

⁴⁶1283

⁴⁷
⁴⁸1284 Veevers, J.J., Saeed, A., 2013. Age and composition of Antarctic sub-glacial bedrock reflected by
⁴⁹
⁵⁰1285 detrital zircons, erratics, and recycled microfossils in the Ellsworth Land–Antarctic Peninsula–
⁵¹
⁵²1286 Weddell Sea–Dronning Maud Land sector (240°E–0°–015°E). *Gondwana Research* 23, 296–332.

⁵³1287

⁵⁴
⁵⁵1288 Von Gosen, W., 2003. Thrust tectonics in the North Patagonian Massif (Argentina): implication for a
⁵⁶
⁵⁷1289 Patagonian plate. *Tectonics* 22, 1005. doi:10.1029/ 2001ITC901039.

⁵⁸1290

⁵⁹

60

61

62

63

64

65

1291 Von Gosen, W., Buggisch, W., Dimieri, L.V., 1990. Structural and metamorphic evolution of the
1 1292 Sierras Australes, Buenos Aires province, Argentina. *Geologische Rundschau* 79, 797–821.
2
3 1293
4
5 1294 Von Gosen, W., Buggisch, W., Krumm, S., 1991. Metamorphism and deformation mechanisms in the
6 1295 Sierras Australes fold and thrust belt (Buenos Aires province, Argentina). *Tectonophysics* 185, 335–
7 1296 356.
8
9

10 1297
11 1298 Zavala, C., Azúa, G., Freige, R.H., Ponce, J.J., 2000. Sistemas deltaicos dominados por avenidas
12 1299 fluviales en el Grupo Curamalal (Paleozoico inferior), cuenca paleozoica de Ventania, provincia de
13 1300 Buenos Aires, Argentina. *Revista de la Asociación Geológica Argentina* 55, 165–178.
14
15

16 1301
17
18 1302 Zimmermann, U., Spalletti, L.A., 2009. Provenance of the Lower Paleozoic Balcarce Formation
19 1303 (Tandilia System, Buenos Aires Province, Argentina): implications for paleogeographic
20 1304 reconstructions of SW Gondwana. *Sedimentary Geology* 219, 7–23.
21
22

23 1305
24

25 1306 **Figure captions**

26
27 1307
28
29 1308 **Figure 1:** Location of the Ventania and Tandilia systems in the province of Buenos Aires,
30 1309 localities mentioned in the text, and main basement provinces of central Argentina and
31 1310 Uruguay (based on Ramos, 2009 and Cingolani, 2011).
32
33

34 1311
35
36 1312 **Figure 2:** Main geological features of the Ventania System in the province of Buenos Aires.
37 1313 Numbers indicate the samples with detrital zircon U/Pb Laser ablation analyses (geology after
38 1314 Schiller, 1930; Harrington, 1947; Suero, 1972).
39
40

41 1315
42
43 1316 **Figure 3:** Main basement exposures of the Ventania System with available ages based on
44 1317 Varela et al. (1987), Rapela et al. (2003), Rapela and Kostadinoff (2005), and Tohver et al.
45 1318 (2012).
46
47

48 1319
49
50 1320 **Figure 4:** Stratigraphic column of the Paleozoic sedimentary rocks of the Ventania System
51 1321 (based on Harrington, 1947), with the stratigraphic positions of the analyzed samples.
52 1322 Paleocurrents after Reinoso (1968), Andreis and Cladera (1992), and López Gamundí and
53 1323 Rossello (1998).
54
55

56 1324
57
58
59
60
61
62
63
64
65

1325 **Figure 5:** Structural cross section of the Gondwanides of northern Patagonia restored for the
1326 end of the Paleozoic. The hinterland region developed in present Somún Cura Massif with
1327 exhumed late Paleozoic arc-granitoids is shown as well as the Ventania System with the fold
1328 and thrust belt and associated Claromecó Basin (based on Von Gosen et al., 1991; Tomezzoli
1329 and Cristallini, 1998; Ploskiewicz, 1999; Ramos, 2008; Pángaro and Ramos, 2012). The
1330 location of potential sutures among Patagonia, Tandilia and Cortijo terranes, as well as the
1331 Tandilia magmatic arc further north, are indicated after Teruggi et al. (1988), Max et al.
1332 (1999), Ramos, (2008) and Cingolani (2011).

1333
1334 **Figure 6:** a) Detail of the sample site; b) U-Pb frequency plot ages from zircons of a
1335 paragneiss (sample VE-02) of the metamorphic basement in the eastern slope of Cerro Pan de
1336 Azúcar, western Sierra de Curamalal (see location in Fig. 2).

1337
1338 **Figure 7:** a) Tectonic lense of mylonitic granite within quartzite layers of La Lola Formation;
1339 b) LA-ICP-MS from concordant zircons of this mylonitic granite (sample SLV-VE-04, see
1340 location in Fig. 2 and analytical data in the supplementary material).

1341
1342 **Figure 8:** U/Pb frequency plot ages from detrital zircons of the Curamalal Group: SLV-VE-
1343 03 from a quartzite clast of the basal conglomerate of the La Lola Formation, and SLV-VE-
1344 05, quartzitic sandstones interfingering in the upper part of the conglomerates; SLV-VE-09
1345 from Mascota Formation from Cerro Colorado area; SLV-VE-10 from Mascota Formation
1346 east of Tornquist (location in Fig. 2).

1347
1348 **Figure 9:** U/Pb frequency plot ages from detrital zircons of lower part of the Ventana Group.
1349 Note the up-sequence decrease of the Paleoproterozoic ages (sample location in Fig. 2) and
1350 clear dominance of Late Neoproterozoic to Cambrian zircons.

1351
1352 **Figure 10:** U/Pb frequency plot ages from detrital zircons of upper part of the Ventana Group.
1353 Note that the samples from the Lolén Formation are more than 10 km distant, but have
1354 coherent patterns (see sample location in Fig. 2).

1355
1356 **Figure 11:** U/Pb frequency plot ages from detrital zircons of Balcarce Formation (samples
1357 FBA 264 and PMOG 233) based on Rapela et al. (2007, 2011). Note the important frequency
1358 peaks of Early Ordovician and Early Cambrian ages (location in Fig. 1).

1359
1360
1361
1362
1363
1364
1365

1359

1
2 1360 **Figure 12:** Comparison of the detrital zircons provenance based on between Curamalal Group
3
4 1361 and lower and upper Ventana Group. Note the prominent frequency peak of Paleoproterozoic
5
6 1362 zircons in the Curamalal Group which is poorly developed in the Ventana Group, and the
7
8 1363 Famatinian peak (475 Ma) in upper Ventana Group, which does not occur in the older units.
9
10 1364 (FAM: Famatinian; BRAS: Brasiliano-Pampean; GRENV: Grenvillian, and TRANS:
11
12 1365 Transamazonian).

13
14 1366
15 1367 **Figure 13:** U/Pb frequency plot ages from detrital zircons of the fine sandstones and shales of
16
17 1368 Pillahuincó Group. Note the prominent frequency peaks of 322-304 Ma and the 291-282 Ma
18
19 1369 peaks may be correlated with igneous ages in the northern Somún Cura Massif (Chernicoff et
20
21 1370 al., 2012a, and cites therein).

22
23 1371
24 1372 **Figure 14:** U/Pb frequency plot ages from zircons from the northern Somún Cura Massif of
25
26 1373 the, a) Sedimentary cover of Sierra Grande Formation (Silurian-Devonian), and b) pre-
27
28 1374 Ordovician metasedimentary basement of the El Jagüelito, Mina Gonzalito, and Nahuel Niyeu
29
30 1375 Formations (after Pankhurst et al., 2006; Naipauer et al., 2011 and Uriz et al., 2011).

31
32 1376
33 1377 **Figure 15:** U/Pb frequency plot ages from detrital zircons of the fine sandstone of González
34
35 1378 Chaves locality. Note the prominent frequency peak at 316 Ma (Late Carboniferous).

36
37 1379
38 1380 **Figure 16:** Hf isotopic analyses of selected samples from the Ventania System. See
39
40 1381 supplementary material for sample number and figure 2 for location.

41
42 1382
43
44 1383 **Figure 17:** U/Pb frequency plot ages from zircons from the Sierra de La Ventana region
45
46 1384 obtained in the present study and the main orogenic events ((FAM: Famatinian; BRAS:
47
48 1385 Brasiliano-Pampean; GRENV: Grenvillian, and TRANS: Transamazonian).

49
50 1386
51 1387 **Figure 18:** U-Pb frequency plots of detrital zircons of Mogotes Formation. Note the different
52
53 1388 pattern with the Balcarce Formation of Fig. 11(after Rapela et al., 2007, 2011).

54
55 1389
56
57 1390 **Figure 19:** Paleogeography of the Ventania System through time; a) Cambrian-Ordovician; b)
58
59 1391 Silurian-Devonian; and c) late Paleozoic times. The Pampean Orogen depicted after Ramos
60
61 1392 (1988), Rapela et al. (1998), and Tohver et al. (2012); the Punta Mogotes Belt based on

62
63
64
65

1393 Gaucher et al. (2005); the Gondwanides Orogen based on Ramos (2008) and Pángaro and
1
2 1394 Ramos (2012).

3
4 1395

5 1396 **Figure 20:** Location of the Ventania Fold Belt in the province of Buenos Aires, Argentina and
6
7 1397 its correlation with the Cape Fold Belt of South Africa as part of the Gondwanides. Tectonic
8
9 1398 framework of the pre-break up of Western Gondwana is based on the reconstruction of
10
11 1399 Pángaro and Ramos (2012).

12
13 1400

14
15 1401

16
17

18

19

20

21

22

23

24

25

26

27

28

29

30

31

32

33

34

35

36

37

38

39

40

41

42

43

44

45

46

47

48

49

50

51

52

53

54

55

56

57

58

59

60

61

62

63

64

65

1 **A provenance study of the Paleozoic Ventania System (Argentina): transient complex**
2 **sources from Western and Eastern Gondwana**

3
4
5 4 Victor A. Ramos^a, Farid Chemale^b, Maximiliano Naipauer^a and Pablo J. Pazos^a
6
7 5

8
9 6 ^a Instituto de Estudios Andinos Don Pablo Groeber, Universidad de Buenos Aires and
10 7 CONICET.

11
12 8 ^b Instituto de Geociências, Universidade de Brasília, Brasília-DF, 70904-970, Brazil
13
14 9

15
16 10 **ABSTRACT**

17
18 11 The U-Pb and Lu-Hf isotopic analyses of the different sedimentary sequences of the Ventania
19 12 System, an old Paleozoic orogenic belt exposed in the southern region of the Río de la Plata
20 13 Craton in the province of Buenos Aires, Argentina, provide new evidence for the
21 14 understanding of the tectonic evolution of the western sector of the Gondwanides mountain
22 15 belt. These ranges formed as result of the late Paleozoic collision of the Patagonia terrane
23 16 against the continental margin of Gondwana. The provenance analysis together with the
24 17 sedimentary paleocurrents confirm a dominant source from the Tandilia System, a
25 18 Paleoproterozoic mountain belt formed during the amalgamation of the Río de la Plata Craton
26 19 at about 1,800-2,200 Ma, and incorporated to Western Gondwana during the Brasiliano
27 20 Orogeny at 550-530 Ma. The local dominant source at the base of the early Paleozoic changed
28 21 to more distant supplies toward the top of the sequences, when is recorded an increasing
29 22 participation of detritus from first, Cambrian (560-520 Ma) zircons from the Pampean
30 23 Orogen, and later on Ordovician (480-460 Ma) zircons from the Famatinian Orogen. The
31 24 detrital zircon patterns and the maximum age of the units shed light on some previous
32 25 discrepancies in the early Paleozoic stratigraphy. The Balcarce Formation, an early Paleozoic
33 26 sedimentary cover of the Tandilia metamorphic and igneous basement, shows striking
34 27 differences when compared with the new data from the Ventania System. The two data-sets
35 28 reveal different sources for the two regions. The late Paleozoic foreland basin deposits mark
36 29 an abrupt change of 180° in the paleocurrent directions, in the petrographic composition of the
37 30 sediments, and in the provenance of detrital zircons. These data indicate a southern
38 31 provenance with the first evidence of Carboniferous and Permian magmatic zircons. The
39 32 oldest Archean zircons together with the finding of clasts with archeocyathids support the
40 33 provenance from Patagonia, which was derived from Eastern Gondwana. The U-Pb ages of
41 34 the ash-fall tuffs in the Tunas Formation confirm the Early Permian age of the *Eurydesma*
42
43
44
45
46
47
48
49
50
51
52
53
54
55
56
57
58
59
60
61
62
63
64
65

35 Fauna in the Ventania System. The U-Pb data together with the Lu-Hf isotopic data enhance
36 the comprehension of the tectonic evolution of the Ventania System as part of the larger
37 Gondwanides Belt that amalgamated to Western Gondwana during Late Permian times with
38 some independent pieces derived from Eastern Gondwana.

39
40 **Keywords:** Gondwanides, *Eurydesma* Fauna, Patagonia, collision, Famatinian and Pampean
41 belts, zircon geochronology, tectonics.

42 43 **1. Introduction**

44 The Ventania System is a complex fold and thrust belt developed in the southwestern
45 margin of Gondwana during late Paleozoic times (Keidel, 1916; Harrington, 1942,1947;
46 Suero, 1972; Killmurray, 1975; Ramos 1986; Von Gosen et al., 1990). Since the early work of
47 Du Toit (1927) it is assumed that Ventania was part of a larger system, which encompasses
48 the Cape Fold Belt of South Africa. Du Toit (1937) named this orogen as the Gondwanides
49 following pioneer work of Keidel (1921), and confirmed later by several works (see Veevers
50 2003, 2004; Milani and De Witt, 2008). In recent years many studies have analyzed the
51 evolution of the Ventania System (Fig. 1) and the adjacent Claromecó foreland basin (Varela
52 et al., 1987; Tomezzoli and Vilas, 1999; Tomezzoli and Cristallini, 1998; Dimieri et al., 2005;
53 Cingolani 2005; Ramos and Kostadinoff, 2005). Current studies were able to track the extent
54 of the Ventania Fold Belt in the offshore based on new seismic and geophysical data,
55 depicting the Colorado Syntaxis (Pángaro and Ramos, 2012). This feature is the mirror image
56 of the Cape Syntaxis and has similar characteristics (De Beer, 1995; Johnston, 2000).

57
58
59
60
61
62
63
64
65
66
67
68
69
70
71
72
73
74
75
76
77
78
79
80
81
82
83
84
85
86
87
88
89
90
91
92
93
94
95
96
97
98
99
100
101
102
103
104
105
106
107
108
109
110
111
112
113
114
115
116
117
118
119
120
121
122
123
124
125
126
127
128
129
130
131
132
133
134
135
136
137
138
139
140
141
142
143
144
145
146
147
148
149
150
151
152
153
154
155
156
157
158
159
160
161
162
163
164
165
166
167
168
169
170
171
172
173
174
175
176
177
178
179
180
181
182
183
184
185
186
187
188
189
190
191
192
193
194
195
196
197
198
199
200
201
202
203
204
205
206
207
208
209
210
211
212
213
214
215
216
217
218
219
220
221
222
223
224
225
226
227
228
229
230
231
232
233
234
235
236
237
238
239
240
241
242
243
244
245
246
247
248
249
250
251
252
253
254
255
256
257
258
259
260
261
262
263
264
265
266
267
268
269
270
271
272
273
274
275
276
277
278
279
280
281
282
283
284
285
286
287
288
289
290
291
292
293
294
295
296
297
298
299
300
301
302
303
304
305
306
307
308
309
310
311
312
313
314
315
316
317
318
319
320
321
322
323
324
325
326
327
328
329
330
331
332
333
334
335
336
337
338
339
340
341
342
343
344
345
346
347
348
349
350
351
352
353
354
355
356
357
358
359
360
361
362
363
364
365
366
367
368
369
370
371
372
373
374
375
376
377
378
379
380
381
382
383
384
385
386
387
388
389
390
391
392
393
394
395
396
397
398
399
400
401
402
403
404
405
406
407
408
409
410
411
412
413
414
415
416
417
418
419
420
421
422
423
424
425
426
427
428
429
430
431
432
433
434
435
436
437
438
439
440
441
442
443
444
445
446
447
448
449
450
451
452
453
454
455
456
457
458
459
460
461
462
463
464
465
466
467
468
469
470
471
472
473
474
475
476
477
478
479
480
481
482
483
484
485
486
487
488
489
490
491
492
493
494
495
496
497
498
499
500
501
502
503
504
505
506
507
508
509
510
511
512
513
514
515
516
517
518
519
520
521
522
523
524
525
526
527
528
529
530
531
532
533
534
535
536
537
538
539
540
541
542
543
544
545
546
547
548
549
550
551
552
553
554
555
556
557
558
559
560
561
562
563
564
565
566
567
568
569
570
571
572
573
574
575
576
577
578
579
580
581
582
583
584
585
586
587
588
589
590
591
592
593
594
595
596
597
598
599
600
601
602
603
604
605
606
607
608
609
610
611
612
613
614
615
616
617
618
619
620
621
622
623
624
625
626
627
628
629
630
631
632
633
634
635
636
637
638
639
640
641
642
643
644
645
646
647
648
649
650
651
652
653
654
655
656
657
658
659
660
661
662
663
664
665
666
667
668
669
670
671
672
673
674
675
676
677
678
679
680
681
682
683
684
685
686
687
688
689
690
691
692
693
694
695
696
697
698
699
700
701
702
703
704
705
706
707
708
709
710
711
712
713
714
715
716
717
718
719
720
721
722
723
724
725
726
727
728
729
730
731
732
733
734
735
736
737
738
739
740
741
742
743
744
745
746
747
748
749
750
751
752
753
754
755
756
757
758
759
760
761
762
763
764
765
766
767
768
769
770
771
772
773
774
775
776
777
778
779
780
781
782
783
784
785
786
787
788
789
790
791
792
793
794
795
796
797
798
799
800
801
802
803
804
805
806
807
808
809
810
811
812
813
814
815
816
817
818
819
820
821
822
823
824
825
826
827
828
829
830
831
832
833
834
835
836
837
838
839
840
841
842
843
844
845
846
847
848
849
850
851
852
853
854
855
856
857
858
859
860
861
862
863
864
865
866
867
868
869
870
871
872
873
874
875
876
877
878
879
880
881
882
883
884
885
886
887
888
889
890
891
892
893
894
895
896
897
898
899
900
901
902
903
904
905
906
907
908
909
910
911
912
913
914
915
916
917
918
919
920
921
922
923
924
925
926
927
928
929
930
931
932
933
934
935
936
937
938
939
940
941
942
943
944
945
946
947
948
949
950
951
952
953
954
955
956
957
958
959
960
961
962
963
964
965
966
967
968
969
970
971
972
973
974
975
976
977
978
979
980
981
982
983
984
985
986
987
988
989
990
991
992
993
994
995
996
997
998
999
1000

FIGURE 1 NEAR HERE

There are two main problems in the tectonic interpretation of Ventania. The first problem is the stratigraphy of the early Paleozoic units as for some authors the Curamalal and Ventana Groups are the same unit tectonically repeated (Killmurray, 1975; Tomezzoli and Cristallini, 2004), although most of the stratigraphers agree about the original sequences proposed by Harrington (1947) where Ventana is younger than Curamalal. The second problem, and perhaps the most important, is if the Ventania fold and thrust belt was originated by collision with an allochthonous Patagonia terrane in the late Paleozoic (Ramos, 1984, 2008; Kay et al., 1989; Sellés Martínez, 1989; Von Gosen, 2003; Chernicoff and Zappettini, 2004; among others), or was an intracratonic basin inverted by contraction and strike-slip tectonics related to oblique subduction further to the south along the present continental margin (Cobbold et al., 1991; López Gamundí et al., 1994, 1995; Rossello et al., 1997;

69 Dalziel et al., 2000; Gregori et al., 2008, among others). Some authors refute the allochthony
70 of Patagonia based on paleogeographic and paleoclimatic reconstructions (López Gamundí
71 and Rossello, 1998). The provenance analyses here presented shed light to both problems and
72 provide a robust answer to previous uncertainties.

73

74 **1.1 Location**

75 The Ventania System is a 30 km wide mountain chain located in the southern part of
76 the province of Buenos Aires in central eastern Argentina. It is surrounded by plains locally
77 known as pampas, and has a length of 180 km with a W-NW trend (Fig. 2).

78 **FIGURE 2 NEAR HERE**

79 These mountains have a maximum height in the Cerro Tres Picos of 1,250 meters.
80 There are several ranges as the Sierras de Curamalal, Ventana and Pillahuincó (Fig. 2), which
81 expose the early and late Paleozoic sequences, tightly folded, with a constant northeast
82 vergence (Harrington, 1947; Suero, 1972).

83

84 **2. Stratigraphy**

85 **2.1 Metamorphic and igneous basement**

86 There are very scarce exposures of the basement in the southwestern slope of the
87 Sierra de Curamalal. Most of the authors recognized the igneous origin of these rocks, which
88 are highly deformed, with typical cataclastic and mylonitic textures (Kilmurray, 1968;
89 Gregori et al., 2005). There are also rhyolites exposed in different sectors further north (Figs.
90 2 and 3) and some isolated outcrops of granites exposed in Cerro Colorado and López Lecube
91 quarries further to the west.

92 **FIGURE 3 NEAR HERE**

93 The available geochronological data indicate an age of 607 ± 5.2 Ma for the deformed
94 granites of Cerro Corral (U-Pb SHRIMP ages in zircons, Rapela et al., 2003), that confirm old
95 Rb-Sr ages of ~ 603 -612 Ma of Varela and Cingolani (1976). New data of the Pan de Azúcar
96 Granite yielded an age of 581 ± 8 Ma (U-Pb SHRIMP ages in zircons, Tohver et al., 2012).
97 The posttectonic granites in Cerro Colorado (531.1 ± 4.1 Ma and 523.8 ± 4 Ma), San Mario
98 (524.3 ± 5.3 Ma), and Los Chilenos (533 ± 12 Ma), as well as the La Ermita Rhyolite ($509 \pm$
99 5.3 Ma and 505 ± 18 Ma), were assigned to the Cambrian (Rapela et al., 2003; Tohver et al.,
100 2012). The Agua Blanca Granite has an inheritance age of 2182 ± 18 Ma that indicates a
101 Paleoproterozoic basement in the area as part of the Río de la Plata Craton (Tohver et al.,
102 2012). The westernmost outcrops of López Lecube quarry yielded an age of 258.5 ± 1.9 Ma

103 by U-Pb SHRIMP in zircons that corresponds to posttectonic granites of the Gondwanide
104 Orogeny and it is not part of the Ventania basement (Rapela and Kostadinoff, 2005).

105 The igneous rocks have been divided in two suites based on their composition and
106 tectonic setting: a calcalkaline orogenic and collisional Neoproterozoic suite and a
107 postorogenic extensional Cambrian suite (Gregori et al., 2005). The last episode was
108 associated with a Cambrian rift by Rapela et al. (2003).

110 **2.2 The Paleozoic sedimentary successions**

111 The early Paleozoic sedimentary succession includes two sequences, the Curamalal
112 and Ventania Groups (Fig. 4) deposited during Ordovician and Devonian times (Harrington,
113 1947; Sellés Martínez, 2001). The late Paleozoic is represented by the Pillahuincó Group (Fig.
114 4), which is mainly Cisuralian (Early Permian). The whole Paleozoic succession is around
115 4,500 m thick, with the two lowermost sequences measuring 2,400 m thick. The upper part of
116 the succession documents a higher subsidence rate compared with the underlying part, but
117 also a contrasting paleocurrent pattern, which varies from SW to SE, with strong NE
118 prograding deltaic lobes in the uppermost part of the sedimentary section. The succession
119 contains mainly sandstones, claystones and conglomerates in the lower part. However, glacial
120 diamictites and glaciomarine deposits constitute a special type of coarse-grained deposits that
121 document the late Paleozoic glaciation (Andreis et al., 1989).

122 The Curamalal Group, which represents the beginning of the sedimentary record in the
123 basin, contains conglomerates with coarse-grained clasts in clast-supported to patchy sandy
124 matrix-supported types, with beds up to 1.5 m in thickness and erosive to sharp bases in the
125 lower part of La Lola Formation. Internally they contain well rounded quartzite clasts
126 showing normal or rarely reverse gradation. The outcrops of the source area remain unknown
127 but the almost monomict composition suggests a quartzite unit situated at a certain distance
128 that allowed the well roundness of clasts by hyperconcentrated flows or diluted debris flows.
129 Sandy deposits include different types of cross-bedding; some of them were interpreted as
130 hummocky cross stratification by Zavala et al. (2000). However, they exhibit a unidirectional
131 pattern and in all cases resemble more bidimensional subaqueous dunes. Giant cross-beds up
132 to 4 m in amplitude are common in medium grained sandstones containing clay chips, and
133 mud drapes. Thin beds show the same sedimentary structures and in cases depict clear
134 bidirectional paleocurrents that document tidal control during the sedimentation. In the
135 Ventana Group, the lower unit (Bravard Formation) has some fine conglomerates with a
136 quartzitic composition of the clasts. The overlying Napostá Formation is well known for its

137 ichnological content that includes *Skolithos*, *Arenicolites* and *Daedalus*. Abundant tidal
138 features have been observed, including herringbone crossbeds and mud drapes. The Lolén
139 Formation is the uppermost unit of the Ventana Group and exhibits more variability in clast
140 composition and contains brachiopods and lycophytid plant remains as *Haplostigma* that have
141 been used to date the top part in the Middle Devonian (Cingolani et al., 2002).

142 A paraconformity separates the Ventana from the overlying Pillahuincó Group,
143 deposited between the latest Carboniferous and the Cisuralian (Early Permian) indicating a
144 prolonged hiatus spanning the Upper Devonian to the middle Pennsylvanian. This group is
145 crucial to understand the evolution of the Ventana System because a thick succession was
146 deposited in a relatively short time. This fact documents a high subsidence rate related to a
147 foreland basin which contrasts with the stable depositional settings for the underlying groups
148 (Fig. 4).

FIGURE 4 NEAR HERE

149 The Sauce Grande Formation rests unconformably over the Ventana Group and is a
150 glaciomarine succession that documents the late Paleozoic glaciation in the Atlantic basins of
151 Argentina. The Sauce Grande Formation represents Late Carboniferous-earliest Permian
152 (Cisuralian) glacial deposits 400 m thick that are also recognized in the Claromecó Basin,
153 which correlates with the Dwyka Formation in the Karoo Basin. This correlation of glacial
154 deposits is known since the pioneer studies of Keidel (1916) and Du Toit (1927). The
155 Malvinas /Falkland Islands also record equivalent glacial deposits in the Lafonia Formation
156 (Frakes and Crowell, 1969; Bellosi and Jalfín, 1984, 1989). The pre-breakup position of the
157 Malvinas (Falkland) Islands based on the early reconstruction of Martin et al. (1981) is south
158 of the Karoo Basin and off the coast of South Africa. Recent studies of the Sauce Grande
159 tillites have found reworked limestone clasts with archeocyathids that indicate a Patagonian
160 derivation from an Antarctic source (González et al., 2011, 2013). Some paleomagnetic
161 studies support a position further to the east, but need a 180° rotation to match the data
162 (Mitchell et al., 1986). Based on these data, López Gamundí and Rossello (1998) conclude
163 that the paleoice flow directions of the Dwyka and the Lafonia glacial sequences were similar,
164 but different from the south-north direction of the Sauce Grande tillites.

165 The Piedra Azul Formation represents early postglacial transgressive deposits, which
166 are overlain by the marine Bonete Formation. These deposits represent the maximum flooding
167 of the basin in the Early Permian and bear the typical Gondwana fauna of *Eurydesma*
168 (Harrington, 1955). This thick-shelled bivalve *Eurydesma* was a cold-resistant and immobile,
169 epifaunal suspension feeder that dominated marine environment of Gondwana in the Early
170

171 Permian (Jones et al., 2006). Above these levels, intertidal plains deposits bear an abundant
172 *Glossopteris* flora, a widespread typical Gondwana flora also known in the Early Permian of
173 Africa, India, Antarctica and Australia (Benedetto, 2010). The upper unit of the group is the
174 Tunas Formation, represented by prodeltaic to subaerial delta plain deposits with
175 paleocurrents that indicate a source area situated to the south-southwest. Very well preserved
176 ichnofossils as *Cochlichnus* and *Gordia* have been observed in the Las Mostazas quarry and
177 cross-bedding exposures that confirm the paleocurrent pattern suggested by Andreis and
178 Cladera (1992) for the unit.

179 Recent studies on the microflora of several wells of the offshore Claromecó Basin
180 have identified on palynological bases almost the entire Permian sequence, including for the
181 first time Lopingian assemblages (Balarino, 2012).

182

183 3. Structure

184 The structure of the Ventania fold and thrust belt was a matter of discussion since the
185 early work of Harrington (1947). Based on the extraordinary ductile folding of the early
186 Paleozoic quartzites described by Keidel (1916) and Du Toit (1927), most of the authors
187 interpreted the structure as a dominant fold-type (Harrington, 1970). Detailed surveys done by
188 Varela et al. (1987), Von Gosen et al. (1990, 1991) and Tomezzoli and Cristallini (1998)
189 recognized the main thrusts and confirmed the old thrust hypothesis of Schiller (1930).
190 Seismic studies performed in the offshore depict those thrusts and their relationship with
191 lower to middle crustal deformed rocks exposed further south in the Somún Curá Massif in
192 the hinterland region (Pángaro and Ramos, 2012). These authors have shown that the
193 Ventania foreland fold and thrust belt is separated from the hinterland by an area of minimum
194 deformation interpreted as a late Paleozoic piggy-back basin. This basin is now beneath the
195 Colorado Basin, a Jurassic to Early Cretaceous aulacogenic basin developed above the suture
196 between Patagonia and Western Gondwana. This suture previously proposed by different
197 authors in land, has been depicted in the offshore by a magnetic anomaly interpreted as
198 evidence of mafic and ultramafic rocks by Max et al. (1999) and Ghidella et al. (1995).

FIGURE 5 NEAR HERE

200 The age of deformation of the Ventania fold and thrust belt is constrained in the Early
201 Permian based on the growth strata of Tunas Formation described by López Gamundí et al.
202 (1995), the paleomagnetic evidence of syndeformational magnetization of Tomezzoli and
203 Vilas (1999), and the illite recrystallization age of Buggish (1987).

204

205 4. Material and methods

206 A systematic field reconnaissance was made of the different Paleozoic units and the
207 metamorphic basement, analyzing their main sedimentological and structural characteristics.
208 A large volume of 24 samples from Curamalal, Ventana and Pillahuincó Groups with detailed
209 sampling in the uppermost tuff layers were collected. The location of the samples is indicated
210 in Figs. 2 and 4 and the sample list and the U-Pb and Lu-Hf analytical data are presented in
211 the electronic supplementary material. Petrographic and geochemistry information of
212 sedimentary and tuff samples can be found in Alessandretti et al. (2013).

213 Samples were crushed and milled using jaw crusher. Then, the zircons were separated
214 by conventional procedures using heavy liquids and an isodynamic magnetic separator after
215 concentration by hand panning. The most clear and inclusion-free zircons from the least
216 magnetic fractions were handpicked. All zircons were mounted in epoxy in 2.5-cm-diameter
217 circular grain mounts and polished until the zircons were just revealed. Images of zircons
218 were obtained using the optical microscope (Leica MZ 125) and back-scatter electron
219 microscope (Jeol JSM 5800) at the Eletron Microscope Center of the Federal University of
220 R rio Grande do Sul, but are only illustrated when necessary to support the interpretation.
221 Zircon grains were dated with laser ablation microprobe (New Wave UP213) coupled to a
222 MC-ICP-MS (Neptune) at the Geochronology Laboratory of the University of Brasilia.

223 U-Pb isotope data were acquired using static mode with spot size of 30 um in
224 diameter. Laser-induced elemental fractional and instrumental mass discrimination were
225 corrected by the reference zircon (GJ-1) (Jackson et al., 2004), following the measurement of
226 two GJ-1 analyses to every four sample zircon spots. The collector configuration used for
227 simultaneous measurements of Th, U, Pb and Hg isotopes was ^{238}U , ^{232}Th and ^{208}Pb in
228 faraday cups (H4, H2 and L4, respectively) and ^{207}Pb , ^{206}Pb , $^{204}\text{Pb}+\text{Hg}$ and ^{202}Hg in Multiplier
229 Ion Counting (MIC) channels attached to the L4 (MICs IC5, IC4, IC3 and IC2, respectively).
230 The external error is calculated after propagation error of the GJ-1 mean and the individual
231 sample zircon (or spot). A detailed description of analytical conditions and data reduction can
232 be found in Chemale et al. (2012). Isoplot 3 software (Ludwig, 2003) was used to generate the
233 concordia diagrams and histograms. For the concordia age calculations and frequency
234 histograms, only the analyses with $100 \pm 10\%$ of concordance were used. All of the calculated
235 ages are reported at the 95% confidence level.

236 Lu, Yb and Hf isotopes in single zircon crystals were acquired using static mode with
237 spot size of 50 um in diameter. The laser spot was driven to the same site or zircon phase
238 dated by the U-Pb method. To minimize aerosol deposition around the ablation pit and to

239 improve transport efficiency, He was flushed along with Ar into the ablation cell. The
240 Faraday collectors were arranged the following way: ^{171}Yb (low 4), ^{173}Yb (low 3), ^{174}Hf (low
241 2), ^{175}Lu (low 1), $^{176}(\text{Hf}+\text{Yb}+\text{Lu})$ (Center), ^{177}Hf (high 1), ^{178}Hf (high 2) and ^{179}Hf (high 3).
242 Detail of operation analytical conditions can be found in Chemale et al. (2011a). To correct
243 for isobaric interferences of Lu and Yb isotopes on mass 176, the isotopes ^{171}Yb , ^{173}Yb and
244 ^{175}Lu were simultaneously monitored during the analyses. The ^{176}Lu and ^{176}Yb concentrations
245 were calculated using a $^{176}\text{Lu}/^{175}\text{Lu}$ ratio of 0.026549 and a $^{173}\text{Yb}/^{171}\text{Yb}$ ratio of 1.123456
246 (Chu et al., 2002; Thirwall and Walder, 1995). Correction of Hf isotopic ratios for
247 instrumental mass bias was based on an exponential law and used the reference $^{179}\text{Hf}/^{177}\text{Hf}$
248 value of 0.7325 (Patchett et al., 1981). Each analytical session included determinations of the
249 βHf and βYb factors for each individual spot. The mass bias behavior of Lu was assumed to
250 follow that of Yb.

251 Lu-Hf model ages (TDM) of zircon grains were calculated based on a depleted mantle
252 source with $^{176}\text{Hf}/^{177}\text{Hf} = 0.28325$ and $^{176}\text{Lu}/^{177}\text{Hf} = 0.0388$ (Andersen et al., 2009). We also
253 calculated model ages of individual zircons for felsic and mafic sources assuming the
254 following parental magma compositions: mafic, $\text{Lu}/\text{Hf} = 0.022$; felsic, $\text{Lu}/\text{Hf} = 0.010$
255 (Pietranik et al., 2008). The values of $\varepsilon\text{Hf}(t)$ were calculated assuming the CHUR $^{176}\text{Hf}/^{177}\text{Hf}$
256 ratio of 0.282785 (Bouvier et al., 2008) and the decay constant of $\lambda^{176}\text{Lu} = 1.867 \times 10^{-11}/\text{a}$
257 (Söderlund et al., 2004).

259 5. Results

260 5.1 Pan de Azúcar mylonitic belt

261 This belt of highly deformed metamorphic rock was identified as the Pan de Azúcar
262 Formation by Cuerda et al. (1975) in the eastern slope of the Cerro Pan de Azúcar beneath the
263 contact with the La Lola Formation. Previous authors interpreted rocks similar to sample
264 SLV-VE 02 (Fig. 6a), as derived from igneous protolith, whereas others as Von Gosen et al.
265 (1990) described paragneisses from these exposures. We interpreted this sample based on the
266 internal textures seen in the back-scattering image and the Th/U ratio in each dated zircon
267 (Fig. 6) as gneiss of igneous origin; apparently deformational and metamorphic process has
268 not affected the detrital zircons. One of the main frequency peaks (Fig. 6b) coincides with the
269 ages of the Cambrian suite proposed by Gregori et al. (2005), although the major frequency
270 peak clearly indicates a Paleoproterozoic component in this rock (Fig. 6 a-b), similar to the
271 age interpreted by Tohver et al. (2012) as a basement inheritance in the granites of Agua
272 Blanca. These ages are between the main magmatic activity (2250–2120 Ma) and the

273 collisional overprint (2100–2080 Ma) recorded in the basement of Tandilia by Cingolani
274 (2011). There are also some few older and younger zircons.

275 **FIGURE 6 NEAR HERE**

276 It is possible that the orthogneiss affected by a post-540 Ma contractional deformation
277 may correlate with the main orogeny of the Saldania Belt recognized by Chemale et al.
278 (2011b) in southernmost Africa. In a Gondwana plate tectonic context, a subduction zone has
279 been proposed at the southern margin of the Kalahari plate, close to the Precambrian-
280 Cambrian boundary, as suggested by Rozendaal et al. (1999), and its extension in the Sierra
281 de la Ventana Orogen (Chemale et al., 2011b). Following Gregori et al. (2005) deformation in
282 Sierra de la Ventana should be older than 533 Ma, which is the age of the posttectonic
283 granites. The age pattern of this orthogneiss shows different inherited zircons.

284 However, another possible alternative would be to consider that sample a highly
285 deformed quartzite of La Lola Formation, due to the similar pattern of zircon ages in
286 comparison with other samples of this unit (see SLV-VE 05 in Fig. 8). This interpretation
287 would indicate that the main deformation of this sample could be Gondwanian in age, instead
288 of Brasiliano.

289 **5.2 Curamalal Group**

291 The base of this group is represented by La Lola Formation, which is nicely exposed
292 in the eastern slope of Cerro Pan de Azúcar (Andreis and López Gamundí, 1989). There is a
293 30 m thick orthoconglomerate dominantly formed by clasts of quartzite (SLV-VE-03). These
294 conglomerates are covered by quartzitic sandstones (SLV-VE-05). It is interesting to remark
295 that tectonically interposed with these quartzites, east of the Abra Mayer, there are some
296 lenses of mylonitic granite. One of these lenses with calcalkaline composition has a unique
297 frequency peak at 541.0 ± 8.4 Ma within the range of basement granites (Figs. 7 a,b).

298 **FIGURE 7 NEAR HERE**

299 The sedimentary facies and provenance of these conglomerates have been studied by
300 Zavala et al. (2000), who recognized a proximal shelfal environment in a flood- dominated
301 fan delta system developed from the Tandilia area. However, the good mineralogical maturity
302 almost dominated by quartzite clasts up to 25 cm in size and good roundness suggest that the
303 source area was closer, indicating that the present day quartzite outcrops of Tandilia extended
304 well into the south. The pattern of detrital zircons of both samples (see samples SLV-03 and
305 SLV-05 in Fig. 8) confirms the proposal of Zavala et al. (2000), and shows that the main peak
306 around 2050-2170 Ma corresponds with the maximum magmatic activity of the Tandilia arc

307 according with Cingolani (2011). The lower levels of La Lola Formation have minor
1 308 Cambrian peaks at 545 and 520 Ma, which indicate exhumation of the post-tectonic rocks in
2
3 309 the surrounding area.

4
5 310 The sample SLV-VE-09 is from the lower part of Mascota Formation from Sierra de
6
7 311 Chasicó, which is unconformably overlying the Cerro Colorado Granite (Harrington,
8
9 312 1968). The maximum age of sedimentation is 534 Ma as indicated by the highest frequency
10
11 313 peak (Fig. 8). This quartzite has been interpreted as being older than the Los Chilenos Granite
12
13 314 (533 Ma, Thover et al, 2012), but the present data may favor that the Mascota Formation is
14
15 315 younger than the granite based on field observations that coincide with criteria used in the
16
17 316 Harrington (1947) map. The sample SLV-VE-10 was collected east of Tornquist (see Fig. 2)
18
19 317 from the Mascota Formation, and presents similar age distribution pattern as sample SLV-
20
21 318 VE-09. In these samples the Paleoproterozoic sources start decreasing and some minor
22
23 319 Mesoproterozoic peaks are visible.

24 320 The analysis of the older units of the Curamalal Group shows an interesting trend in
25
26 321 their sources (Fig. 8) with a continuous decrease in the Paleoproterozoic provenance from the
27
28 322 La Lola Formation at the base of the Curamalal Group upwards, parallels the increase of the
29
30 323 Cambrian zircons towards the top of the Mascota Formation. This increase of Cambrian peaks
31
32 324 of 545 and 534 Ma may indicate a potential derivation from Eastern Sierras Pampeanas (see
33
34 325 Fig. 1) which has been exhumed at that time. The input of Grenville-age zircons around 1200
35
36 326 Ma in the Mascota Formation is somewhat older to be derived from the Namaqua belt of
37
38 327 western Kalahari craton, but similar ages recorded in the detrital zircons of the Punta Mogotes
39
40 328 basement from a borehole core, were interpreted as derived from the western Kaapval Craton
41
42 329 by Rapela et al. (2011). Similar age zircons were also recognized in the Cerro Largo
43
44 330 Formation from Tandilia by Gaucher et al. (2008). However, the most potential Grenville-age
45
46 331 source based on the rank of ages observed could be the Eastern Sierras Pampeanas where ages
47
48 332 from 1000 to 1200 Ma are common (Escayola et al., 2007).

49 333 FIGURE 8 NEAR HERE

50 334 **5.3 Ventana Group**

51 335 The different units of the Ventana Group are conformably deposited on the Curamalal
52
53 336 Group. The provenance analysis based on the detrital zircons shows as the most important
54
55 337 frequency peak Brasiliano ages around (564-540 Ma) (Fig. 9). The Paleoproterozoic ages of
56
57 338 Tandilia are less significant and tend to disappear. Some minor evidence of Ordovician
58
59 339 zircons (482 Ma) is seen in the Napostá Formation, as well as in the Bravard Formation,
60
61 340 which will be dominant in the upper part of the sequence. Uriz et al. (2012) analyzed a sample
62
63
64
65

341 from the Napostá Formation and detected an important frequency peak of 473 Ma, partially
342 equivalent to the Ordovician peak found by us.

343 FIGURE 9 NEAR HERE

344 The zircons of Providencia Formation follow the same trend of the lower section of
345 the Ventana Group (compare with Fig. 10), but an important change is recorded in the Lolén
346 Formation, already recognized by Uriz et al. (2011). There, an important peak of Early
347 Ordovician zircons is seen for the first time (490 Ma), as well as increasingly old Brasiliano
348 ages (641-612 Ma). The first occurrence of an Ordovician frequency peak in the Lolén
349 Formation is very similar to the one recognized by Rapela et al. (2007) further to the
350 northeast, in somewhat equivalent nearshore quartzitic sandstones of the Balcarce Formation.
351 This unit is exposed nearby the town of Balcarce (see location in Fig.1), and is
352 unconformably deposited on the metamorphic basement of the Tandilia System and pinch out
353 over the glacial diamictites of the Volcán Formation (Pazos et al., 2008).

354 There are not precise biostratigraphic constraints for its age, but it was assumed to be
355 broadly between Ordovician and Early Silurian based on its trace fossils (Borrello, 1966).
356 According to Rapela et al. (2007) who reported detrital zircon ages as young as 475–480 Ma,
357 the Balcarce Formation is not older than Early Ordovician, suggesting a Late Ordovician to
358 Early Silurian sedimentation age. Moreover, the trace fossils described by Seilacher et al.
359 (2002) from several localities, differ significantly from the familiar Arenigian suite. Rather,
360 they resemble the Lower Silurian ichnofaunas of Libya, Chad and Benin, with trilobite
361 tunnels (*Cruziana ancora*), palmate *Arthropycus alleghaniensis* and *Gyrochorte zigzag* as
362 shared elements (Seilacher et al., 2002), but also *Diplocraterion* conforming monospecific
363 suites has been observed. These authors therefore assigned an Early Silurian age to the
364 Balcarce Formation and they mentioned that the ichnofauna possibly signals an even further
365 southward extension of the Malvinocaffric Province. It is interesting to remark that the matrix
366 of the Cerro Volcán diamictites, a four meters thick level underlying typical quartzites of the
367 Balcarce Formation, has detrital zircons 485-490 Ma old and a maximum peak of 530 Ma
368 (Zimmermann and Spalletti, 2009; Van Staden et al., 2010). These data reinforce the
369 assignation to the Silurian of this unit since these glacial deposits could be interpreted as
370 representing the Hirnantian glaciation of the end of the Ordovician.

371 FIGURE 10 NEAR HERE

372 The siliciclastic deposits of the Balcarce Formation were developed in a nearshore and
373 inner shelf environment on a tide dominated platform, affected by storm events in a marine
374 system that was open to the south based on the pattern of progradational clinofolds (Poiré et

375 al., 2003). Paleocurrents indicate a north dominant sediment supply for the western and
1 376 central areas of the Balcarce Formation, while in the eastern part of the basin the main
2 377 transport directions are east-west oriented (Teruggi, 1964).
3
4

5 378 The Lolén Formation is the only unit bearing marine invertebrate fossils in the lower
6
7 379 Paleozoic sequences of the Ventania System and the occurrence of brachiopods is known
8
9 380 since the early work of Harrington (1947). Benedetto (2010) analyzed these brachiopods and
10
11 381 assigned them to *Cryptonella*, an Early Devonian genus. Based on the age of these
12
13 382 brachiopods, Newton and Cingolani (1990) correlated the Lolén Formation with the
14
15 383 Bokkeveld Group of the Cape Fold Belt, confirming the correlation of Du Toit (1937).
16

17 384 Therefore, a partial correlation between Lolén and Balcarce Formations is proposed
18 385 based on the detrital zircon pattern (Fig. 11), not only the Early Ordovician sources, but also
19
20 386 the range of Brasiliano ages (640-610 Ma), which are older than previous ages recorded in
21
22 387 the early Paleozoic of Ventania. The Ordovician provenance of both units should come from
23
24 388 the northwest, derived from the Western Sierras Pampeanas Orogen, the only sector that
25
26 389 records plutonic and volcanic rocks of Famatinian age at these latitudes (Ramos et al., 2010).
27

28
29
30
31
32
33
34
35
36
37
38
39
40
41
42
43
44
45
46
47
48
49
50
51
52
53
54
55
56
57
58
59
60
61
62
63
64
65

FIGURE 11 NEAR HERE

5.4 Comparison between the Curamalal and the Ventana Groups

391 Kilmurray (1975) proposed that both groups were result of a tectonic repetition based
392
393 on an apparent similarity between the quartzitic sandstones. Tomezzoli and Cristallini (2004)
394 formalized Kilmurray' hypothesis in their study of the structure of Sierras de la Ventana and
395 Curamalal through a viable structural section of these ranges, which shows both groups as a
396 single sequence tectonically repeated. However, our present results indicate a striking
397 difference between the detrital zircon patterns of both groups. When the pattern of La Lola
398 Formation (Fig. 8) is compared with the lower part of the Ventana Group, in particular the
399 Bravard and Napostá Formations (Fig. 9), it is clear the absence of Paleoproterozoic
400 population in these units (Fig. 12).
401

FIGURE 12 NEAR HERE

402 The Curamalal Group begins with a high frequency peak of Paleoproterozoic ages
403 with a minor peak in the Brasiliano ages, showing exhumation of the Tandilia rocks at that
404 time. An irregular exposed topography extended to the south of the present ranges that
405 explains the zircon detrital pattern and facies of the conglomerates of La Lola Formation. The
406 absence of carbonate clasts contrasts with the abundance of carbonates in the Neoproterozoic
407 sedimentary cover of Tandilia. This could be explained by a combination of climate and
408 transport that favored resistant lithologies over carbonates.

409 The maximum frequency in the base of Ventana Group shows exhumation of the
410 Brasiliano rocks and almost no existence of Paleoproterozoic ages, contrasting with the
411 Curamalal Group pattern. These different patterns also characterize the upper part of the
412 Curamalal and Ventana Groups (see Figs. 8 and 10). The major difference is the first
413 occurrence of Ordovician zircons which is exclusive of the Ventana Group and Balcarce
414 Formation (Fig. 12). The Cerro Largo Formation in the Tandilia System has been considered
415 correlatable with the Balcarce Formation, but Pazos and Rapalini (2011) kept the unit in the
416 Precambrian as traditionally suggested in agreement with the detrital pattern of this unit.

417 These evidences permit to discard the correlation of both groups and reevaluate the
418 early proposed stratigraphy of Harrington (1947) which, at the present level of knowledge, is
419 the one that best explains the data.

421 **5.5 Pillahuincó Group**

422 The late Paleozoic deposits of this group indicate the inception of a foreland basin
423 stage in the evolution of the Ventania System (Ramos, 1984; López Gamundí and Rossello,
424 1992, among others). The unconformity that separates the Ventana and Pillahuincó Group,
425 although quite elusive in the structural evidence (López Gamundí and Rossello, 1993),
426 coincides with an important change in the petrography of the sandstones (Andreis and
427 Cladera, 1992). Compositionally, the initial passive margin phase of the continental platform
428 was characterized by quartz-rich, craton-derived detritus, but was followed by a foreland
429 phase that shows a paleocurrent reversal and dominance of arc/foldbelt-derived material
430 (López Gamundí and Rossello, 1998).

431 The recent finding of subrounded clasts with archeocyathids in the glaciomarine Sauce
432 Grande Formation in Ventania derived from Antarctica (González et al., 2013) as well as in
433 the Lafonia (Fitzroy) tillites in the Malvinas (Falkland) Islands, and in the Dwyka tillites
434 (South Africa) support the correlation of these glacial deposits (Veevers and Saeed, 2013).

435 The analysis of the detrital zircon provenance of the late Paleozoic deposits (Fig. 13)
436 shows several differences regarding the early Paleozoic sequences. The first important
437 difference is that in the Sauce Grande Formation there are Archean zircons with conspicuous
438 ages of 2729, 2990 and 3200 Ma, not seen in the lower Paleozoic sequence of Ventania. As
439 the Tandil area shows strong evidence supporting the derivation from a Neoproterozoic crust
440 (less than 2.65 Ga) as inferred by Cingolani (2011) based on the positive ϵ_{Hf} data, those
441 zircons together with the reversal of the paleocurrents indicate a different old cratonic source
442 south of the study area. The second striking difference is the frequency peaks of 319-322 Ma

443 in the Piedra Azul, Bonete, and Tunas formations that are characteristic from northern
1 444 Patagonia, as well as the Silurian 432-417 Ma peaks, similar to the age recorded in Los
2 445 Pájaros Island in northeastern Patagonia granites (Nuñez et al., 1975). The Piedra Azul
3 446 Formation represents early postglacial transgressive deposits, which are overlain by the
4 447 marine deposits of the Bonete Formation bearing the typical *Eurydesma* Gondwana fauna
5 448 (Harrington, 1955), which represent the maximum flooding of the basins in the Early
6 449 Permian. Above this fauna, some intertidal plain deposits bear an abundant *Glossopteris* flora,
7 450 a typical Gondwana flora also known in the Early Permian of Africa, India, Antarctica and
8 451 Australia (Benedetto, 2010).

16 452 FIGURE 13 NEAR HERE

18 453 The other frequency peaks (Fig. 13) are common ages in the crystalline basement of
19 454 northern Somún Cura Massif. Zircons ages of Grenvillian (1100-1000 Ma), Brasiliano (584-
20 455 532 Ma), and Ordovician (491-450) have been widely reported by Pankhurst et al. (2001,
21 456 2006); Ramos (2008), and Naipauer et al. (2010). This spectrum of frequency peaks is
22 457 duplicated by the detrital zircons of the Sierra Grande Formation (Fig. 14), a Siluro-Devonian
23 458 sedimentary cover unconformably deposited over the crystalline basement (Uriz et al., 2011).

29 459 FIGURE 14 NEAR HERE

31 460 There are some minor outcrops of sandstones near González Chaves, 113 km east of
32 461 the Coronel Pringles in the middle of the Claromecó Basin (Figs. 1 and 2) (Llambías and
33 462 Prozzi, 1975). Monteverde (1937) correlated these sandstones with the quartzites of Las
34 463 Mostazas in the southeastern part of the Sierra de Pillahuincó (Tunas Formation). Furque
35 464 (1965) described similar quartzites with rest of lepidophytes in a similar setting 50 km further
36 465 east of González Chaves. A representative sample of these outcrops near González Chaves
37 466 was dated (SLV-VE 24, Fig. 15).

44 467 FIGURE 15 NEAR HERE

45 468 The detrital zircon ages show two important frequency peaks, one in the Late
46 469 Carboniferous (316 Ma), and another in the Early Devonian (406 Ma), a pattern characteristic
47 470 of other Pillahuincó Group rocks (Fig. 13). It is important to note that the youngest
48 471 sedimentary deposits exposed in the Claromecó Basin belong to this group, although
49 472 Tomezzoli and Vilas (1997) and Tomezzoli (2009) indicated that these exposures are
50 473 consistent with an Early to Late Permian age based on paleomagnetic grounds. This has been
51 474 challenged by Domeier et al. (2011), who supported younger ages based on recent dating in
52 475 Sierra Chica.

60 476

477 5.6 The Permian ash-fall tuffs of Tunas Formation

1 478 The occurrence of pyroclastic levels in the Tunas Formation first described by Iñiguez
2 et al. (1988) is one of the best time-lines to constrain the age of the late Paleozoic sequences.
3 479 The age of this unit was based on the *Eurydesma* Fauna and the *Glossopteris* Flora in the
4 480 deposits underlying the Tunas Formation, both of Early Permian age (Harrington 1947, 1955;
5 481 Benedetto, 2010). The upper part of the Tunas Formation bears the *Gangamopteris* Flora of
6 482 latest Early Permian age according to Archangelsky and Cúneo (1984).
7 483

8 484 Several ash-fall tuffs levels were sampled in the Abra del Despeñadero, in the
9 485 southeastern sector of Sierra de Pillahuincó. There, thin beds of smectite-rich claystones have
10 486 been identified in the predominantly sandy upper half of the Tunas Formation and are
11 487 characterized by abundant vitroclasts and fragments of vitric tuffs (Iñiguez et al., 1988; López
12 488 Gamundí, 2006). The dated zircons of three beds yielded an average $^{206}\text{Pb}/^{238}\text{U}$ age of 304
13 489 Ma, that corresponds to some sort of mixing of zircons formed between 280 and 288 Ma
14 490 (interpreted as juvenile zircons based on ϵHf data) and zircons formed between 290 to 315
15 491 Ma. Alessandreti et al. (2013) presented for the same SLV-VE-19 sample an U-Pb in situ LA-
16 492 MC-ICPMS age of 284 ± 15 Ma.
17 493

18 494 One tuff layer of the same outcrop as the samples SLV-VE-19, 20 and 21 has been
19 495 dated by Tohver et al. (2008) and yielded an age of 282.4 ± 2.8 Ma (U-Pb-SHRIMP). A
20 496 similar age of 280.9 ± 1.9 Ma (U-Pb SHRIMP) was recently reported by López-Gamundí et
21 497 al. (2013) on volcanic zircons from a tuff layer in the uppermost section of the Tunas
22 498 Formation. Both SHRIMP U-Pb ages are more reliable.
23 499

24 500 Based on these data, it is assumed that the tuff layers with the younger frequency
25 501 peaks, have crystallization ages close to 280 and 288 Ma (see Fig. 13), indicating a middle
26 502 Early Permian age, consistent with SHRIMP recent ages and the biochron of the fossil fauna
27 503 and flora.
28 504

29 505 The intimate relationship between volcanic activity inboard of the paleo-Pacific
30 506 margin, deformation in the adjacent orogenic belt, and subsidence and sedimentation in the
31 507 contiguous foreland basin led López Gamundí and Rossello (1998) to interpret the magmatic
32 508 belt as an Andean-type margin related to the paleo-Pacific margin. This proposal was
33 509 followed by Turner (1999) and Dalziel et al. (2000), among others. The main problem of this
34 510 interpretation is that the magmatic arc, as pointed out by Turner (1999) was located over
35 1,000 km away from the continental margin. No subduction related magmatism can exist that
36 far from the margin, even if a flat-subduction is proposed. A magmatic arc belt cannot be
37 developed further than 300-400 km away of the trench. Some authors proposed an
38
39
40
41
42
43
44
45
46
47
48
49
50
51
52
53
54
55
56
57
58
59
60
61
62
63
64
65

511 intermediate location (Pankhurst et al., 2006), but still inconsistent with a magmatic arc along
1 512 northern Patagonia in the Somún Cura Massif. Recent work of Chernicoff et al. (2012 a)
2 513 demonstrates that a series of calc-alkaline orthogneisses are Permian in age and represent the
3 514 relicts of the late Paleozoic magmatic arc developed in the northern Patagonia as proposed by
4 515 different authors (Ramos, 2008, and cites therein).
5 516

6 517 Although, the classic interpretation to explain the pyroclastic levels in the Las Tunas
7 518 Formation and in the Paraná Basin in southern Brazil is a source in the Choiyoi volcanic rocks
8 519 (Kay et al., 1989), we favor a more proximal origin. Based on U-Pb SHRIMP ages around
9 520 281.4 ± 2.5 Ma from Los Reyunos Formation, lower section of the Choiyoi volcanic rocks,
10 521 Rocha Campos et al. (2011) correlated these rocks with the older tuffs of the Paraná Basin.
11 522 This correlation is supported by the northeast paleocurrent directions measured in the aeolian
12 523 sandstones of Los Reyunos Formation by Pazos et al. (2011). However, if we want to use the
13 524 same Choiyoi source for the pyroclastic deposits of Las Tunas Formation, even with similar
14 525 ages, the dominant winds should be to the southeast, different from what was measured in the
15 526 Choiyoi intercalated aeolian sandstones. The distance is closer from Somún Cura, the ages are
16 527 similar, and the required paleowind direction is also to the northeast. Therefore, we prefer as a
17 528 potential source the Early Permian widespread calderas and rhyolites of the same age found in
18 529 the Somún Cura Massif. This interpretation also explains the source of the large amount of
19 530 volcanic debris and igneous Carboniferous detrital zircons found in Las Tunas Formation.
20 531

21 532

22 533 **6. Lu-Hf-Isotope analyses**

23 534 Hf isotopes have been analyzed in 65 detrital zircons of samples from the Cambrian
24 535 paragneiss (SLV-VE-02), and from the Lolén (SLVE-01) and Tunas (SLV-VE 20/21)
25 536 Formations, in order to understand the characteristics of the source region (Fig. 16).
26 537

27 538 Several zircons from different representative sources have been analyzed in the sample
28 539 of metamorphic basement (SLV-VE-02). Two Neoproterozoic zircons yielded negative values of
29 540 $\epsilon_{\text{Hf}}(t)$ of -7.06 and -5.11 and TDM ages 2.98 and 3.22 Ga; one Mesoproterozoic zircon has an
30 541 $\epsilon_{\text{Hf}}(t)$ of +1.73 with a TDM age of 3.06 Ga. The Paleoproterozoic source was analyzed in
31 542 eight zircons, which yielded values of $\epsilon_{\text{Hf}}(t)$ between + 2.19 and -1.8. These values are
32 543 typical of the juvenile arc granitoids of Tandilia (Fig. 16). The younger zircon of 1,782 Ma
33 544 gave a quite negative value of -5.57 far from the previous ones; the TDM ages yielded
34 545 between 2.57 and 2.19 Ga. This 1.78 Ga corresponds to the age of post-collisional granites in
35 546 the Tandilia area (Cingolani, 2011), which clearly shows important crustal recycling (Fig. 16).
36 547
37 548
38 549
39 550
40 551
41 552
42 553
43 554
44 555
45 556
46 557
47 558
48 559
49 560
50 561
51 562
52 563
53 564
54 565
55 566
56 567
57 568
58 569
59 570
60 571
61 572
62 573
63 574
64 575
65 576

544 A few Mesoproterozoic zircons analyzed have disperse $\epsilon\text{Hf}(t)$ values from -14.8 and an TDM
1 age of 2.05 Ga, to $\epsilon\text{Hf}(t)$ positives and TDM ages 1.87 and 1.62 Ga. The other well
2 545 represented fraction is the Neoproterozoic (ca. 552 Ma) with $\epsilon\text{Hf}(t)$ values between -5.4 and -
3 546 3.08 with similar TDM Mesoproterozoic ages between 1.34 and 1.26 Ga within the range
4 547 described for the Sierras Pampeanas by Dahlquist et al. (2013).
5 548

9 549 FIGURE 16 NEAR HERE

10
11 550 In the Lolén Formation 35 zircons have been analyzed from sample (SL-VE-01)
12 551 representing different sources (Fig. 16). The Paleoproterozoic source yielded values of $\epsilon\text{Hf}(t)$
13 552 of +2.86 and -1.57 and TDM ages between 2.49 and 2.31 Ga; however, a few zircons yielded
14 553 $\epsilon\text{Hf}(t)$ values more negatives between -4.04 and -20.68 and older TDM ages between 2.81 and
15 554 2.59 Ga. Grenville-age zircons yielded similar $\epsilon\text{Hf}(t)$ values, but highly positive, between
16 555 +12.75 and +7.22, and model ages close to the crystallization ages, between 1.27 and 1.50 Ga,
17 556 showing their juvenile nature (Fig. 16). The Neoproterozoic zircons have variable
18 557 characteristics with a group of highly negative $\epsilon\text{Hf}(t)$ values between -35.17 and -18.22 and
19 558 model ages between 2.52 and 1.80 Ga; a second group has less negative $\epsilon\text{Hf}(t)$ values
20 559 between -5.64 and -0.73 and younger TDM ages between 1.16 and 1.35 Ga. The Paleozoic
21 560 sources can also be grouped in two sets, a group of Cambrian, Ordovician, and Devonian
22 561 zircons with very negative $\epsilon\text{Hf}(t)$ values (-43.93 and -11.09) and TDM ages between 2.61 and
23 562 1.47 Ga; the other group has more positive $\epsilon\text{Hf}(t)$ values (+28.71 and -5.01) and younger
24 563 TDM ages (1.26 and 1.03 Ga).
25 564

26 565 The last samples from the Tunas Formation (SLV-VE 20/21), which have late
27 566 Paleozoic zircons (290-340 Ma) yielded $\epsilon\text{Hf}(t)$ values between +10.51 and -1.87, with TDM
28 567 ages restricted between 0.98 and 0.80 Ga. These zircons probably belong to the juvenile
29 568 magmatic arc of northern Patagonia (see Ramos, 2008). There is also a crystal with highly
30 569 negative $\epsilon\text{Hf}(t)$ value (-30.82) and a model age of 1.82 Ga, very distinct of the rest of the
31 570 group (Fig. 16). Those highly negative values were also recorded by Chernicoff et al. (2012
32 571 a).
33 572

34 573 7. Analyses of the provenance

35 574 Based on the previous detrital zircon analyses, together with conventional
36 575 petrographic and paleocurrents studies performed by Reinoso (1968), Andreis and Cladera
37 576 (1992) and López Gamundí and Rossello (1998), among others, a tentative paleogeography
38 can be reconstructed along a series of stages.
39
40
41
42
43
44
45
46
47
48
49
50
51
52
53
54
55
56
57
58
59
60
61
62
63
64
65

577

7.1 Cambrian-Ordovician

The provenance at this stage looks simple and conditioned by the basement exposed at that time. The Paleoproterozoic of Tandilia is the main source, a clear indication that these mountains were conspicuous at that time. Through time, the Pampean basement of Ventania starts being exhumed and Cambrian and Neoproterozoic granitoids became the main source (Fig. 17).

FIGURE 17 NEAR HERE

The proposed paleogeography shows an old mountain system being exhumed, represented by the Tandilia mountains, surrounded to the west (present coordinates) by the Pampean orogenic belt of Eastern Sierras Pampeanas. The exhumation of this belt produced an increased participation of this source through time. At the eastern side the Punta Mogotes Belt, a Brasiliano orogen related to the final closure of Adamastor Ocean at Early Cambrian times (Gaucher et al., 2005), was one of the last events related to the amalgamation of Gondwana. However, this orogen was not source of the analyzed samples of Ventania. The comparison of the different units of the Curamalal Group (Figs. 7 and 8) with the Mogotes Formation detrital zircon patterns shows striking differences (Fig.18).

FIGURE 18 NEAR HERE

The Cambrian-Ordovician paleogeography is illustrated in Fig. 19. The drainage should have an important component from the west or northwest to explain the lack of zircons from the Punta Mogotes Belt seen in the frequency peaks of Fig. 18. Note that these peaks are partially recognized in the younger Balcarce Formation (Fig. 11).

FIGURE 19 NEAR HERE

7.2 Silurian-Devonian

At this time the main dominant provenance was from the west and northwest. The Pampean basement of Eastern Sierras Pampeanas as described by Rapela et al. (1998), Ramos et al. (2010) and Chernicoff et al. (2009, 2012 b), was the main source of the lower Ventana Group (Fig. 17). The angular unconformity between the Balcarce Formation and the Neoproterozoic and Early Cambrian sedimentary cover of Tandilia (Cingolani, 2011) may be either the result of the collision of Pampia with the Río de la Plata Craton (Early Cambrian), or the Famatinian collision (Middle Ordovician). The sedimentary record of Balcarce Formation indicates a post Hirnantian glaciation age (Late Ordovician). The Pampean unconformity is seen in different places of Eastern Sierras Pampeanas and was dated in 530 Ma by Escayola et al. (2007) and Ianizzotto et al. (2013). But, as the main source is coming

611 from Eastern Sierras Pampeanas which is closer to Tandilia, it is more probable that
612 deformation is related to the Pampean orogen (see further details in Pazos and Rapalini,
613 2011).

614 Through time, the Pampean Belt had the relief partially eroded, and during Silurian
615 times the first Ordovician zircons were recorded, indicating that either the Famatinian Belt
616 was supplying zircons to the area, or some scarce Ordovician granitoids in the Eastern
617 Pampean Belt were exhumed. Also, Grenvillian-age zircons began to appear in the pattern of
618 provenance, suggesting that the Mesoproterozoic basement of Cuyania and/or Pampia was
619 also exhumed (Sato et al., 2000). The relief of Tandilia was almost non-existent as a source.
620 At this time, an important source from Punta Mogotes Belt is recorded in the Balcarce
621 Formation, indicating that this belt was actively exhumed. In Silurian times the
622 paleogeography was characterized by higher mountains in the Famatinian Belt in the west, a
623 partially eroded Pampean Belt, almost non-existent Tandilia Mountains, and an important
624 relief in the Punta Mogotes Belt. Some sort of by-pass existed through the Pampean Belt in
625 order to register Ordovician zircons in the Balcarce and Lolén Formations. The continental
626 margin was opened to the present south (Fig. 19).

628 **7.3 Late Paleozoic**

629 A drastic change in paleogeography was produced at this time. A volcanic relief
630 associated with a magmatic arc was located to the south, in present northern Patagonia.
631 Volcanic debris (Andreis and Cladera, 1992) together with magmatic zircons were recorded in
632 Ventania from 320 to 270 Ma. Classic petrographic provenance studies in Ventania and Cape
633 Fold Belt of South Africa indicate a dissected arc source for these rocks (López Gamundí and
634 Rossello, 1998). The older data of Late Carboniferous age observed as detrital zircons are in
635 agreement with their derivation from the northern late Paleozoic magmatic arc proposed by
636 Ramos (2008) in northern Patagonian along the Somún Cura Massif. Recent studies of
637 Chernicoff et al. (2012 a) in the Yaminué region in the Somún Cura Massif show that a biotite
638 paraschist has a maximum U/Pb SHRIMP age of 318 ± 5 Ma coherent with the frequency
639 peaks of several units of the Pillahuincó Group of the Ventania System. On the other hand,
640 the tonalitic orthogneiss has a crystallization age of 261.3 ± 2.7 Ma, which is broadly coeval
641 with deformation, and Neoproterozoic inheritance, indicating the occurrence of
642 Archean crust in this sector of Patagonia. Hf TDM ages of Permian zircons are mainly Meso-
643 Paleoproterozoic (2.97–3.35 Ga) with highly negative $\epsilon(\text{Hf})$ values (ca. -33) according to
644 Chernicoff et al. (2012 a). It is interesting to remark that the first Archean zircons observed in

645 Ventania are the 2729, 2990 and 3200 Ma frequency peaks of Sauce Grande Formation,
646 within the range of inherited Archean zircons of the Yaminué region described by these
647 authors.

648 The obtained zircon dates of the ash-fall tuffs of the Tunas Formation indicate an
649 Early Permian age, close to the depositional age of this unit (López Gamundí et al., 1995),
650 which was interpreted as synorogenic deposits based on the occurrence of growth strata. The
651 age of deformation is consistent with the deformation ages of the orthogneisses in north
652 Patagonia in the adjacent Somún Cura Massif (Chernicoff et al., 2012a).

653 A Permian very juvenile poorly dissected relief dominated the Somún Cura Massif and
654 the uplifted Ventania fold belt providing immature detritus to the Claromecó Basin. The
655 Ventania fold and thrust belt continues in the offshore in the Colorado syntaxis (Pángaro and
656 Ramos, 2012), a mirror image of the Cape Syntaxis (Fig. 20).

657

658 **8. Correlation with the Cape Fold Belt in South Africa**

659 It is important to note that in South Africa, the Cape Fold Belt was developed at the
660 same time that the Ventania Belt (Fig. 20) as parts of the Gondwanides Orogen (Keidel, 1916,
661 1921). There is consensus in the correlation of the different units of the Neoproterozoic-
662 Cambrian basement and the Paleozoic sedimentary sequences since the early work of Keidel
663 (1916) and DuToit (1927) followed by Harrington (1947). This correlation was based on the
664 rock types and age of the basement as proposed by Rapela et al. (2003), Milani and DeWitt
665 (2008), and Chemale et al. (2011b). On fossiliferous grounds the correlation was based on the
666 *Eurydesma* fauna and the *Glossopteris* flora, as well as in the Devonian marine fossils
667 (Harrington, 1955; Benedetto, 2010). Another piercing point is the correlation of the glacial
668 deposits of Sauce Grande and the Dwyka Tillite, which has been identified since the early
669 work of Keidel (1913), and corroborated several times by more recent works (López Gamundi
670 and Rossello, 1998).

671

FIGURE 20 NEAR HERE

672 A recent study on the detrital zircons of several pre-Carboniferous units of the Cape
673 Supergroup shows striking differences and similarities with the Ventania System (Fourie et
674 al., 2011). The main difference is the dominant Mesoproterozoic (1.0-1.2 Ga) provenance of
675 the Cape Supergroup that points out to the Namaqua Belt as the source area. The Curamalal
676 and Ventana Groups have the Paleoproterozoic ages from Tandilia Belt (2.2-2.0 Ga) as the
677 main Precambrian source. The similarities are the Neoproterozoic-Cambrian ages derived in
678 the present study from the Eastern Sierras Pampeanas, and from the pan-African belts and the

1
2
3
4
5
6
7
8
9
10
11
12
13
14
15
16
17
18
19
20
21
22
23
24
25
26
27
28
29
30
31
32
33
34
35
36
37
38
39
40
41
42
43
44
45
46
47
48
49
50
51
52
53
54
55
56
57
58
59
60
61
62
63
64
65

679 Cape Granites for Fourie et al. (2011). Both studies have also a striking coincidence in the
1
2 680 Ordovician ages. The analyses performed in the pre-Carboniferous rocks of the Cape Fold
3
4 681 Belt have a noticeable frequency peak at 469 Ma, similar to the frequency peak of 475 Ma of
5
6 682 Lolén Formation in the Ventania Belt that in the present study is straight forward derived
7
8 683 from the Famatinian Belt of Western Sierras Pampeanas. A similar Ordovician peak (478 Ma,
9
10 684 see Fig. 11) was identified in the Balcarce Formation by Rapela et al. (2011). Nonetheless,
11
12 685 Fourie et al. (2011) assumed that the source area could be either the Ross Orogen in
13
14 686 Antarctica or the Patagonian Deseado Massif of Argentina. As we noticed, the abrupt change
15
16 687 in provenance occurred after the collision of Patagonia, where a very different provenance is
17
18 688 recorded for the first time.

18 689 Based on the evaluation of both detrital zircon data bases we consider the Ordovician
19
20 690 (480-460 Ma) provenances in both Ventania and Cape belts, as derived from Western Sierras
21
22 691 Pampeanas, while the Neoproterozoic-Cambrian (560-530 Ma) zircons have local sources.
23
24 692 Zircons are derived in the Ventania Belt from Eastern Sierra Pampeanas, but in the Cape Fold
25
26 693 Belt come from local pan-African belts.

27 694

28 29 695 **9. Concluding remarks**

30
31 696 The obtained data permit to confirm some hypotheses and discard some previous
32
33 697 interpretations. The comparison of the provenance between the Curamalal and Ventana
34
35 698 Groups allows once more to confirm the stratigraphy of Harrington (1947), and to reject some
36
37 699 hypotheses that interpreted these units as tectonic repetitions of the same succession. These
38
39 700 pre-Carboniferous sequences of the Ventania Belt have a pattern derived from the Tandilia
40
41 701 Belt, as well as from Eastern and Western Sierras Pampeanas. These characteristics can be
42
43 702 compared with the detrital zircon pattern of the pre-Carboniferous Cape Fold Belt sequences.
44
45 703 Differences and similarities can be explained with common and local sources; both belts share
46
47 704 a similar Early to Middle Ordovician age zircons, which seem to be derived from the Sierras
48
49 705 Pampeanas Belt.

49 706 The change in provenance between the early Paleozoic deposits of the Ventana Group
50
51 707 and the late Paleozoic foreland sequences of the Pillahuincó Group indicates a different
52
53 708 source region from these deposits. A series of Carboniferous to Permian zircons, absent in the
54
55 709 previous units, together with the drastic change in paleocurrents indicate their derivation from
56
57 710 northern Patagonia as part of the Gondwanides Belt. The source area for the Pillahuincó
58
59 711 Group matches one to one the lithological characteristics of the Somún Cura Massif (see
60
61 712 location in Fig. 1), and the U-Pb ages of the main igneous and metamorphic rocks.

62
63
64
65

713 The occurrence of clasts with archeocyathids in the Somún Cura Massif sequences,
1 714 together with the detrital zircon patterns, are compatible with a source in Eastern Antarctica
2
3 715 (González et al., 2011; Naipauer et al., 2011; Ramos and Naipauer, 2012; Veevers and Saeed,
4
5 716 2013). The recent finding of archeocyathids in clasts of the Sauce Grande tillites (González et
6
7 717 al., 2013), reinforces this provenance. This match indicates that Patagonia should have
8
9 718 originated in Eastern Gondwana, and that it was transferred to Western Gondwana during the
10
11 719 Gondwanan orogeny. For further details see the recent analysis of Ramos and Naipauer
12
13 720 (2013 and cites there in). Although some recent papers proposed a continuation of the
14
15 721 magmatic activity in the early Paleozoic from the Sierras Pampeanas to the Somún Cura area
16
17 722 (Rapalini et al., 2013), a classic proposal advanced by Braccini (1960), it is not able to
18
19 723 elucidate the presence of archeocyathids (see discussion in Ramos and Naipauer, 2013).
20
21 724 Rapalini et al. (2013) follow the arguments of Dalziel et al. (2013) who propose a continuous
22
23 725 archeocyathid reef along the margin of Antarctica. However, this argument needs a magmatic
24
25 726 arc located in the Somún Cura arc more than thousand kilometers away from the Pacific
26
27 727 margin (see discussion in Ramos, 2008).

28
29 728 The integrated evolution of the Gondwanides in this sector of the southwestern
30
31 729 Gondwana margin with the general evolution of the Terra Australis Orogen as defined by
32
33 730 Cawood (2005) and modified by Ramos (2009), shows some interesting features. The early
34
35 731 Paleozoic continental margin of Ventania interrupts the almost continuous Famatinian-Ross
36
37 732 orogens. The Famatinian Orogen characterizes an active continental margin with a
38
39 733 voluminous magmatic arc developed along the proto-Andean margin of Western Gondwana
40
41 734 from Venezuela and Colombia through most of Argentina down to Ventania, during latest
42
43 735 Cambrian and Middle Ordovician times. The Ross Orogen (Stump, 1995; Myrow et al., 2001)
44
45 736 continues to the present east from Patagonia all along the Transantarctic Mountains and
46
47 737 Australia, and has a latest Cambrian to Early Ordovician magmatic arc. The Ventania early
48
49 738 Paleozoic basin is devoid of any magmatic activity in these intervals, representing a passive
50
51 739 continental margin. The tectonic causes of such differences are beyond the present research.

52
53 740

54 741 **Acknowledgements**

55 742 The authors want to thank Dr. Silvia Japas and Dr. Claudia Marsicano from the
56
57 743 Universidad de Buenos Aires for their help in the field work as well as to grants to VAR and
58
59 744 FC. We want to express our recognition to Dr. Eric Thover and an anonymous reviewer for
60
61 745 their critical and positive comments. This is the contribution R-90 of the Instituto de Estudios
62
63 746 Andinos “Don Pablo Groeber” (IDEAN).
64
65

References

749

750 Alessandreti, L, Philipp, R.P., Chemale Jr., F., Brückmann, M.P., Zvirtes, G., Matté, V., Ramos, V.A.,
751 2013. Geochemistry, provenance, and tectonic setting of the Paleozoic Ventania Fold Belt and the
752 Claromecó Foreland Basin: implications on sedimentation and volcanism along the southwestern
753 Gondwana margin. *Journal South American Earth Sciences* (in press).

754

755 Andersen, T., Graham, S., Aberg, G, Simonsen, S.L., 2009. Granitic magmatism by melting of
756 juvenile continental crust: new constraints on the source of Palaeoproterozoic granitoids in
757 Fennoscandia from Hf isotopes in zircon. *Journal of the Geological Society* 166, 233–247.

758

759 Andreis, R.R., Cladera, G., 1992. Las epiclastitas pérmicas de la cuenca Sauce Grande (Sierras
760 Australes, Buenos Aires, Argentina). Parte I: composición y procedencia de detritos. 4° Reunión
761 Argentina de Sedimentología (La Plata), Actas, p. 127–134.

762

763 Andreis, R., López Gamundi, O., 1989. Interpretación paleoambiental de la secuencia paleozoica del
764 Cerro Pan de Azúcar, Sierras Australes, Prov. de Buenos Aires. 1° Jornadas Geológicas Bonaerenses
765 (Tandil), Actas, p. 953–966, Bahía Blanca.

766

767 Andreis, R.R., Iñiguez, A.M., Lluch, J.J., Rodriguez, S., 1989. Cuenca Paleozoica de Ventania, Sierras
768 Australes, Buenos Aires. In: Chebli, G., Spalletti, L. (Eds.), *Cuencas Sedimentarias Argentinas:*
769 *Universidad Nacional de Tucumán, Correlación Geológica Serie 6*, p. 265–298.

770

771 Archangelsky, S., Cúneo, R., 1984. Zonación del Pérmico continental argentino sobre la base de sus
772 plantas fósiles. 3° Congreso Latinoamericano de Paleontología (México), *Memorias*, p. 143–153.

773

774 Balarino, M.L., 2012. Palinología del Pérmico de la cuenca de Claromecó-Colorado, Argentina.
775 *Ameghiniana* 49, 343–364.

776

777 Bellosi, E.S., Jalfin, G.A., 1984. Litoestratigrafía y evolución paleoambiental neopaleozoica de las
778 islas Malvinas, Argentina. 9° Congreso Geológico Argentino (Bariloche), Actas 5, p. 66–86.

779

780 Bellosi, E.S., Jalfin, G.A., 1989. Cuencas neopaleozoicas de la Patagonia extraandina e Islas Malvinas.
781 In: Chebli, G., Spalletti, L. (Eds.), *Cuencas Sedimentarias Argentinas: Universidad Nacional de*
782 *Tucumán, Correlación Geológica Serie, 6*, p. 379–394.

780

781

782

783

784

785

786

783

- 1 784 Benedetto, J.L., 2010. El continente de Gondwana a través del tiempo. Una introducción a la Geología
2 Histórica. Academia Nacional de Ciencias, Córdoba, 384 p.
- 3 785
4
5 786
- 6 787 Borrello, A.V., 1966. Trazas, restos tubiformes y cuerpos fósiles problemáticos de la Formación La
7 Tinta, Sierras Septentrionales de la Provincia de Buenos Aires. Comisión de Investigaciones
8 788 Científicas de la Provincia de Buenos Aires. *Paleontografía Bonaerense* 5, 1–42.
9
10 789
11 790
- 12
13 791 Bouvier, A., Vervoort, J.D., Patchett, P.J., 2008. The Lu–Hf and Sm–Nd isotopic composition of
14 CHUR: Constraints from unequilibrated chondrites and implications for the bulk composition of
15 792 terrestrial planets. *Earth and Planetary Science Letters* 273, 48–57.
16 793
17
18 794
- 19
20 795 Braccacini, O., 1960. Lineamientos principales de la evolución estructural de la Argentina.
21 796 *Petrotecnica, Revista del Instituto Argentino del Petróleo* 10(6), 57–69.
22
23 797
- 24
25 798 Buggisch, W., 1987. Stratigraphy and very low grade metamorphism of the Sierras Australes of the
26 799 Province of Buenos Aires, Argentina and implications in Gondwana correlations. *Zentralblatt*
27 *Mineralogie Geologie Paläontologie* 1, 819–837.
28 800
29
30 801
- 31
32 802 Cawood, P.A., 2005. Terra Australis orogen: Rodinia breakup and development of the Pacific and
33 803 Iapetus margins of Gondwana during the Neoproterozoic and Paleozoic. *Earth-Science Reviews* 69,
34 804 249–279.
35
36 805
- 37
38 806 Chemale Jr., F., Philipp, R.P., Dussin, I.A., Formoso, M.L.L., Kawashita, K., Bertotti, A.L., 2011a.
39 807 Lu-Hf and U-Pb age determinations of Capivarita Anorthosite in the Dom Feliciano Belt, Brazil.
40 808 *Precambrian Research* 186, 117–126.
41
42 809
- 43
44
45 810 Chemale Jr., F., Scheepers, R., Gresse, P.G., Van Schmus, W.R., 2011b. Geochronology and sources
46 811 of late Neoproterozoic to Cambrian granites of the Saldania Belt. *International Journal of Earth*
47 812 *Sciences (Geologische Rundschau)* 100, 431–444.
48
49 813
- 50
51
52 814 Chemale Jr., F., Kawashita, K., Dussin, I. A., Ávila, J. N., Justino, D., Bertotti, Anelise L., 2012. U-Pb
53 815 zircon in situ dating with LA-MC-ICP-MS using a mixed detector configuration. *Anais da Academia*
54 816 *Brasileira de Ciências* 84, 275–295.
55
56 817
- 57
58 818 Chernicoff, J., Zapettini, E., 2004. Geophysical evidence for terrane boundaries in South-Central
59 819 Argentina. *Gondwana Research* 7, 1105–1117.
60
61
62
63
64
65

- 1 821 Chernicoff, C.J., Zappettini, E.O., Villar, L.M., Chemale Jr., F., Hernández, L., 2009. The belt of
2 metagabros of La Pampa: Lower Paleozoic back-arc magmatism in south-central Argentina. *Journal of*
3 822 *South American Earth Sciences* 28, 383–397.
- 4
5 823
6 824
- 7
8 825 Chernicoff, C.J., Zappettini, E.O., Santos, J.O.S., Godeas, M.C, Belousova, E., McNaughton, N.K.,
9
10 826 2012 a. Identification and isotopic studies of early Cambrian magmatism (El Carancho Igneous
11 827 Complex) at the boundary between Pampia terrane and the Río de la Plata craton, La Pampa province,
12 Argentina. *Gondwana Research* 21, 378–393.
- 13 828
14
15 829
- 16 830 Chernicoff, C.J., Zappettini, E.O., Santos, J.O.S., McNaughton, N.J., Belousova , E., 2012 b.
17
18 831 Combined U-Pb SHRIMP and Hf isotope study of the Late Paleozoic Yaminué Complex, Rio Negro
19 832 Province, Argentina: Implications for the origin and evolution of the Patagonia Composite Terrane.
20
21 833 *Geoscience Frontiers*, doi: 10.1016/j.gsf.2012.06.003.
- 22 834
- 23 835 Chu, N.C., Taylor, R.N., Chavagnac, V., Nesbitt, R.W., Boella, M., Milton, J.A., 2002. Hf isotope
24
25 836 ratio analysis using multi-collector inductively coupled plasma mass spectrometry: an evaluation of
26
27 837 isobaric interference corrections. *Journal Analytic Atmospheric Spectrom* 17, 1567–1574.
- 28
29 838
- 30 839 Cingolani, C., 2005. Unidades morfoestructurales (y estructuras menores) de la provincia de Buenos
31
32 840 Aires. In: de Barrio, R.E., Etcheverry, R.O., Caballé, M.F., Llambías, E. (Eds.) *Geología y recursos*
33
34 841 *minerales de la Provincia de Buenos Aires. 16° Congreso Geológico Argentino, Relatorio*, p. 21–30,
35
36 842 *La Plata*.
- 37 843
- 38 844 Cingolani, C., 2011. The Tandilia System of Argentina as a southern extension of the Río de la Plata
39
40 845 craton: an overview. *International Journal of Earth Sciences (Geologische Rundschau)* 100, 221–242.
- 41
42 846
- 43 847 Cingolani, C., Berry, C.M., Morel, E., Tomezzoli, R., 2002. Middle Devonian lycosids from high
44
45 848 southern palaeolatitudes of Gondwana (Argentina). *Geological Magazine* 139, 641–649.
- 46
47 849
- 48 850 Cobbold, P.R., Gapais, D., Rossello, E.A., 1991. Partitioning of transpressive motions within a
49
50 851 sigmoidal foldbelt: the Variscan Sierras Australes, Argentina. *Journal of Structural Geology* 13, 743–
51
52 852 758.
- 53 853
- 54
55 854 Cuerda, A., Cingolani, C., Barranquero, H., 1975. *Estratigrafía del basamento Precámbrico en la*
56
57 855 *comarca de los cerros Pan de Azúcar del Coral, Sierras Australes, prov. de Buenos Aires, Rep.*
- 58
59
60
61
62
63
64
65

856 Argentina. 2° Congreso Iberoamericano de Geología Económica (Buenos Aires), Actas 1, p. 57–64,
1 857 Buenos Aires.
2
3 858
4
5 859 Dahlquist, J.A., Pankhurst, R.J., Gaschnig, R.M., Rapela, C.W., Casquet, C., Alasino, P.H., Galindo,
6 860 C., Baldo, E.G., 2013. Hf and Nd isotopes in Early Ordovician to Early Carboniferous granites as
7
8 861 monitors of crustal growth in the Proto-Andean margin of Gondwana. *Gondwana Research* 23, 1617–
9
10 862 1630.
11
12 863
13 864 Dalziel, I.W.D., Lawver, L.A., Murphy, J.B., 2000. Plumes, orogenesis, and supercontinental
14
15 865 fragmentation. *Earth and Planetary Science Letters* 178, 1–11.
16
17 866
18 867 Dalziel, I.W.D., Lawver, L.A., Norton, I.O., Gahagan, L.M., 2013. The Scotia Arc: Genesis,
19
20 868 Evolution, Global Significance. *Annual Reviews in Earth and Planetary Sciences* 41, 1–27.
21
22 869
23 870 de Beer, C.H., 1995. Fold interference from simultaneous shortening in different directions: the Cape
24
25 871 Fold Belt syntaxis. *Journal of African Earth Sciences* 21, 157–169.
26
27 872
28 873 Domeier, M., Van der Voo, R., Tohver, E., Tomezzoli, R.N., Vizan, H., Torsvik, T.H., Kirshner, J.,
29
30 874 2011. New Late Permian Constraints on the Apparent Polar Wander Path and Paleo-Marginal
31
32 875 Deformation of Gondwana. *Geochemistry, Geophysics, Geosystems*, 12, Q07002.
33
34 876
35 877 Dimieri, L., Delpino, S., Turienzo, M., 2005. Estructura de las Sierras Australes de Buenos Aires. In:
36
37 878 de Barrio, R., Etcheverry, O., Caballé, M.F., Llambías E. (Eds.), *Geología y recursos minerales de la*
38
39 879 *Provincia de Buenos Aires. 16° Congreso Geológico Argentino, Relatorio*, p. 101–118, La Plata.
40
41 880
42 881 Du Toit, A.L., 1927. A geological comparison of South America with South Africa. *Publications*
43
44 882 *Carnegie Institute* 381, 1–157.
45
46 883
47 884 Du Toit, A.L., 1937. Our wandering continents. An hypothesis of continental drifting. Oliver & Boyd,
48
49 885 London, 366 p.
50
51 886
52 887 Escayola, M., Pimentel, M., Armstrong, R., 2007. Neoproterozoic backarc basin: Sensitive high-
53
54 888 resolution ion microprobe U-Pb and Sm-Nd isotopic evidence from the Eastern Pampean Ranges,
55
56 889 Argentina. *Geology* 36, 495–498.
57
58 890
59 891 Fourie, P.H., Zimmermann, U., Beukes, N.J., Naidoo, T., Kobayashi, K., Kosler, J., Nakamura, E.,
60
61 892 Tait, J., Theron, J.N., 2011. Provenance and reconnaissance study of detrital zircons of the Palaeozoic
62
63
64
65

893 Cape Supergroup in South Africa: revealing the interaction of the Kalahari and Rio de la Plata cratons.
1 894 International Journal of Earth Sciences 100, 527–541.
2
3 895
4
5 896 Frakes, L.A., Crowell, J.C., 1969. Late Paleozoic glaciation. Part I. South America. Geological
6 897 Society America, Bulletin 80, 1007–1042.
7
8 898
9
10 899 Furque, G., 1965. Nuevos afloramientos del Paleozoico en la provincia de Buenos Aires. Revista del
11 900 Museo de la Plata, n.s. 5 (Geología 25), 239–243.
12
13 901
14 902 Gaucher, C., Poiré, D.G., Gómez Peral, L., Chiglino, L., 2005. Litoestratigrafía, bioestratigrafía y
15 903 correlaciones de las sucesiones sedimentarias del Neoproterozoico-Cámbrico del Cratón del Río de la
16 904 Plata (Uruguay y Argentina). Latinamerican Journal of Sedimentology and Basin Analysis 12, 145–
17 905 160.
18
19 906
20
21 907 Gaucher, C., Finney, S.C., Poiré, D.G., Valencia, V.A., Grove, M., Blanco, G., Pamoukaghlián, K.,
22 908 Gómez Peral, L., 2008. Detrital zircon ages of Neoproterozoic sedimentary successions in Uruguay
23 909 and Argentina: insights into the geological evolution of the Río de la Plata Craton. Precambrian
24 910 Research 167, 150–170.
25
26 911
27
28 912 Ghidella, M.E., Paterlini, C.M., Kovacs, L.C., Rodríguez, G.A., 1995. Magnetic anomalies on the
29 913 Argentina Continental Shelf. Fourth International Congress of the Brazilian Geophysical Society and
30 914 First Latin American Geophysical Conference (Río de Janeiro), Expanded Abstracts 1, 269–272.
31
32 915
33
34 916 Goodge, J.W., Vervoort, J.D., 2006. Origin of Mesoproterozoic A-type granites in Laurentia: Hf
35 917 isotope evidence. Earth and Planetary Science Letters 243, 711–731.
36
37 918
38
39 919 González, P.D., Tortello, M.F., Damborenea, S.E., 2011. Early Cambrian archaeocyathan limestone
40 920 blocks in low-grade meta-conglomerate from El Jagüelito Formation (Sierra Grande, Río Negro,
41 921 Argentina). Geologica Acta 9, 159–174.
42
43 922
44
45 923 González, P.D., Tortello, M.F., Damborenea, S.E., Naipauer, M. Sato, A.M., Varela, R., 2013.
46 924 Archaeocyaths from South America: review and a new record. Geological Journal 48, 114–125.
47
48 925
49
50 926 Gregori, D.A., López, V.L., Grecco, L.E., 2005. A Late Proterozoic–Early Paleozoic magmatic cycle
51 927 in Sierra de la Ventana, Argentina. Journal of South American Earth Sciences 19, 155–171.
52
53 928
54
55
56
57
58
59
60
61
62
63
64
65

929 Gregori, D.A., Kostadinoff, J., Strazzere, L., Raniolo, A., 2008. Tectonic significance and
1 930 consequences of the Gondwanide orogeny in northern Patagonia, Argentina. *Gondwana Research* 14,
2 429–450.
3 931
4
5 932
6 933 Griffin, W.L., Pearson, N.J., Belousova, E., Jackson, S.E., van Achterbergh, E., O'Reilly, S.Y., Shee,
7 934 S.R., 2000. The Hf isotope composition of cratonic mantle: LAM-MC-ICPMS analysis of zircon
8 935 megacrysts in kimberlites. *Geochimica et Cosmochimica Acta* 64, 133–147.
9
10 936
11
12 937 Harrington, H.J., 1942. Algunas consideraciones sobre el sector argentino del geosinclinal de
13 938 SAMFRAU. Primer Congreso Panamericano de Ingeniería, Minería y Geología (Santiago), *Anales* 2,
14 319–339.
15 939
16
17 940
18 941 Harrington, H.J., 1947. Explicación de las Hojas 33m y 34m, Sierras de Curamalal y de la Ventana,
19 942 provincia de Buenos Aires. *Boletín Dirección Nacional de Geología y Minería* 6, 1-56, Buenos Aires.
20 943
21
22 944 Harrington, H.J., 1955. The Permian *Eurydesma* fauna of eastern Argentina. *Journal of Paleontology*
23 945 29, 112–128.
24
25 946
26 947 Harrington, H.J., 1968. Desarrollo paleogeográfico de Sudamérica. Universidad Nacional de
27 948 Tucumán, Instituto Miguel Lillo, *Miscelánea* 26, 1–74.
28 949
29
30 950 Harrington, H.J., 1970. Las Sierras Australes de Buenos Aires, República Argentina: cadena
31 951 aulacogénica. *Revista de la Asociación Geológica Argentina* 25, 151–181.
32 952
33
34 953 Iannizzotto, N.F., Rapela, C.W., Baldo, E., Galindo, C., Fanning, C.M., Pankhurst, R., 2013. The
35 954 Sierra Norte-Ambargasta batholith: Late Ediacaran–Early Cambrian magmatism associated with
36 955 Pampean transpressional tectonics. *Journal of South American Earth Sciences* 42, 127–143.
37 956
38
39 957 Iñíguez, A.M., Andreis, R.R., Zalba, P.E., 1988. Eventos piroclásticos en la Formación Tunas
40 958 (Pérmico), Sierras Australes, provincia de Buenos Aires, República Argentina. 2° Jornadas Geológicas
41 959 Bonaerenses (Bahía Blanca), *Actas*, p. 383–395.
42 960
43
44 961 Jackson, S.E., Pearson, N.J., Griffin, W.L., Belousov, E.A., 2004. The application of laser ablation-
45 962 inductively coupled plasma-mass spectrometry to in situ U–Pb zircon geochronology. *Chemical*
46 963 *Geology* 211, 47–69.
47 964
48
49
50
51
52
53
54
55
56
57
58
59
60
61
62
63
64
65

- 965 Johnston, S.T., 2000. The Cape Fold Belt and syntaxis and the rotated Falkland Islands: dextral
1 966 transpressional tectonics along the southwest margin of Gondwana. *Journal of African Earth Sciences*
2 31, 4–13.
3 967
4
5 968
6 969 Jones, A.T., Franck, T.D., Fielding, C.R., 2006. Cold climate in the eastern Australian mid to late
7 Permian may reflect cold upwelling waters. *Palaeogeography, Palaeoclimatology, Palaeoecology* 237,
8 970 370–377.
9 971
10 972
11 973 Kay, S.M., Ramos, V.A., Mpodozis, C., Sruoga, P., 1989. Late Paleozoic to Jurassic silicic
12 magmatism at the Gondwana margin: analogy to the Middle Proterozoic in North America? *Geology*
13 17, 324–328.
14 974
15 975
16 976
17 977 Keidel, J., 1913. Über das Alter, die Verbreitung und die gegenseitigen Beziehungen der
18 verschiedenen tektonischen strukturen in den argentinischen Gebirgen. 12° Session du Congrès
19 Géologique International (Toronto), *Compte Rendus*, p. 671–687.
20 978
21 979
22 980
23 981 Keidel, J., 1916. La geología de las Sierras de la Provincia de Buenos Aires y sus relaciones con las
24 montañas de Sudáfrica y Los Andes. Ministerio de Agricultura de la Nación, Sección Geología,
25 Mineralogía y Minería, *Anales* 11, 1–78, Buenos Aires.
26 982
27 983
28 984
29 985 Keidel, J., 1921. Sobre la distribución de los depósitos glaciares del Pérmico conocidos en la
30 Argentina y su significación para la estratigrafía de la serie del Gondwana y la paleogeografía del
31 Hemisferio Austral. *Academia Nacional de Ciencias, Boletín* 25, 239–368.
32 986
33 987
34 988
35 989 Kilmurray, J.O., 1968. Petrología de las rocas cataclásticas y el skarn del anticlinal del cerro Pan de
36 Azúcar, partido de Saavedra, provincia de Buenos Aires. 3° Jornadas Geológicas Argentinas
37 (Comodoro Rivadavia), *Actas* 3, p. 217–239.
38 990
39 991
40 992
41 993 Kilmurray, J.O., 1975. Las Sierras Australes de la provincia de Buenos Aires. Las fases de
42 deformación y nueva interpretación estratigráfica. *Revista de la Asociación Geológica Argentina* 30,
43 994 331–348.
44 995
45 996
46 997 Llabrés, E., Prozzi, C.R., 1975. Ventania. In: *Geología de la Provincia de Buenos Aires, 6° Congreso*
47 Geológico Argentino, *Relatorio*, p. 79–101, Buenos Aires.
48 998
49 999
50
51
52
53
54
55
56
57
58
59
60
61
62
63
64
65

- 1000 López Gamundí, O., 2006. Permian plate margin volcanism and tuffs in adjacent basins of west
1 1001 Gondwana: Age constraints and common characteristics. *Journal of South American Earth Sciences*
2 22, 227–238.
3 1002
4
5 1003
6 1004 López Gamundí, O.R., Rossello, E.A., 1992. La Cuenca interserrana (Claromecó) de Buenos Aires,
7 Argentina: un ejemplo de cuenca hercínica de antepais. 3° Congreso Geológico de España y 8°
8 1005 Congreso Latinoamericano de Geología (Salamanca), Actas 4, p. 55–59.
9 1006
10 1007
11 1008 López Gamundí, O.R., Rossello, E.A., 1993. The Devonian-Carboniferous unconformity in Argentina
12 and its relation to the Eo-Hercynian orogeny in southern South America. *Geologische Rundschau* 82,
13 1009 136–147.
14
15 1010
16 1011
17 1012 López Gamundí, O.R., Rossello, E.A., 1998. Basin fill evolution and paleotectonic patterns along the
18 Samfrau geosyncline: the Sauce Grande basin–Ventana foldbelt (Argentina) and Karoo basin-Cape
19 1013 foldbelt (South Africa) revisited. *Geologische Rundschau* 86, 819–834.
20
21 1014
22 1015 López Gamundí, O.R., Espejo, I.S., Conaghan, P.J., Powell, C., 1994. Southern South America.
23 1016 *Geological Society of America, Memoir* 184, 281–330.
24
25 1017
26 1018 López Gamundí, O.R., Conaghan, P.C., Rossello, E.A., Cobbold, P.R., 1995. The Tunas Formation
27 1019 (Permian) in the Sierras Australes foldbelt, East Central Argentina: evidence for syntectonic
28 1020 sedimentation in a foreland basin. *Journal of South American Earth Sciences* 8, 129–142.
29
30 1021
31 1022 López Gamundí, O., Fildani, A., Weislogel, A., Rossello, E.A., 2013. The age of the Tunas Formation
32 1023 in the Sauce Grande basin-Ventana foldbelt (Argentina): implications for the Permian evolution of the
33 1024 southwestern margin of Gondwana. *Journal of South American Earth Sciences* (in press).
34
35 1025
36 1026 Ludwig, K.R., 2003. *Isoplot 3.00: A geochronological toolkit for Microsoft Excel*. Berkeley
37 1027 Geochronological Center, Special Publication 4, 70p.
38
39 1028
40 1029 Martin, A.K., C.J.H., Hartnady, Goodland, S.W., 1981. A revised fit of South America and South
41 1030 Central Africa. *Earth and Planetary Science Letters* 54, 293–305.
42
43 1031
44 1032 Max, M.D., Ghidella, M., Kovacs, L., Paterlini, M., Valladares, J.A., 1999. Geology of the Argentine
45 1033 continental shelf and margin from aeromagnetic survey. *Marine and Petroleum Geology* 16, 41–64.
46
47 1034
48 1035
49
50
51
52
53
54
55
56
57
58
59
60
61
62
63
64
65

- 1036 Milani, E.J., DeWitt, M.J., 2008. Correlations between the classic Paraná and Cape–Karoo sequences
1 of South America and southern Africa and their basin infills flanking the Gondwanides: du Toit
2 1037 revisited. In: Pankhurst, R.J., Trouw, R.A.J., Brito Neves, B.B., De Wit, M.J. (Eds.), West Gondwana:
3 1038 Pre-Cenozoic Correlations Across the South Atlantic Region. Geological Society, Special Publications
4 1039 294, p. 319–342.
5 1040
6 1041
7 1042 Monteverde, A., 1937. Nuevo yacimiento de material pétreo en González Chaves. Revista Minera 8,
8 1043 116–124.
9 1044
10 1045 Myrow, P.M., Pope, M.C., Goodge, J.W., Fischer, W., Palmer, A.R., 2001. Depositional history of
11 1046 pre-Devonian strata and timing of Ross orogenic tectonism in the central Transantarctic Mountains,
12 1047 Antarctica. Geological Society of America, Bulletin 114, 1070–1088.
13 1048
14 1049 Mitchell, C., Taylor, G.K., Cox, K.G., Shaw, J., 1986. Are the Falkland Islands a rotated microplate?
15 1050 Nature 319, 131–134.
16 1051
17 1052 Naipauer, M., Sato, A.M., González, P.D., Chemale Jr. F., Varela, R., Llambías, E.J., Greco, G.A.,
18 1053 Dantas, E., 2010. Eopaleozoic Patagonia–East Antarctica connection: fossil and U-Pb evidence from
19 1054 El Jagüelito Formation. 7° South American Symposium on Isotope Geology (Brasilia), Extended
20 1055 Abstracts, 602–605.
21 1056
22 1057 Naipauer, M., González, P.D., Varela, R., Sato, A.M., Chemale Jr., F., Llambías, E., Greco, G., 2011.
23 1058 Edades U-Pb (LA-ICP-MS) en circones detríticos del Miembro Polke, Formación Sierra Grande, Rio
24 1059 Negro: ¿Una nueva unidad cambro-ordovícica? 18° Congreso Geológico Argentino (Neuquén), Actas
25 1060 in CD, 113.
26 1061
27 1062 Newton, A.A., Cingolani, C.A., 1990. Aspectos estratigráficos y estructurales comparativos entre las
28 1063 secuencias siluro-devónicas de la Sierra de la Ventana (Argentina) y el Cinturón Plegado del Cabo
29 1064 (Sudáfrica). Revista Técnica de YPF 11, 59–63.
30 1065
31 1066 Nuñez, E., Bachmann, E.W. de, Ravazzoli, I., Britos, A., Franchi, M., Lizuaín, A., Sepúlveda, E.,
32 1067 1975. Rasgos geológicos del sector oriental del Macizo Somuncurá, provincia de Río Negro,
33 1068 República Argentina. 2° Congreso Iberoamericano Geología Económica (Buenos Aires), Actas 4, p.
34 1069 247–266.
35 1070
36 1071 Pángaro, F., Ramos, V.A., 2012. Paleozoic crustal blocks of onshore and offshore central Argentina:
37 1072 new pieces of the southwestern Gondwana collage and their role in the accretion of Patagonia and the
38
39
40
41
42
43
44
45
46
47
48
49
50
51
52
53
54
55
56
57
58
59
60
61
62
63
64
65

- 1073 evolution of Mesozoic south Atlantic sedimentary basins. *Marine and Petroleum Geology* 37, 162–
1074 183.
- 1075
- 1076 Pankhurst, R.J., Rapela, C.W., Fanning, C.M., 2001. The Mina Gonzalito Gneiss: Early Ordovician
1077 Metamorphism in Northern Patagonia. 3^o South American Symposium on Isotope Geology (Pucón),
1078 Actas electrónicas Session 6(4), 1–4.
- 1079
- 1080 Pankhurst, R.J., Rapela, C.W., Fanning, C.M., Márquez, M., 2006. Gondwanide continental collision
1081 and the origin of Patagonia. *Earth Science Reviews* 76, 235–257.
- 1082
- 1083 Patchett, P.J., Kuovo, O., Hedge, C.E., Tatsumoto, M., 1981. Evolution of continental crust and
1084 mantle heterogeneity: evidence from Hf isotopes. *Contribution to Mineralogy and Petrology* 78, 279–
1085 297.
- 1086
- 1087 Pazos, P.J., Rapalini, A., 2011. The controversial stratigraphy of the glacial deposits in the Tandilia
1088 System, Argentina. In: Arnaud, E., Halverson, G.P., Shields-Zou, G. (Eds.), *The Geological Record of*
1089 *Neoproterozoic Glaciations*, Geological Society, Memoirs 36, 565–569.
- 1090
- 1091 Pazos, P.J., Bettucci, L.S., Loureiro, J., 2008. The Neoproterozoic glacial record in the Río de la Plata
1092 Craton: a critical reappraisal. In: Pankhurst, R.J., Trouw, R.A.J., Brito Neves, B.B., De Wit, M.J.
1093 (Eds.), *West Gondwana: Pre-Cenozoic Correlations Across the South Atlantic Region*. Geological
1094 Society, Special Publications 294, p. 343–364.
- 1095
- 1096 Pazos, P.J., Rey, F., Marsicano, C., Ottone, G., de la Fuente, M., 2011. Permian unroofing,
1097 palaeoenvironmental and palaeoclimate evolution in the San Rafael foreland basin, Mendoza,
1098 Argentina. *Gondwana 14, Reuniting Gondwana: East meets West (Buzios)*, Abstracts , p. 149.
- 1099
- 1100 Pietranik, A.B., Hawkesworth, C.J., Storey, C.D., Kemp, T.I., Sircombe, K.N., Whitehouse, M.J.,
1101 Bleeker, W., 2008. Episodic, mafic crust formation from 4.5 to 2.8 Ga: New evidence from detrital
1102 zircons, Slave craton, Canada. *Geology* 36, 875–878.
- 1103
- 1104 Ploszkiewicz, J.V., 1999. ¿Será Buenos Aires una nueva provincia petrolera? Antecedentes, hipótesis
1105 y certezas. *Boletín de Informaciones Petroleras* 58, 56–45.
- 1106
- 1107 Poiré, D.G., Spalletti, L.A., del Valle, A., 2003. The Cambrian-Ordovician siliciclastic platform of the
1108 Balcarce Formation (Tandilia System, Argentina): Facies, trace fossils, palaeoenvironments and
1109 sequence stratigraphy. *Geologica Acta* 1, 41–60.

- 1110
- ¹1111 Ramos, V.A., 1984. Patagonia: un continente a la deriva? 9º Congreso Geológico Argentino
²
³1112 (Bariloche), Actas 2, p. 311–328.
⁴
- ⁵1113
- ⁶1114 Ramos, V.A., 1986. Tectonostratigraphy, as applied to analysis of South African Phanerozoic Basins
⁷
⁸1115 by H. de la R. Winter, discussion. Transactions Geological Society South Africa 87, 169–179.
⁹
- ¹⁰1116
- ¹¹1117 Ramos, V.A., 1988. Tectonic of the Late Proterozoic-Early Paleozoic: a collisional history of the
¹²
¹³1118 southern South American. Episodes 12, 168–174.
¹⁴
- ¹⁵1119
- ¹⁶1120 Ramos, V.A., 2008. The basement of the Central Andes: the Arequipa and related terranes. Annual
¹⁷
¹⁸1121 Review on Earth and Planetary Sciences 36, 289–324.
¹⁹
- ²⁰1122
- ²¹1123 Ramos, V.A., 2009. Anatomy and global context of the Andes: Main geologic features and the Andean
²²
²³1124 orogenic cycle. In: Kay, S.M., Ramos, V.A., Dickinson, W. (Eds.), Backbone of the Americas:
²⁴
²⁵1125 Shallow Subduction, Plateau Uplift, and Ridge and Terrane Collision, Geological Society of America,
²⁶
²⁷1126 Memoir 204, p. 31–65.
²⁸
- ²⁹1127
- ³⁰1128 Ramos, V.A., Kostadinoff, J., 2005. La cuenca de Claromecó. In: de Barrio, R.E., Etcheverry, R.O.,
³¹
³²1129 Caballé, M.F., Llambías, E. (Eds.), Geología y recursos minerales de la Provincia de Buenos Aires.
³³1130 16º Congreso Geológico Argentino, Relatorio, p. 473–480.
³⁴
- ³⁵1131
- ³⁶1132 Ramos, V.A., Naipauer, M., 2012. Patagonia: an allochthonous terrane accreted to the Western
³⁷
³⁸1133 Gondwana and its contribution to the formation of the paleo-Andes in the late Paleozoic. In: Heredia
³⁹
⁴⁰1134 Carballo, N., Colombo Piñol, F., García Sansegundo, J. (Eds.) Geology of the Andean Cordillera and
⁴¹
⁴²1135 its foreland, Geo-Temas 13, 1903–1906.
⁴³
- ⁴⁴1136
- ⁴⁵1137 Ramos, V.A., Naipauer, M., 2013. Patagonia: Where does it come from? Journal of Iberian Geology
⁴⁶
⁴⁷1138 (in press).
⁴⁸
- ⁴⁹1139
- ⁵⁰1140 Ramos, V.A., Vujovich, G., Martino, R., Otamendi, J., 2010. Pampia: a large cratonic block missing in
⁵¹
⁵²1141 the Rodinia supercontinent. Journal of Geodynamics 50, 243–255.
⁵³
- ⁵⁴1142
- ⁵⁵1143 Rapalini, A., López de Luchi, M., Tohver, E., Cawood, P.A., 2013. The South American ancestry of
⁵⁶
⁵⁷1144 the North Patagonian Massif: geochronological evidence for an autochthonous origin? Terra Nova doi:
⁵⁸1145 10.1111/ter.12043.
⁵⁹
- ⁶⁰1146
- ⁶¹
- ⁶²
- ⁶³
- ⁶⁴
- ⁶⁵

- 1147 Rapela, C.W., Kostadinoff, J., 2005. El basamento de Sierra de la Ventana: historia tectonomagmática.
1
2 1148 In: de Barrio, R.E., Etcheverry, R.O., Caballé, M.F., Llambías, E. (Eds.), Geología y recursos
3 1149 minerales de la Provincia de Buenos Aires. 16° Congreso Geológico Argentino, Relatorio, p. 69–84.
4
5 1150
- 6 1151 Rapela, C.W., Pankhurst, R.J., Casquet, C., Baldo, E., Saavedra, J., Galindo, C., Fanning, C.M., 1998.
7
8 1152 The Pampean orogeny of the southern proto-Andes: Cambrian continental collision in the Sierras de
9
10 1153 Córdoba. In: Pankhurst, R.J., Rapela, C.W. (Eds.), The Proto-Andean Margin of Gondwana.
11
12 1154 Geological Society, Special Publication 142, p. 181–217.
13
14 1155
- 15 1156 Rapela, C.W., Pankhurst, R.J., Fanning, C.M., Grecco, L.E., 2003. Basement evolution of the Sierra
16
17 1157 de la Ventana Fold Belt: new evidence for Cambrian continental rifting along the southern margin of
18 1158 Gondwana. *Journal of the Geological Society* 160, 613–628.
19
20 1159
- 21 1160 Rapela, C.W., Pankhurst, R.J., Casquet, C., Fanning, C.M., Baldo, E.G., González-Casado, J.M.,
22
23 1161 Galindo, C., Dahlquist, J., 2007. The Río de la Plata craton and the assembly of SW Gondwana. *Earth-*
24
25 1162 *Science Reviews* 83, 49–82.
26
27 1163
- 28 1164 Rapela, C.W., Fanning, C.M., Casquet, C., Pankhurst, R.J., Spalletti, L., Poiré, D., Baldo, E.G., 2011.
29
30 1165 The Río de la Plata craton and the adjoining Pan-African/brasiliano terranes: Their origins and
31
32 1166 incorporation into south-west Gondwana. *Gondwana Research* 20, 673–690.
33
34 1167
- 35 1168 Reinoso, M., 1968. Paleocorrientes en la Formación Providencia. Devónico, Sierras Australes de la
36
37 1169 provincia de Buenos Aires. *Revista de la Asociación Geológica Argentina* 23, 287–296.
38
39 1170
- 40 1171 Rocha Campos, A.C., Basei, M.A., Nutman, A.P., Kleiman, L.E., Varela, R., Llambias, E., Canile,
41
42 1172 F.M., da Rosa, O. de C.R., 2011. 30 million years of Permian volcanism recorded in the Choiyoi
43 1173 igneous province (W Argentina) and their source for younger ash fall deposits in the Paraná Basin:
44
45 1174 SHRIMP U–Pb zircon geochronology evidence. *Gondwana Research* 19, 509–523.
46
47 1175
- 48 1176 Rossello, E., Massabie, A.C., López Gamundí, O.R., Cobbold, P.R., Gapais, D., 1997. Late Paleozoic
49
50 1177 transpression in Buenos Aires and Northeast Patagonian ranges, Argentina. *Journal of South American*
51
52 1178 *Earth Sciences* 10, 389–402.
53
54 1179
- 55 1180 Rozendaal, A., Gresse, P.G., Scheepers, R., Le Roux, J.P., 1999. Neoproterozoic to Early Cambrian
56
57 1181 Crustal Evolution of the Pan-African Saldania Belt, South Africa. *Precambrian Research* 97, 303–323.
58
59 1182
60
61
62
63
64
65

- 1183 Sato, A.M., Tickyj, H., Llambías, E.J., Sato, K., 2000. The Las Matras tonalitic-trondhjemitic pluton,
1184 central Argentina: Grenvillian-age constraints, geochemical characteristics, and regional implications.
1185 Journal of South American Earth Sciences 13, 587–610.
1186
- 1187 Schiller, W., 1930. Investigaciones geológicas en las montañas del sudoeste de la Provincia de Buenos
1188 Aires. Anales del Museo de La Plata 4 (2a. Serie), 9–84.
1189
- 1190 Seilacher, A., Cingolani, C.A., Varela, R., 2002. Ichnostratigraphic correlation of Early Paleozoic
1191 sandstones in North Africa and Central Argentina. In: Salem, M., Oun, K. (Eds.), Geology of
1192 Northwest Libya, Earth Sci Soc Lybia, 1, 275–292.
1193
- 1194 Sellés Martínez, J., 1989. The structure of the Sierras Australes (Buenos Aires province, Argentina): an
1195 example of folding in a transpressive environment. Journal of South American Earth Sciences 3, 317–
1196 329.
1197
- 1198 Sellés Martínez, J., 2001. Geología de la Ventania (Provincia de Buenos Aires (Argentina)). Journal of
1199 Iberian Geology 27, 43–69.
1200
- 1201 Söderlund, U., Patchett, P.J., Vervoort, J.D., Isachsen, C.E., 2004. The ^{176}Lu decay constant
1202 determined by Lu–Hf and U–Pb isotope systematics of Precambrian mafic intrusions. Earth Planetary
1203 Science Letters 219, 311–324.
1204
- 1205 Stacey, J.S., Kramers, J.D., 1975. Approximation of terrestrial lead isotope evolution by a two-stage
1206 model. Earth and Planetary Science Letters 26, 207–221.
1207
- 1208 Stump, E., 1995. The Ross Orogeny of the Transantarctic Mountains. Cambridge University Press,
1209 Cambridge, 284 p.
1210
- 1211 Suero, T., 1972. Compilación geológica de las Sierras Australes de la provincia de Buenos Aires.
1212 LEMIT (La Plata), Anales 3, 135–147.
1213
- 1214 Teruggi, M.E., 1964. Paleocorrientes y paleogeografía de las ortocuarcitas de la Serie de La Tinta
1215 (provincia de Buenos Aires). Comisión de Investigaciones Científicas de la provincia de Buenos
1216 Aires, Anales 5, 1–27.
1217
1218
1219
1220
1221
1222
1223
1224
1225
1226
1227
1228
1229
1230
1231
1232
1233
1234
1235

- 1218 Teruggi, M.E., Leguizamón, M.A., Ramos, V.A., 1988. Metamorfitas de bajo grado con afinidades
1 1219 oceánicas en el basamento de Tandil: sus implicaciones geotectónicas, provincia de Buenos Aires.
2
3 1220 Revista de la Asociación Geológica Argentina 43, 366–374.
4
5 1221
6 1222 Thirwall, M.F., Walder, A.J., 1995. In situ hafnium isotope ratio analyses of zircon by inductively
7
8 1223 coupled plasma mass spectrometry. *Chemical Geology* 122, 241–247.
9
10 1224
11 1225 Tohver, E., Cawood, P.A., Rossello, E., López de Luchi, M.G., Rapalini, A., Jourdan, F., 2008. New
12
13 1226 SHRIMP U-Pb and ⁴⁰Ar/³⁹Ar constraints on the crustal stabilization of southern South America,
14
15 1227 from the margin of the Rio de Plata (Sierra de Ventana) craton to northern Patagonia. American
16
17 1228 Geophysical Union, Fall Meeting, EOS (Abstract), T23C-2052.
18
19 1229
20 1230 Tohver, E., Cawood, P.A., Rossello, E.A., Jourdan, F., 2012. Closure of the Clymene Ocean and
21
22 1231 formation of West Gondwana in the Cambrian: Evidence from the Sierras Australes of the
23
24 1232 southernmost Rio de la Plata craton, Argentina. *Gondwana Research* 21, 394–405.
25
26 1233
27 1234 Tomezzoli, R.N., 2009. The apparent polar wander path for South America during the
28
29 1235 Permian-Triassic. *Gondwana Research* 15, 209–215.
30
31 1236
32 1237 Tomezzoli, R.N., Cristallini, E.O., 1998. Nuevas evidencias sobre la importancia del fallamiento en la
33
34 1238 estructura de las Sierras Australes de la Provincia de Buenos Aires. *Revista de la Asociación*
35
36 1239 *Geológica Argentina* 53, 117–129.
37
38 1240
39 1241 Tomezzoli, R.N., Cristallini, E.O., 2004. Secciones estructurales de las Sierras Australes de la
40
41 1242 provincia de Buenos Aires: Repetición de la secuencia estratigráfica a partir de fallas inversas? *Revista*
42
43 1243 *de la Asociación Geológica Argentina* 59, 330–340.
44
45 1244
46 1245 Tomezzoli, R.N., Vilas, J.F., 1997. Estudios paleomagnéticos preliminares y de fábrica magnética en
47
48 1246 afloramientos de López Lecube (38° lat S, 62° long. O) y González Chaves (38° lat. S, 60° long. O), en
49
50 1247 las cercanías de las Sierras Australes de la provincia de Buenos Aires, Argentina. *Revista de la*
51
52 1248 *Asociación Geológica Argentina* 52, 419–432.
53
54 1249
55 1250 Tomezzoli, R.N., Vilas, J.F., 1999. Paleomagnetic constraints on the age of deformation of the Sierras
56
57 1251 Australes thrust and fold belt, Argentina. *Geophysical Journal Interior* 138, 857–870.
58
59 1252
60 1253 Turner, B.R., 1999. Tectonostratigraphical development of the Upper Karoo foreland basin: orogenic
61
62 1254 unloading versus thermally-induced Gondwana rifting. *Journal of African Earth Sciences* 28, 215–238.
63
64
65

1255

¹1256 Uriz, N.J., Cingolani, C.A., Chemale Jr, F., Macambira, M.B., Armstrong, R., 2011. Isotopic studies
²
³1257 on detrital zircons of Silurian–Devonian siliciclastic sequences from Argentinean North Patagonia and
⁴
⁵1258 Sierra de la Ventana regions: comparative provenance. *International Journal of Earth Sciences*
⁶1259 (Geologische Rundschau) 100, 571–589.

⁸1260

⁹
¹⁰1261 Uriz, N.J., Cingolani, C.A., Marques, J., 2012. Procedencia sedimentaria del Paleozoico inferior –
¹¹1262 medio del Grupo Ventana y de la Formación Sierra Grande. *Nuevas edades U-Pb (LA-ICP.MS) en*
¹²
¹³1263 *circones detríticos. 13° Reunión Argentina de Sedimentología (Salta), Actas, 215–216.*

¹⁵1264

¹⁶1265 Van Staden, A., Zimmermann, U., Gutzmer, J., Chemale, F. Jr, Germs, G., 2010. Correlation of
¹⁷
¹⁸1266 Ordovician diamictites from Argentina and South Africa using detrital zircon dating. *Journal of the*
¹⁹
²⁰1267 *Geological Society* 167, 217–220.

²¹1268

²³1269 Varela, R., Cingolani, C.A., 1976. Nuevas edades radimétricas del basamento aflorante en el perfil del
²⁴
²⁵1270 cerro Pan de Azúcar - Cerro del Corral y consideraciones sobre la evolución geocronológica de las
²⁶
²⁷1271 rocas ígneas de las Sierras Australes, Buenos Aires. 6° Congreso Geológico Argentino (Bahía Blanca),
²⁸1272 *Actas 1, 543–556.*

³⁰1273

³¹1274 Varela, R., Leone, E.M., Manceda, R., 1987. Estructura tectónica en la zona del cerro del Corral,
³²
³³1275 Sierras Australes de Buenos Aires. *Revista de la Asociación Geológica Argentina* 41, 256–261.

³⁵1276

³⁶1277 Veevers, J.J., 2003. Pan-African is Pan-Gondwanaland: oblique convergence drives rotation during
³⁷
³⁸1278 650– 500 Ma assembly. *Geology* 31, 501–504.

⁴⁰1279

⁴¹1280 Veevers, J.J., 2004. Gondwanaland from 650– 500 Ma assembly through 320 Ma merger in Pangea to
⁴²
⁴³1281 185– 100 Ma breakup: supercontinental tectonics via stratigraphy and radiometric dating. *Earth-*
⁴⁴
⁴⁵1282 *Science Reviews* 68, 1–132.

⁴⁶1283

⁴⁸1284 Veevers, J.J., Saeed, A., 2013. Age and composition of Antarctic sub-glacial bedrock reflected by
⁴⁹
⁵⁰1285 detrital zircons, erratics, and recycled microfossils in the Ellsworth Land–Antarctic Peninsula–
⁵¹
⁵²1286 Weddell Sea–Dronning Maud Land sector (240°E–0°–015°E). *Gondwana Research* 23, 296–332.

⁵³1287

⁵⁴
⁵⁵1288 Von Gosen, W., 2003. Thrust tectonics in the North Patagonian Massif (Argentina): implication for a
⁵⁶
⁵⁷1289 Patagonian plate. *Tectonics* 22, 1005. doi:10.1029/ 2001ITC901039.

⁵⁸1290

⁵⁹

60

61

62

63

64

65

1291 Von Gosen, W., Buggisch, W., Dimieri, L.V., 1990. Structural and metamorphic evolution of the
1292 Sierras Australes, Buenos Aires province, Argentina. *Geologische Rundschau* 79, 797–821.
1293
1294 Von Gosen, W., Buggisch, W., Krumm, S., 1991. Metamorphism and deformation mechanisms in the
1295 Sierras Australes fold and thrust belt (Buenos Aires province, Argentina). *Tectonophysics* 185, 335–
1296 356.
1297
1298 Zavala, C., Azúa, G., Freige, R.H., Ponce, J.J., 2000. Sistemas deltaicos dominados por avenidas
1299 fluviales en el Grupo Curamalal (Paleozoico inferior), cuenca paleozoica de Ventania, provincia de
1300 Buenos Aires, Argentina. *Revista de la Asociación Geológica Argentina* 55, 165–178.
1301
1302 Zimmermann, U., Spalletti, L.A., 2009. Provenance of the Lower Paleozoic Balcarce Formation
1303 (Tandilia System, Buenos Aires Province, Argentina): implications for paleogeographic
1304 reconstructions of SW Gondwana. *Sedimentary Geology* 219, 7–23.

1305
1306

Figure captions

1307
1308

Figure 1: Location of the Ventania and Tandilia systems in the province of Buenos Aires, localities mentioned in the text, and main basement provinces of central Argentina and Uruguay (based on Ramos, 2009 and Cingolani, 2011).

1311
1312

Figure 2: Main geological features of the Ventania System in the province of Buenos Aires. Numbers indicate the samples with detrital zircon U/Pb Laser ablation analyses (geology after Schiller, 1930; Harrington, 1947; Suero, 1972).

1315
1316

Figure 3: Main basement exposures of the Ventania System with available ages based on Varela et al. (1987), Rapela et al. (2003), Rapela and Kostadinoff (2005), and Tohver et al. (2012).

1319
1320

Figure 4: Stratigraphic column of the Paleozoic sedimentary rocks of the Ventania System (based on Harrington, 1947), with the stratigraphic positions of the analyzed samples.

1322
1323

Paleocurrents after Reinoso (1968), Andreis and Cladera (1992), and López Gamundí and Rossello (1998).

1324
1325

1326
1327

1328
1329

1330
1331

1332
1333

1325 **Figure 5:** Structural cross section of the Gondwanides of northern Patagonia restored for the
1326 end of the Paleozoic. The hinterland region developed in present Somún Cura Massif with
1327 exhumed late Paleozoic arc-granitoids is shown as well as the Ventania System with the fold
1328 and thrust belt and associated Claromecó Basin (based on Von Gosen et al., 1991; Tomezzoli
1329 and Cristallini, 1998; Ploskiewicz, 1999; Ramos, 2008; Pángaro and Ramos, 2012). The
1330 location of potential sutures among Patagonia, Tandilia and Cortijo terranes, as well as the
1331 Tandilia magmatic arc further north, are indicated after Teruggi et al. (1988), Max et al.
1332 (1999), Ramos, (2008) and Cingolani (2011).

1333
1334 **Figure 6:** a) Detail of the sample site; b) U-Pb frequency plot ages from zircons of a
1335 paragneiss (sample VE-02) of the metamorphic basement in the eastern slope of Cerro Pan de
1336 Azúcar, western Sierra de Curamalal (see location in Fig. 2).

1337
1338 **Figure 7:** a) Tectonic lense of mylonitic granite within quartzite layers of La Lola Formation;
1339 b) LA-ICP-MS from concordant zircons of this mylonitic granite (sample SLV-VE-04, see
1340 location in Fig. 2 and analytical data in the supplementary material).

1341
1342 **Figure 8:** U/Pb frequency plot ages from detrital zircons of the Curamalal Group: SLV-VE-
1343 03 from a quartzite clast of the basal conglomerate of the La Lola Formation, and SLV-VE-
1344 05, quartzitic sandstones interfingered in the upper part of the conglomerates; SLV-VE-09
1345 from Mascota Formation from Cerro Colorado area; SLV-VE-10 from Mascota Formation
1346 east of Tornquist (location in Fig. 2).

1347
1348 **Figure 9:** U/Pb frequency plot ages from detrital zircons of lower part of the Ventana Group.
1349 Note the up-sequence decrease of the Paleoproterozoic ages (sample location in Fig. 2) and
1350 clear dominance of Late Neoproterozoic to Cambrian zircons.

1351
1352 **Figure 10:** U/Pb frequency plot ages from detrital zircons of upper part of the Ventana Group.
1353 Note that the samples from the Lolén Formation are more than 10 km distant, but have
1354 coherent patterns (see sample location in Fig. 2).

1355
1356 **Figure 11:** U/Pb frequency plot ages from detrital zircons of Balcarce Formation (samples
1357 FBA 264 and PMOG 233) based on Rapela et al. (2007, 2011). Note the important frequency
1358 peaks of Early Ordovician and Early Cambrian ages (location in Fig. 1).

1359
1360
1361
1362
1363
1364
1365

1359

1
2 1360 **Figure 12:** Comparison of the detrital zircons provenance based on between Curamalal Group
3
4 1361 and lower and upper Ventana Group. Note the prominent frequency peak of Paleoproterozoic
5
6 1362 zircons in the Curamalal Group which is poorly developed in the Ventana Group, and the
7
8 1363 Famatinian peak (475 Ma) in upper Ventana Group, which does not occur in the older units.
9
10 1364 (FAM: Famatinian; BRAS: Brasiliano-Pampean; GRENV: Grenvillian, and TRANS:
11
12 1365 Transamazonian).

13
14 1366
15 1367 **Figure 13:** U/Pb frequency plot ages from detrital zircons of the fine sandstones and shales of
16
17 1368 Pillahuincó Group. Note the prominent frequency peaks of 322-304 Ma and the 291-282 Ma
18
19 1369 peaks may be correlated with igneous ages in the northern Somún Cura Massif (Chernicoff et
20
21 1370 al., 2012a, and cites therein).

22
23 1371
24 1372 **Figure 14:** U/Pb frequency plot ages from zircons from the northern Somún Cura Massif of
25
26 1373 the, a) Sedimentary cover of Sierra Grande Formation (Silurian-Devonian), and b) pre-
27
28 1374 Ordovician metasedimentary basement of the El Jagüelito, Mina Gonzalito, and Nahuel Niyeu
29
30 1375 Formations (after Pankhurst et al., 2006; Naipauer et al., 2011 and Uriz et al., 2011).

31
32 1376
33 1377 **Figure 15:** U/Pb frequency plot ages from detrital zircons of the fine sandstone of González
34
35 1378 Chaves locality. Note the prominent frequency peak at 316 Ma (Late Carboniferous).

36
37 1379
38 1380 **Figure 16:** Hf isotopic analyses of selected samples from the Ventania System. See
39
40 1381 supplementary material for sample number and figure 2 for location.

41
42 1382
43
44 1383 **Figure 17:** U/Pb frequency plot ages from zircons from the Sierra de La Ventana region
45
46 1384 obtained in the present study and the main orogenic events ((FAM: Famatinian; BRAS:
47
48 1385 Brasiliano-Pampean; GRENV: Grenvillian, and TRANS: Transamazonian).

49
50 1386
51 1387 **Figure 18:** U-Pb frequency plots of detrital zircons of Mogotes Formation. Note the different
52
53 1388 pattern with the Balcarce Formation of Fig. 11(after Rapela et al., 2007, 2011).

54
55 1389
56
57 1390 **Figure 19:** Paleogeography of the Ventania System through time; a) Cambrian-Ordovician; b)
58
59 1391 Silurian-Devonian; and c) late Paleozoic times. The Pampean Orogen depicted after Ramos
60
61 1392 (1988), Rapela et al. (1998), and Tohver et al. (2012); the Punta Mogotes Belt based on

62
63
64
65

1393 Gaucher et al. (2005); the Gondwanides Orogen based on Ramos (2008) and Pángaro and
1
2 1394 Ramos (2012).

3
4 1395

5 1396 **Figure 20:** Location of the Ventania Fold Belt in the province of Buenos Aires, Argentina and
6
7 1397 its correlation with the Cape Fold Belt of South Africa as part of the Gondwanides. Tectonic
8
9 1398 framework of the pre-break up of Western Gondwana is based on the reconstruction of
10
11 1399 Pángaro and Ramos (2012).

12
13 1400

14
15 1401

16
17

18

19

20

21

22

23

24

25

26

27

28

29

30

31

32

33

34

35

36

37

38

39

40

41

42

43

44

45

46

47

48

49

50

51

52

53

54

55

56

57

58

59

60

61

62

63

64

65

Figure 1
[Click here to download high resolution image](#)

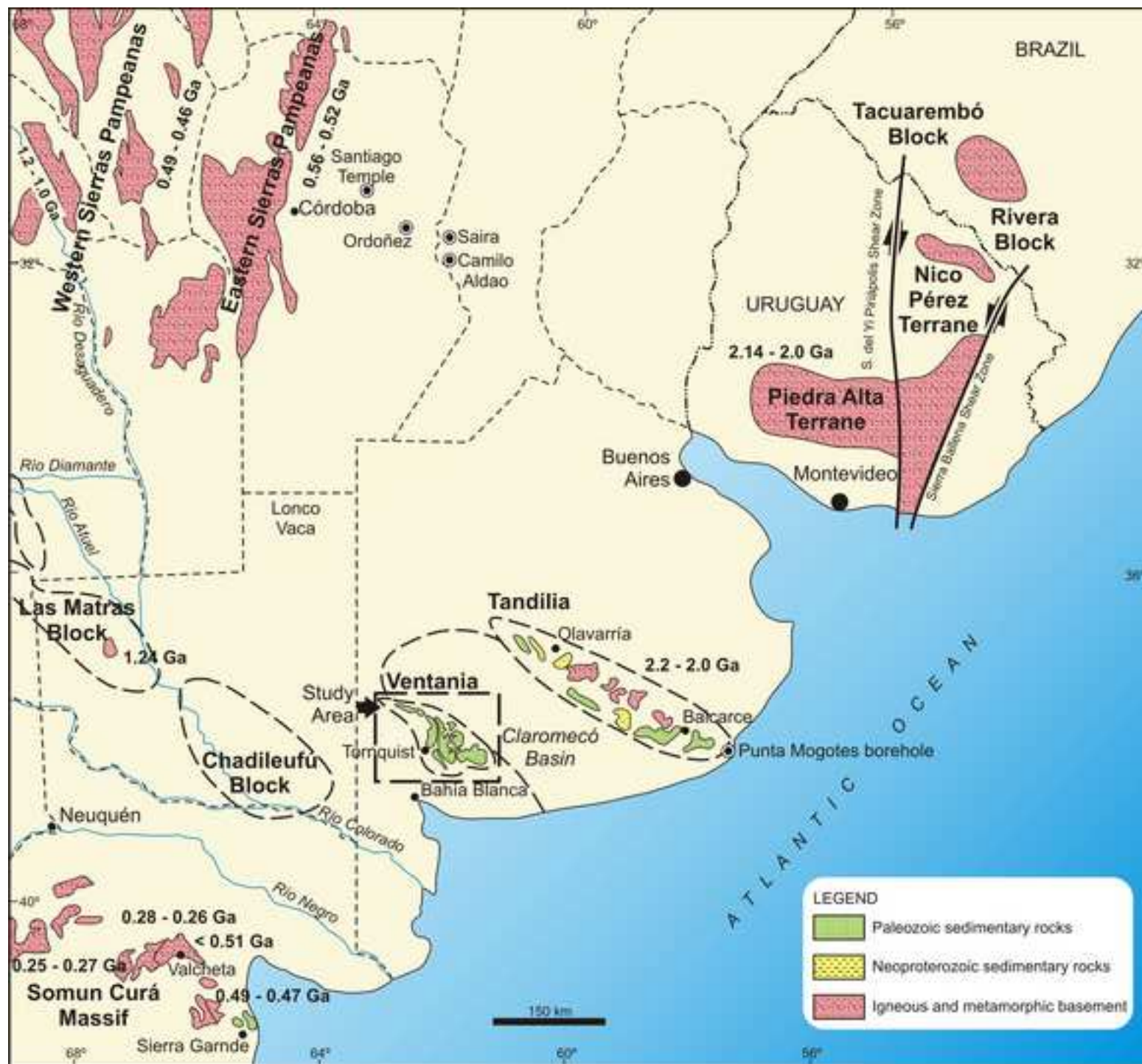
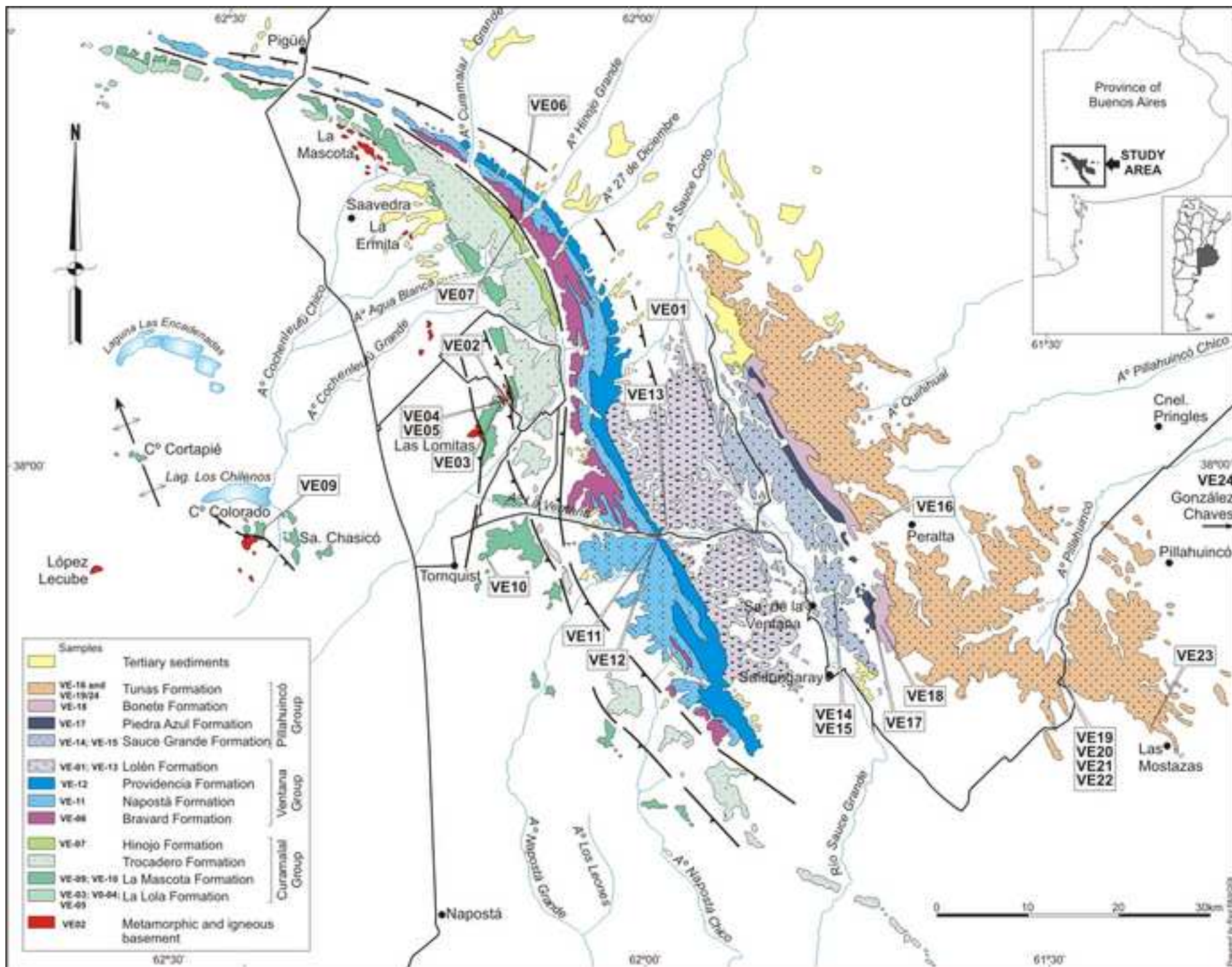


Figure 2
[Click here to download high resolution image](#)



New Figure 3

[Click here to download high resolution image](#)

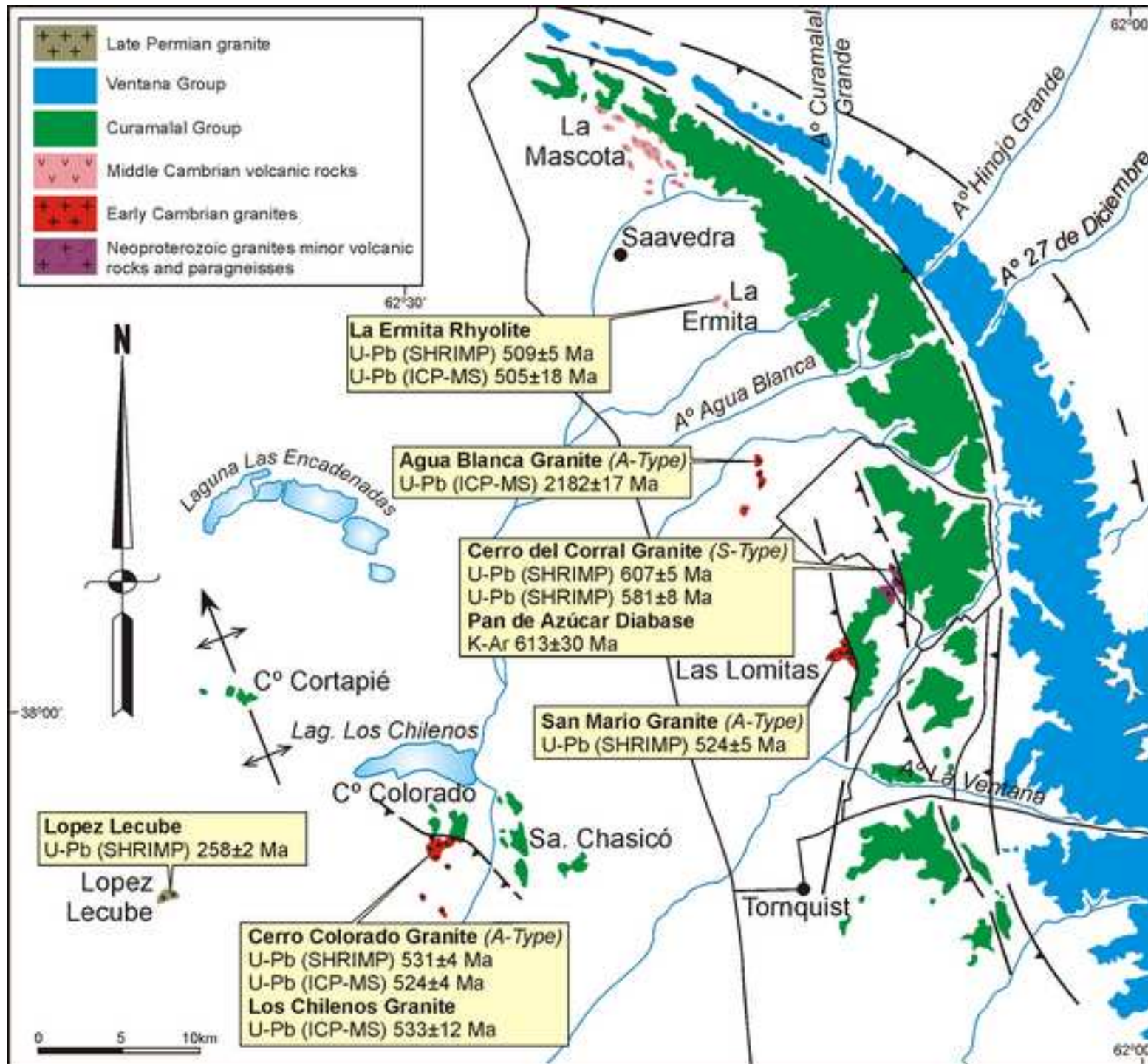


Figure 4
[Click here to download high resolution image](#)

STRATIGRAPHIC COLUMN OF THE VENTANIA SYSTEM

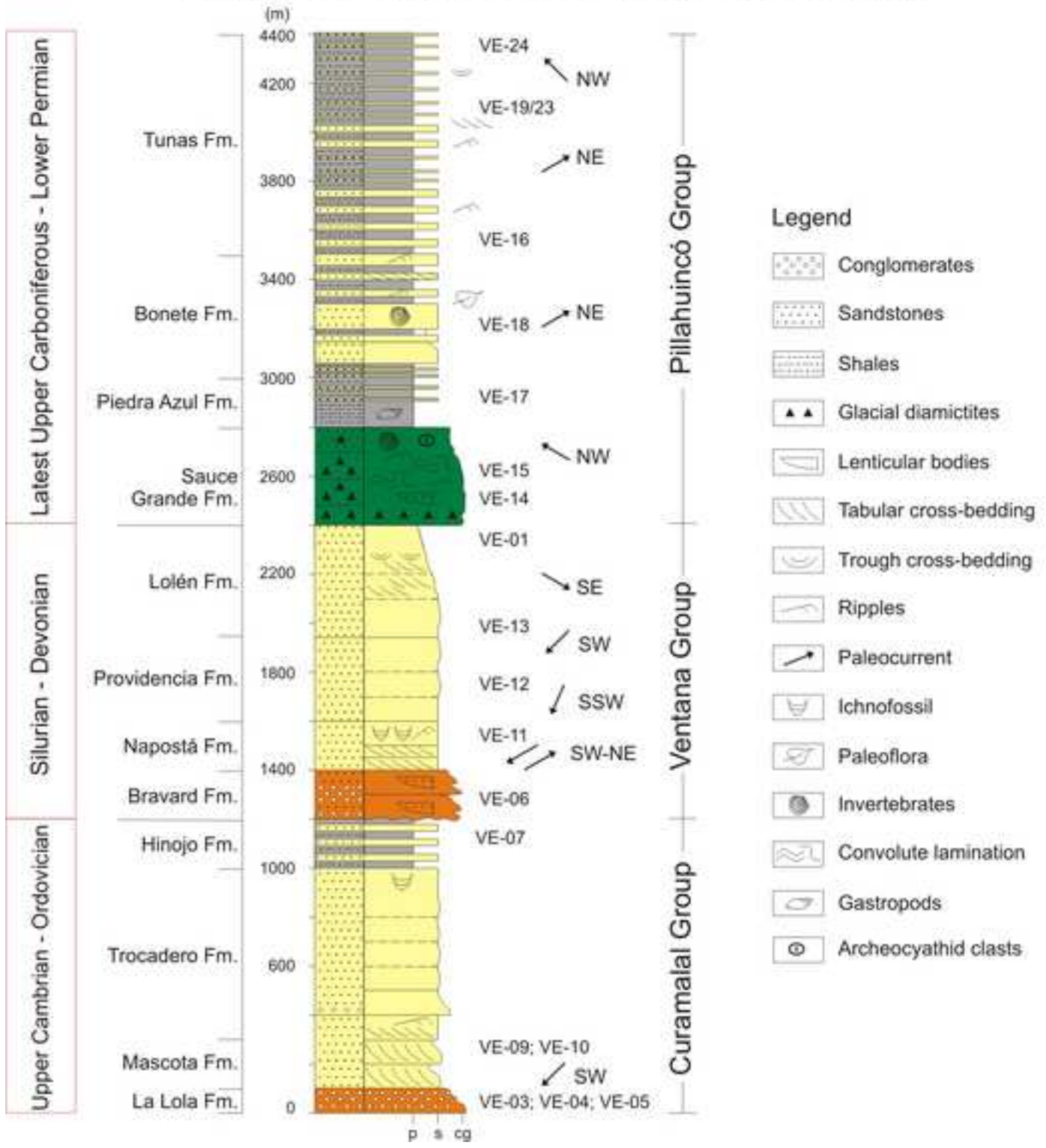
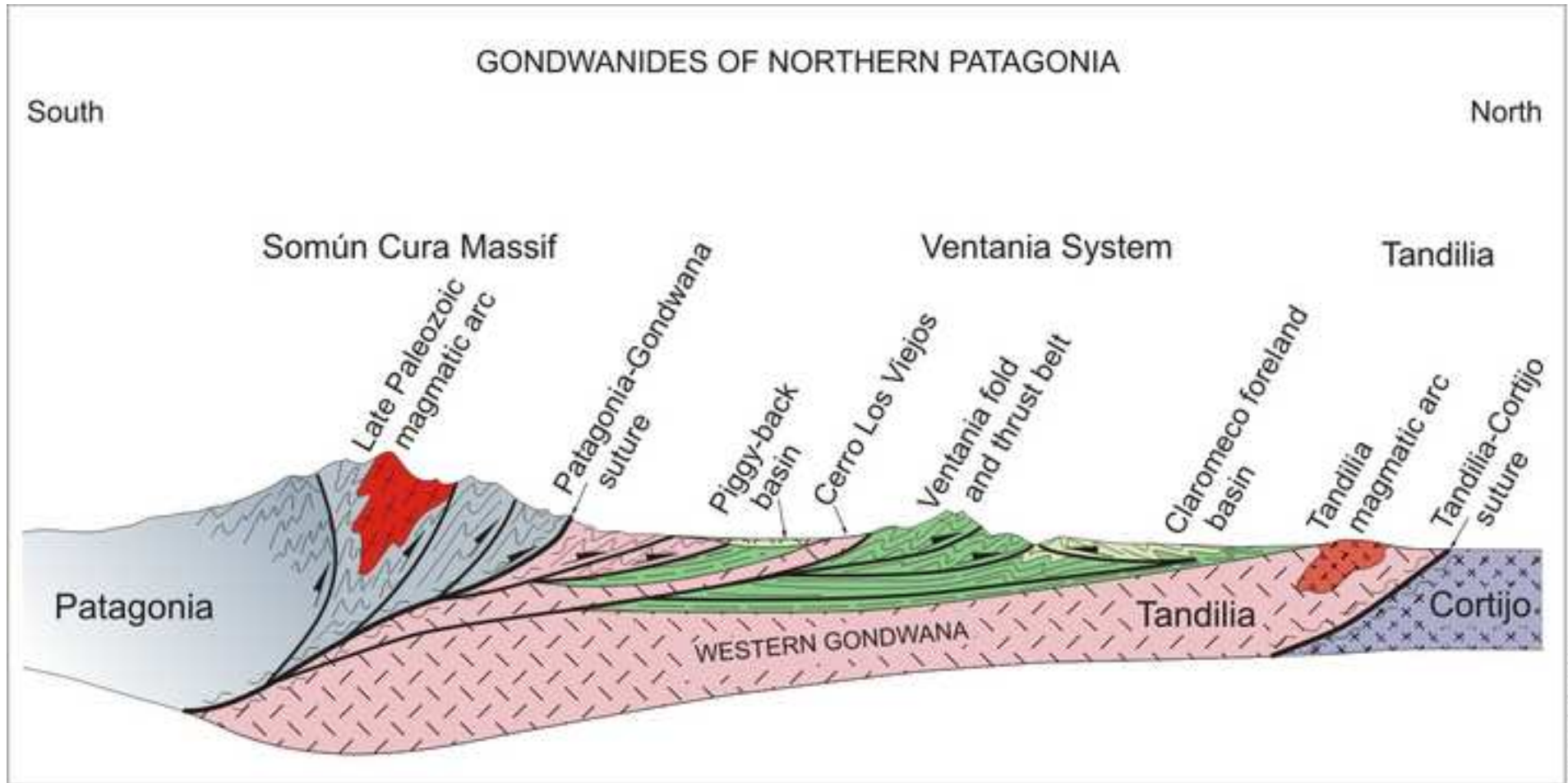
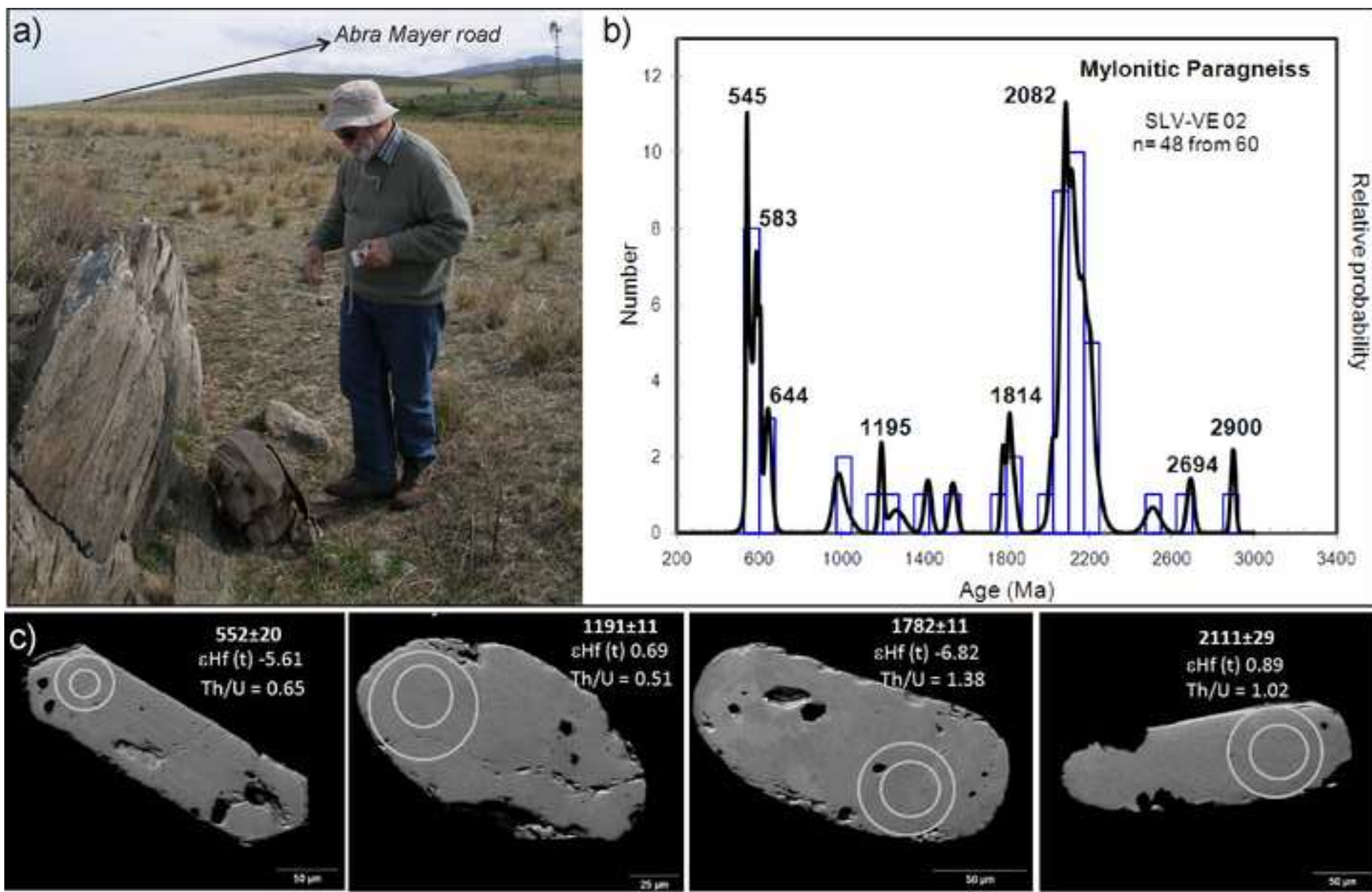
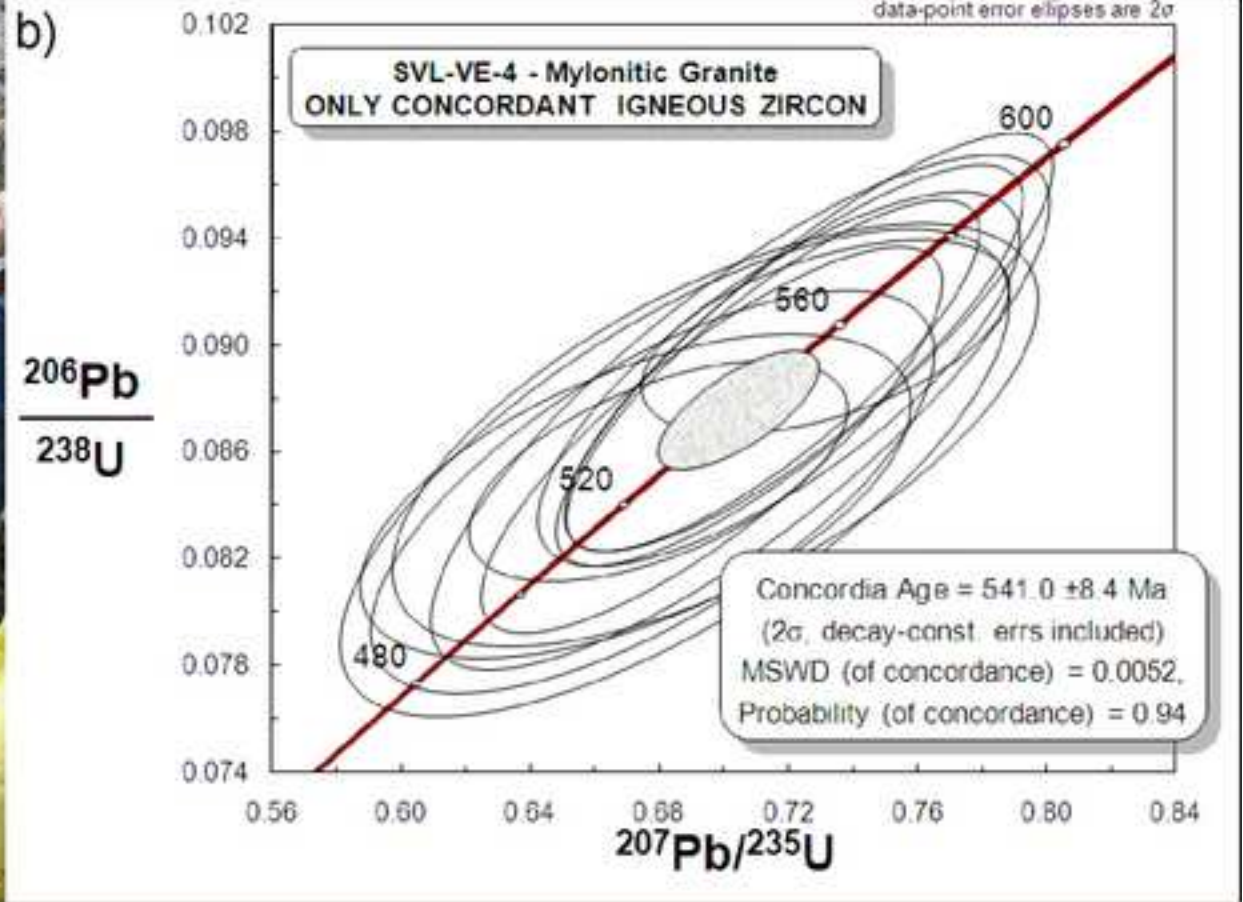


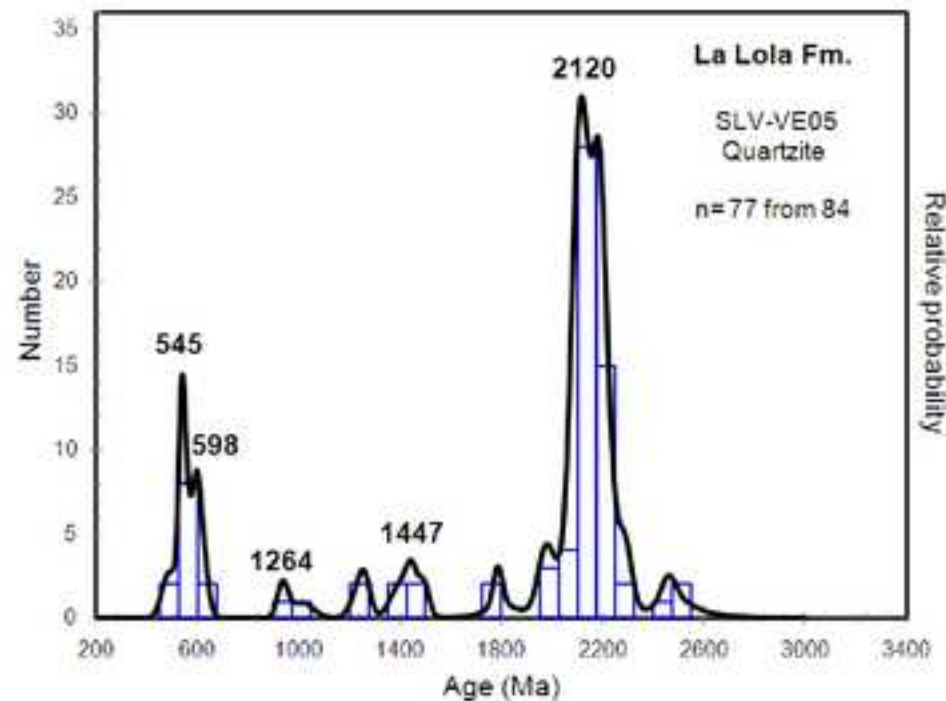
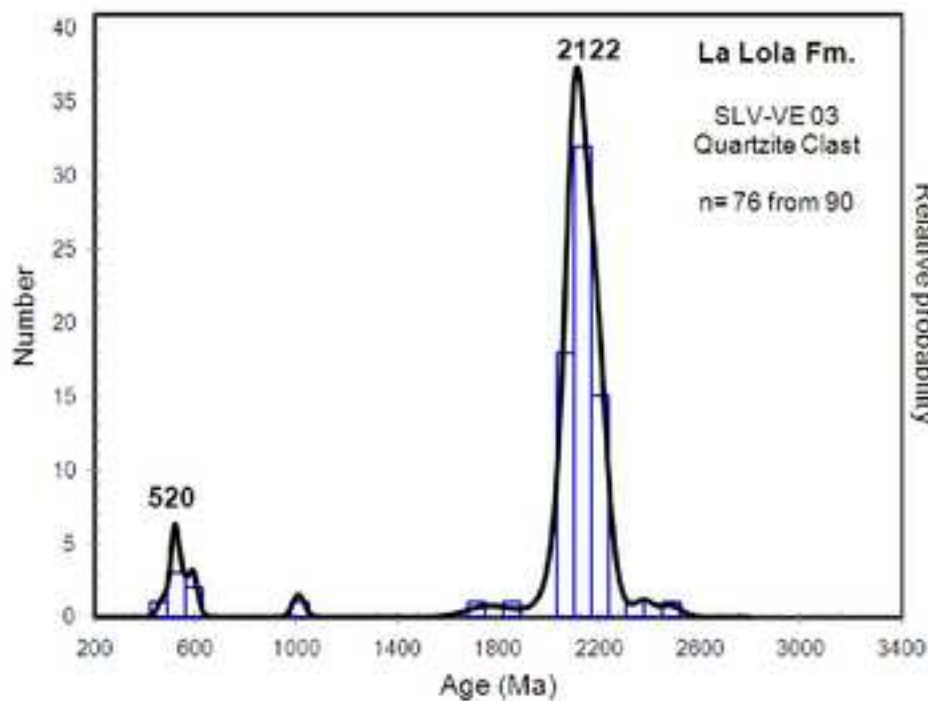
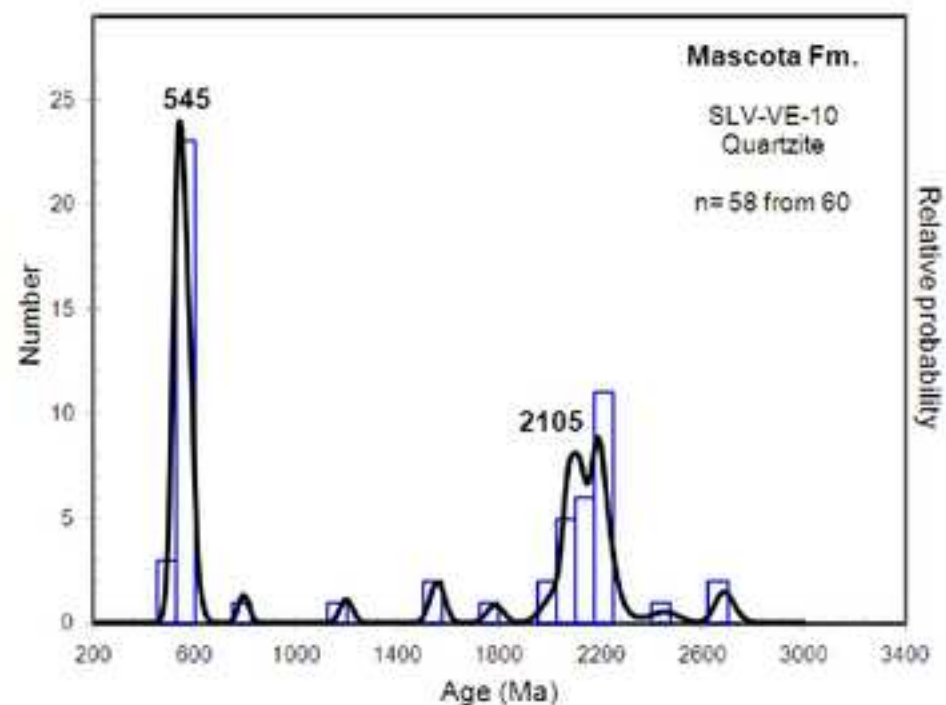
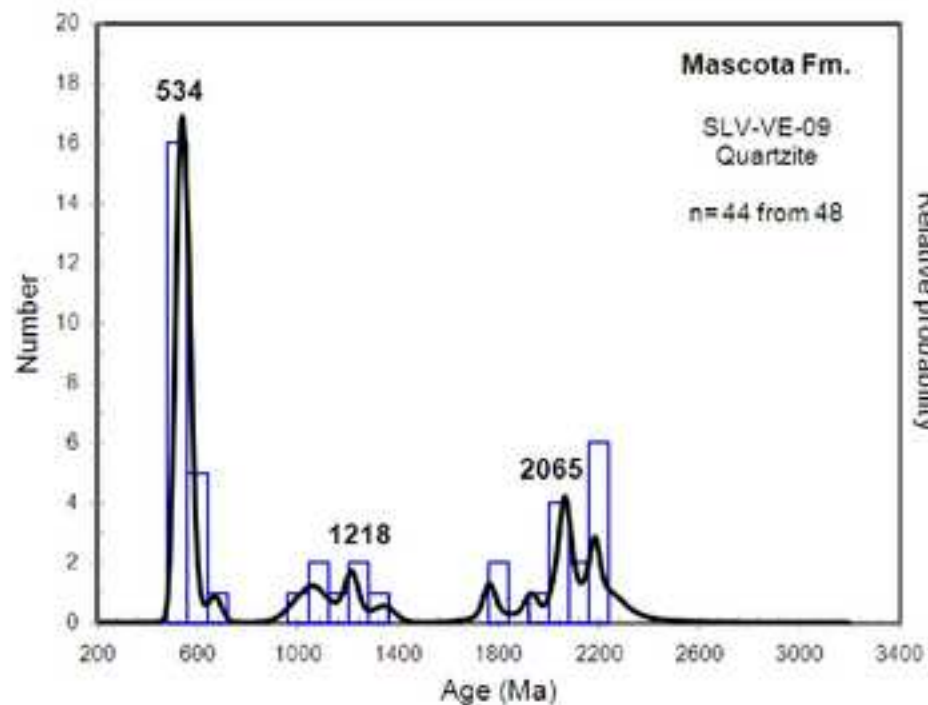
Figure 5
[Click here to download high resolution image](#)

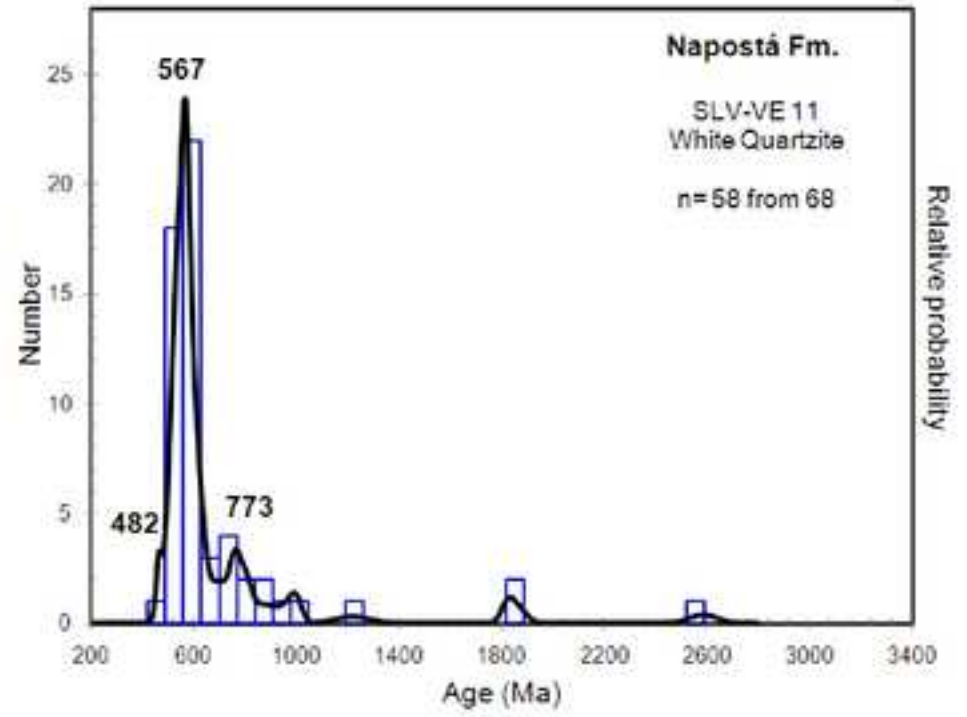
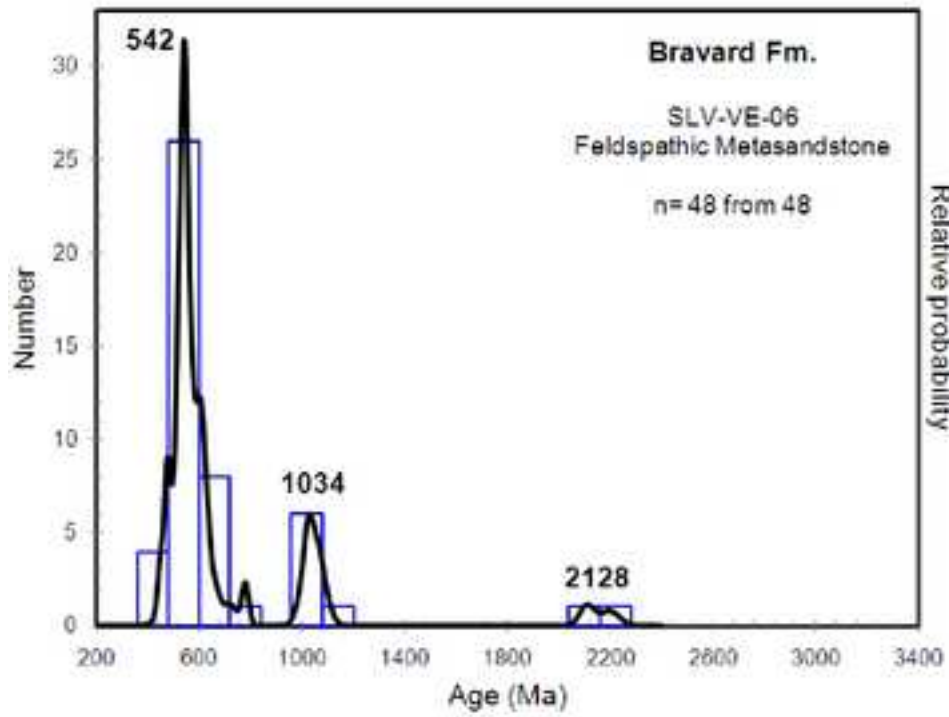






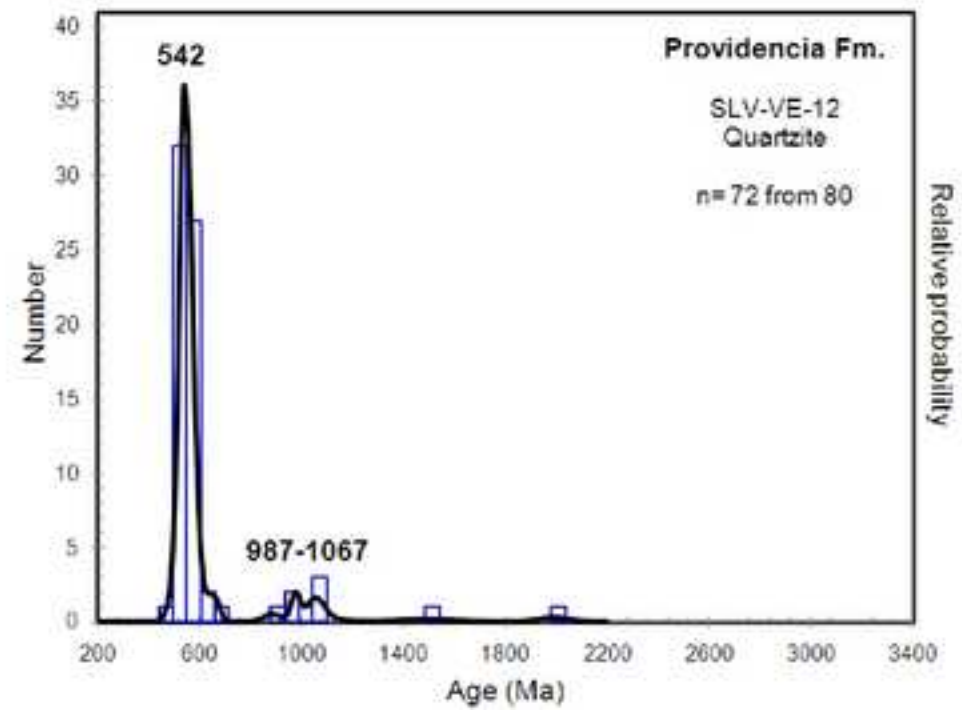
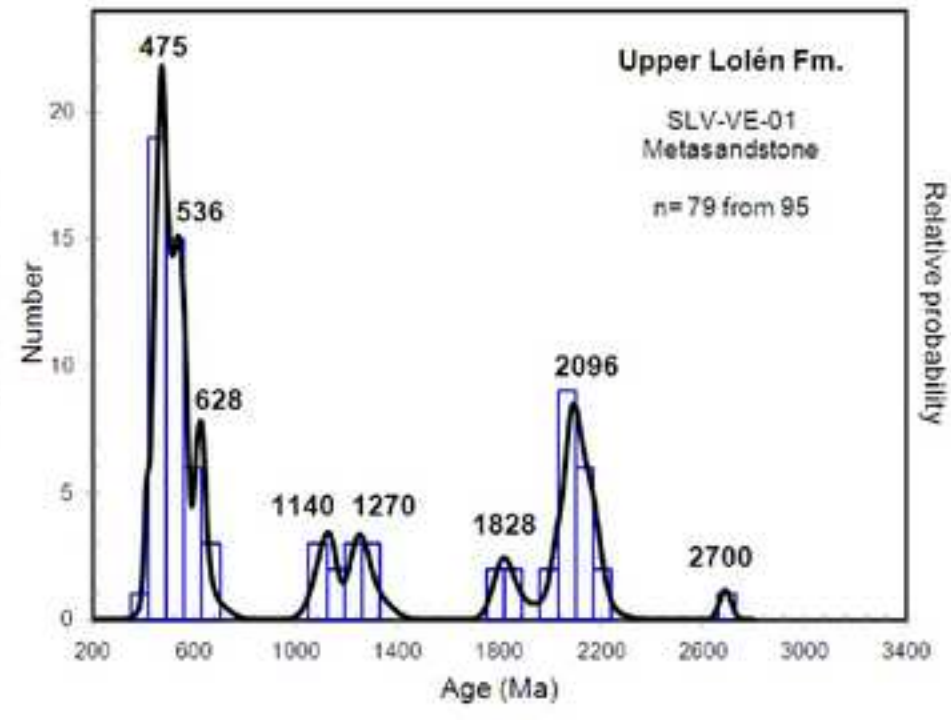
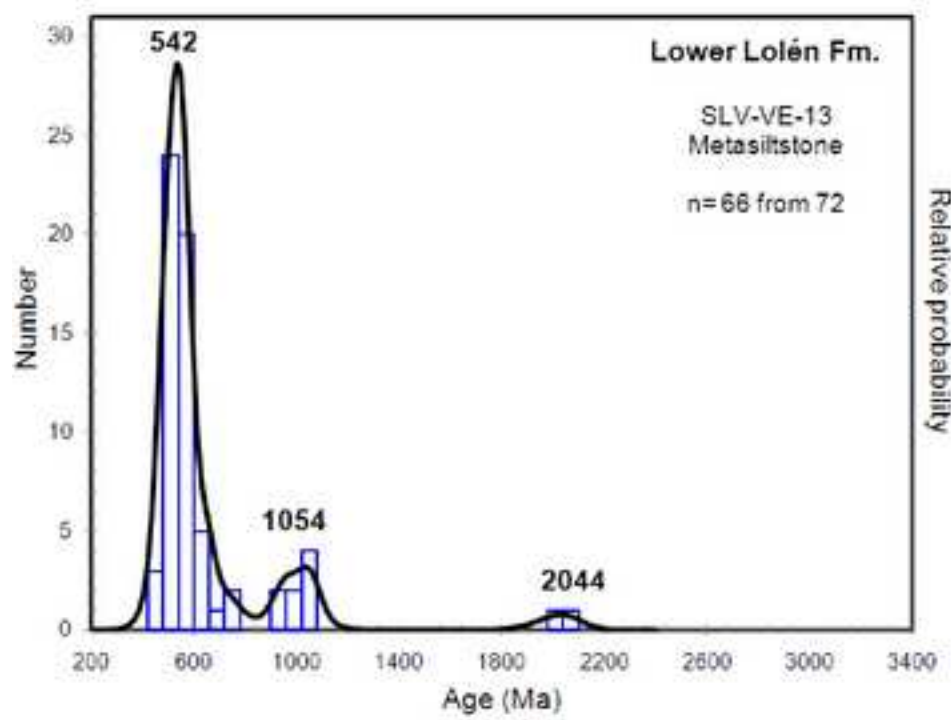
New Figure 8
[Click here to download high resolution image](#)

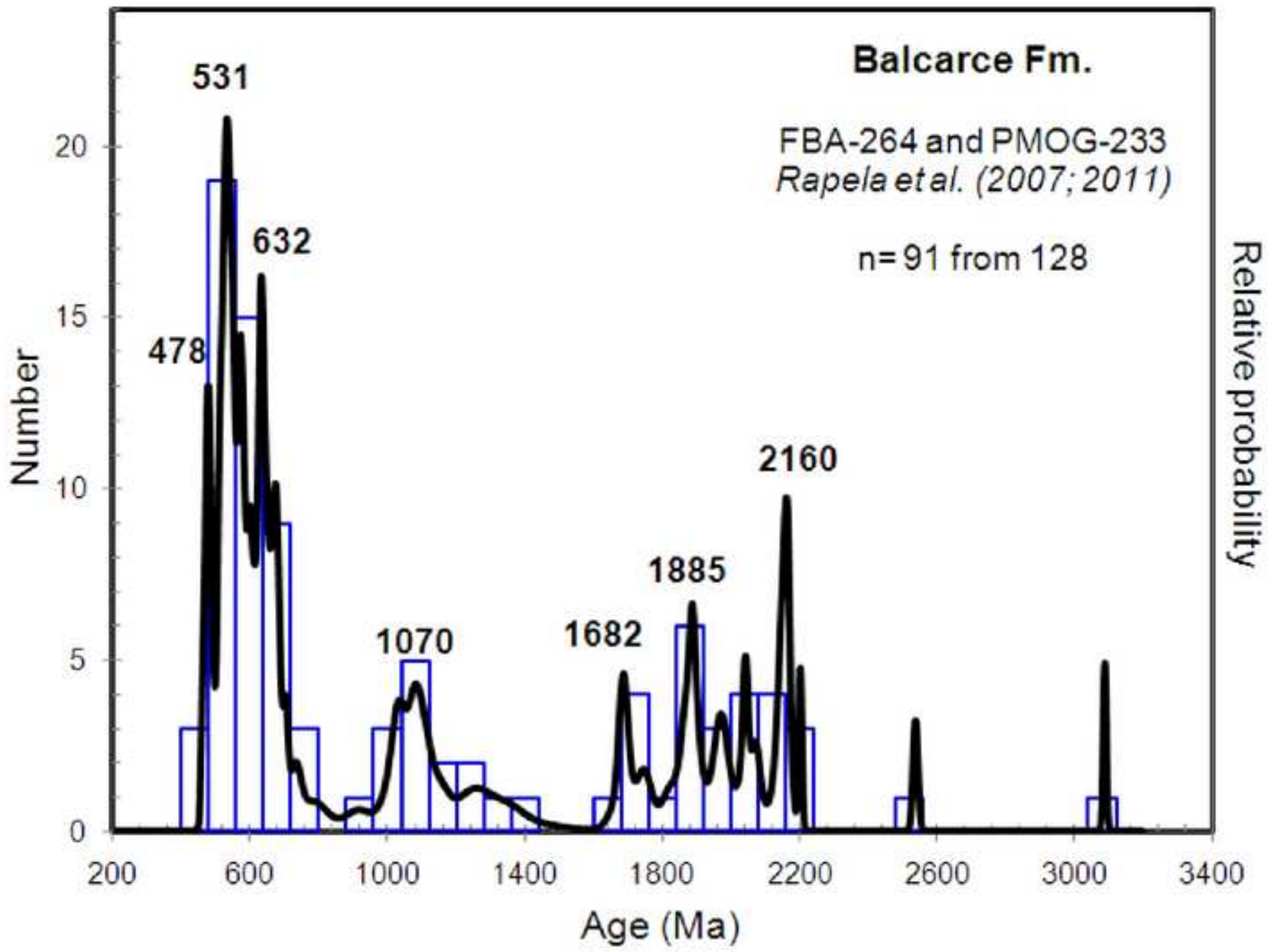


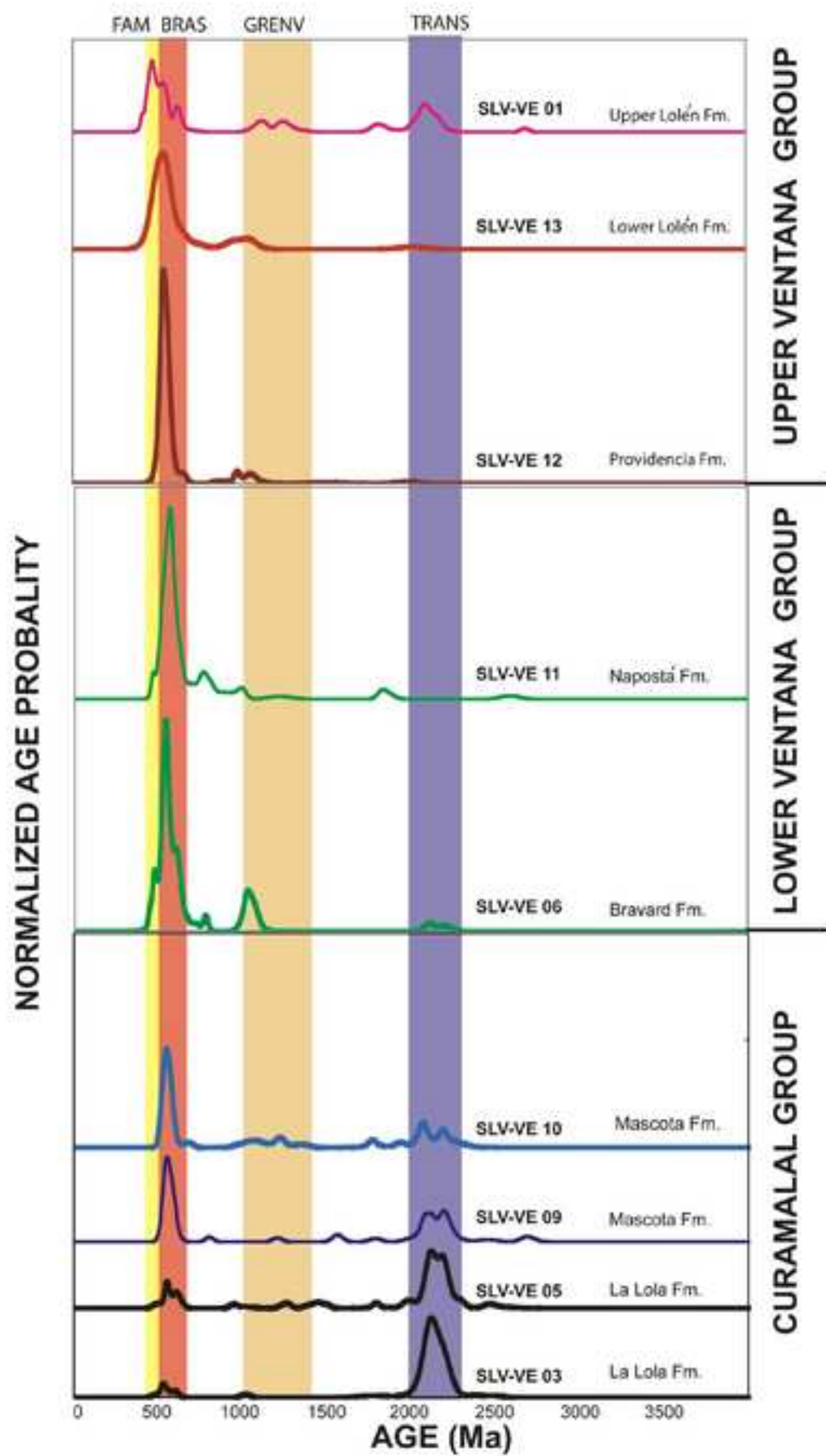


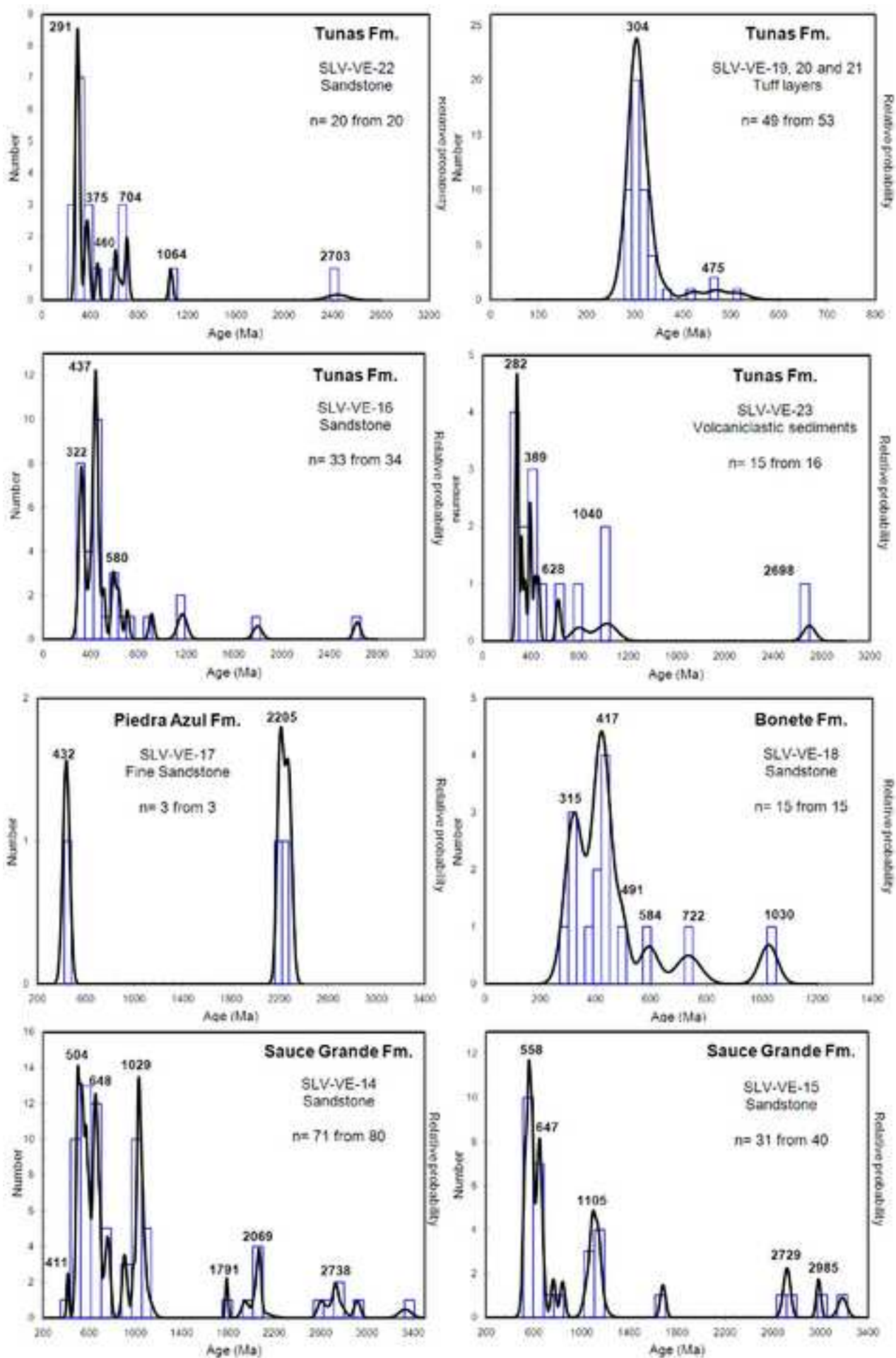
New Figure 10

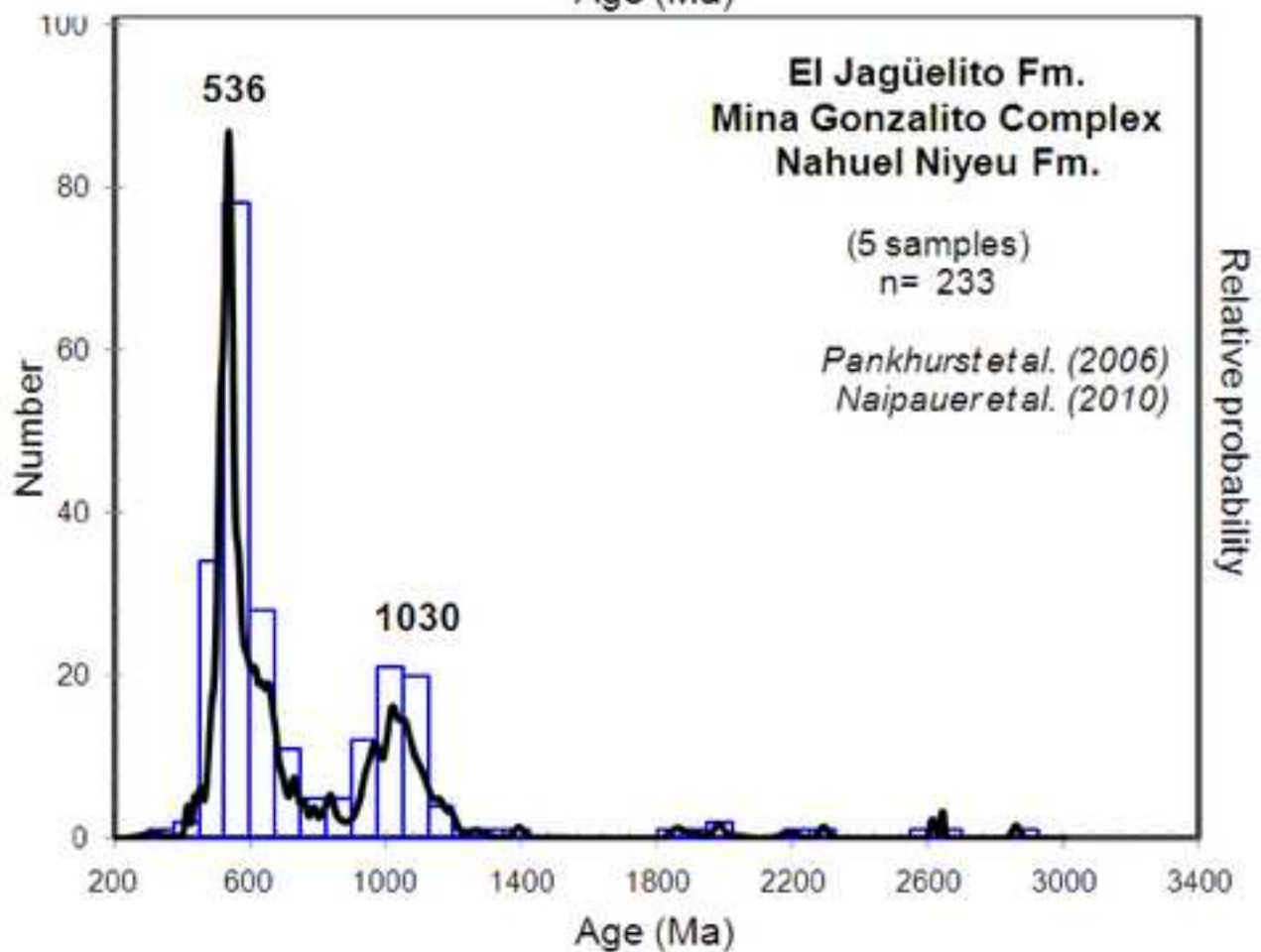
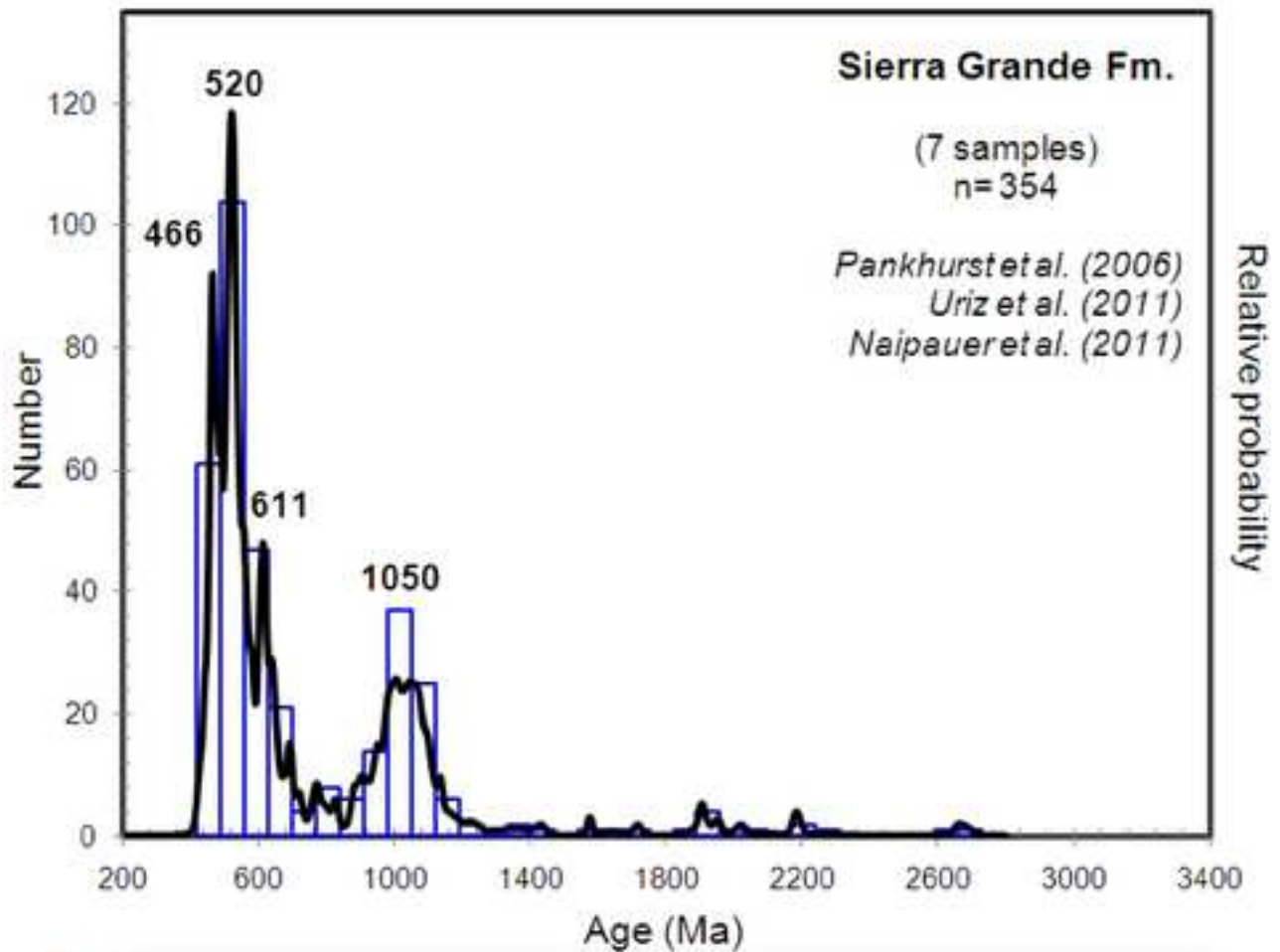
[Click here to download high resolution image](#)

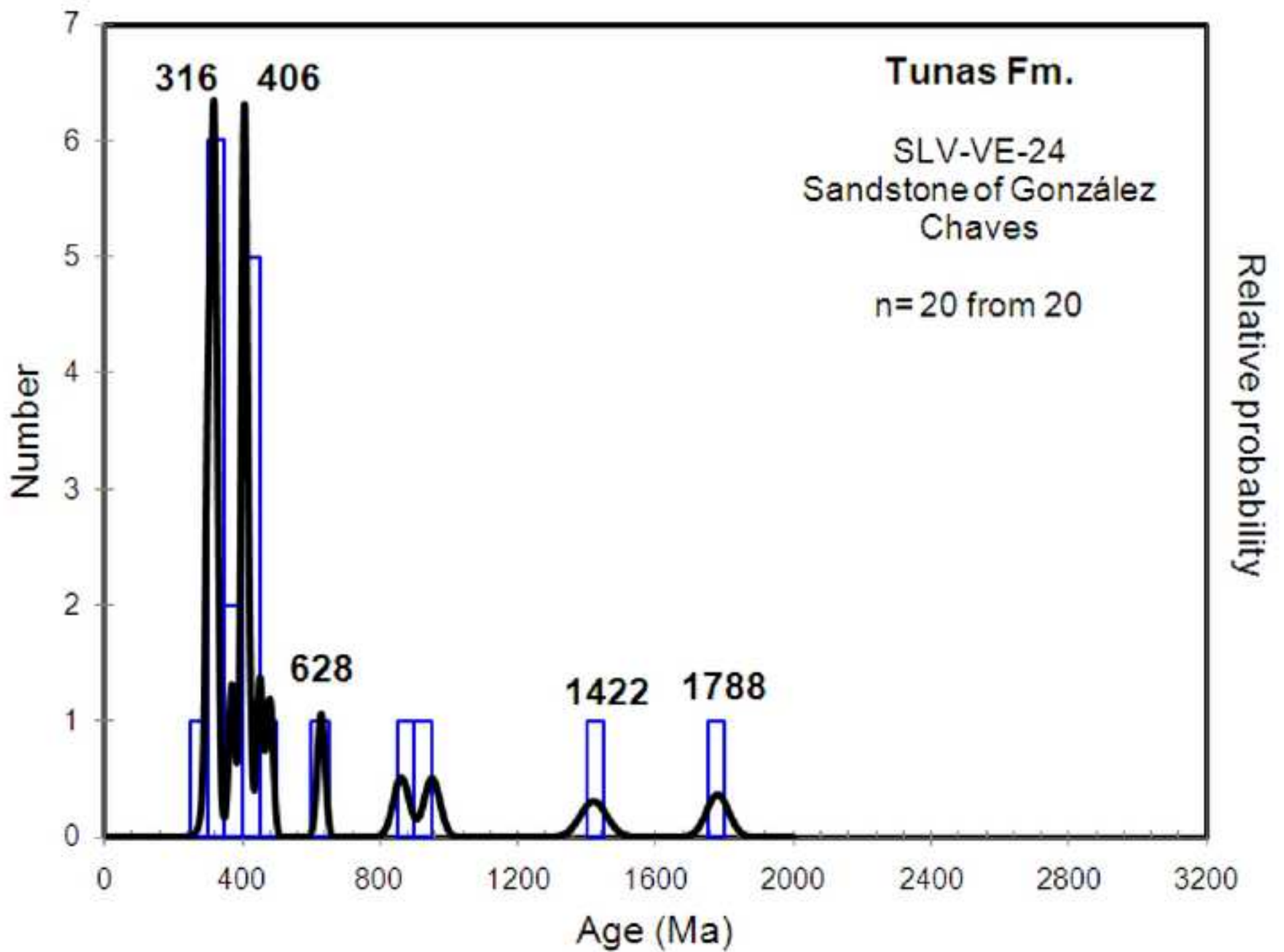












New Figure 16

[Click here to download high resolution image](#)

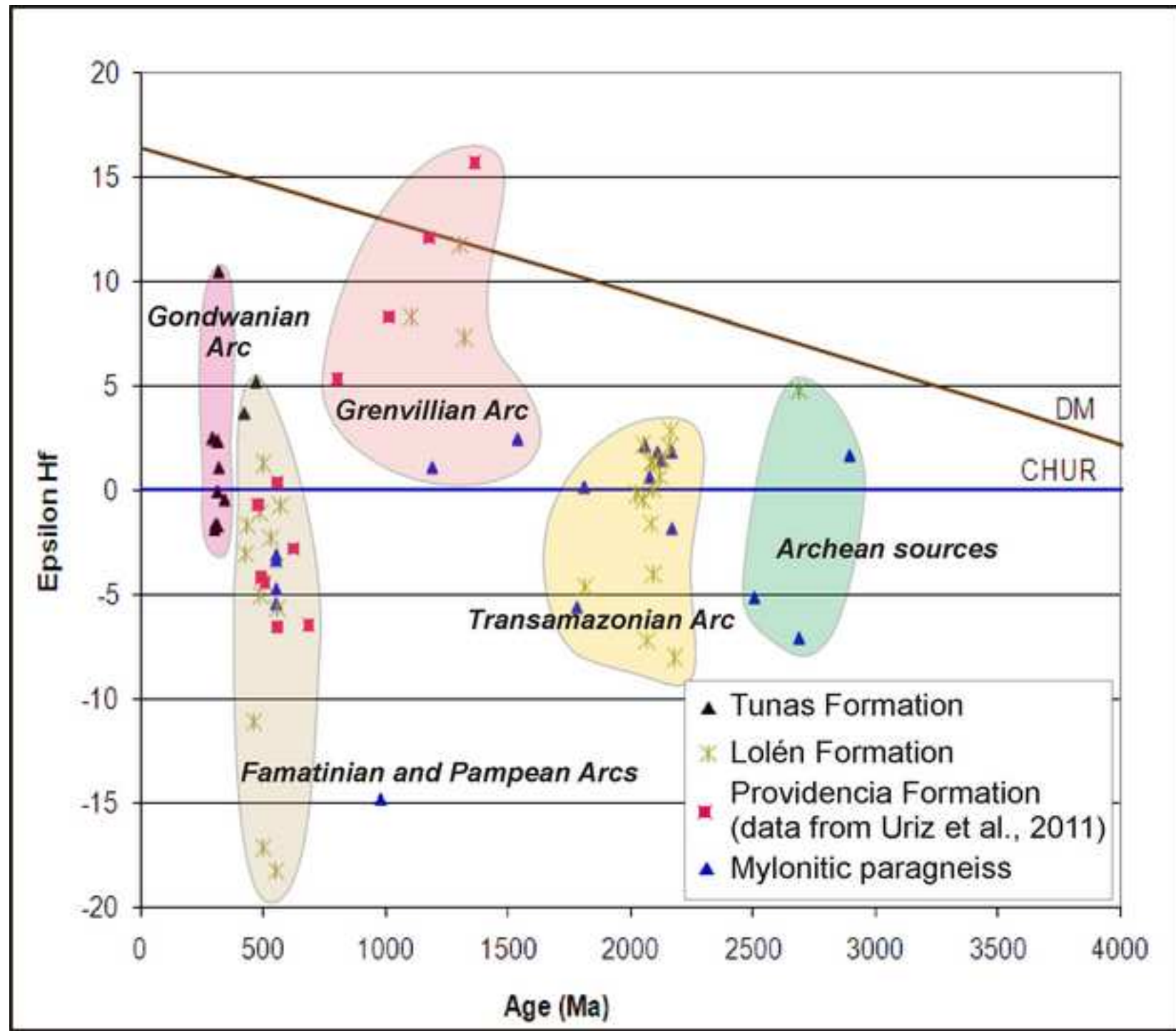
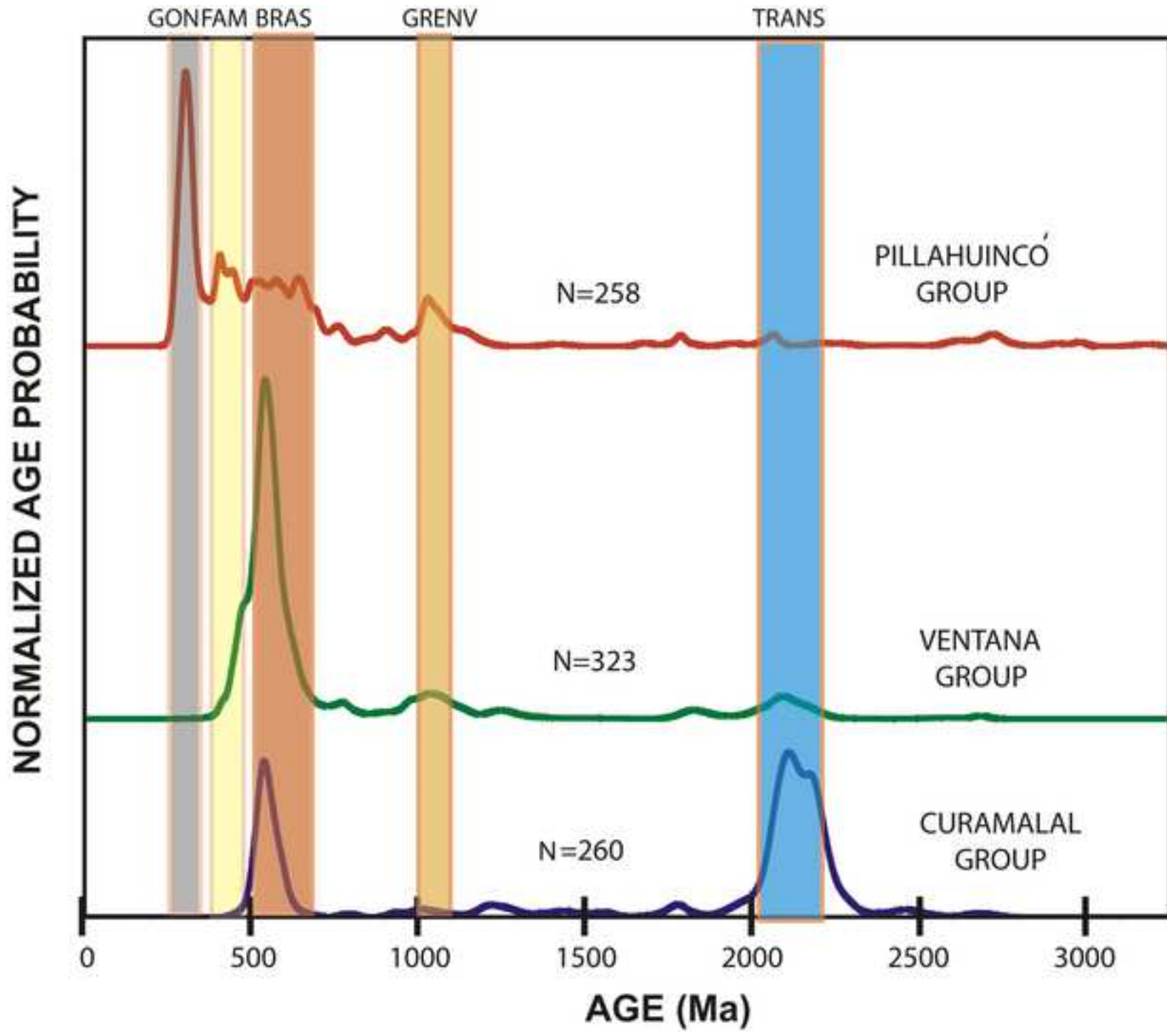
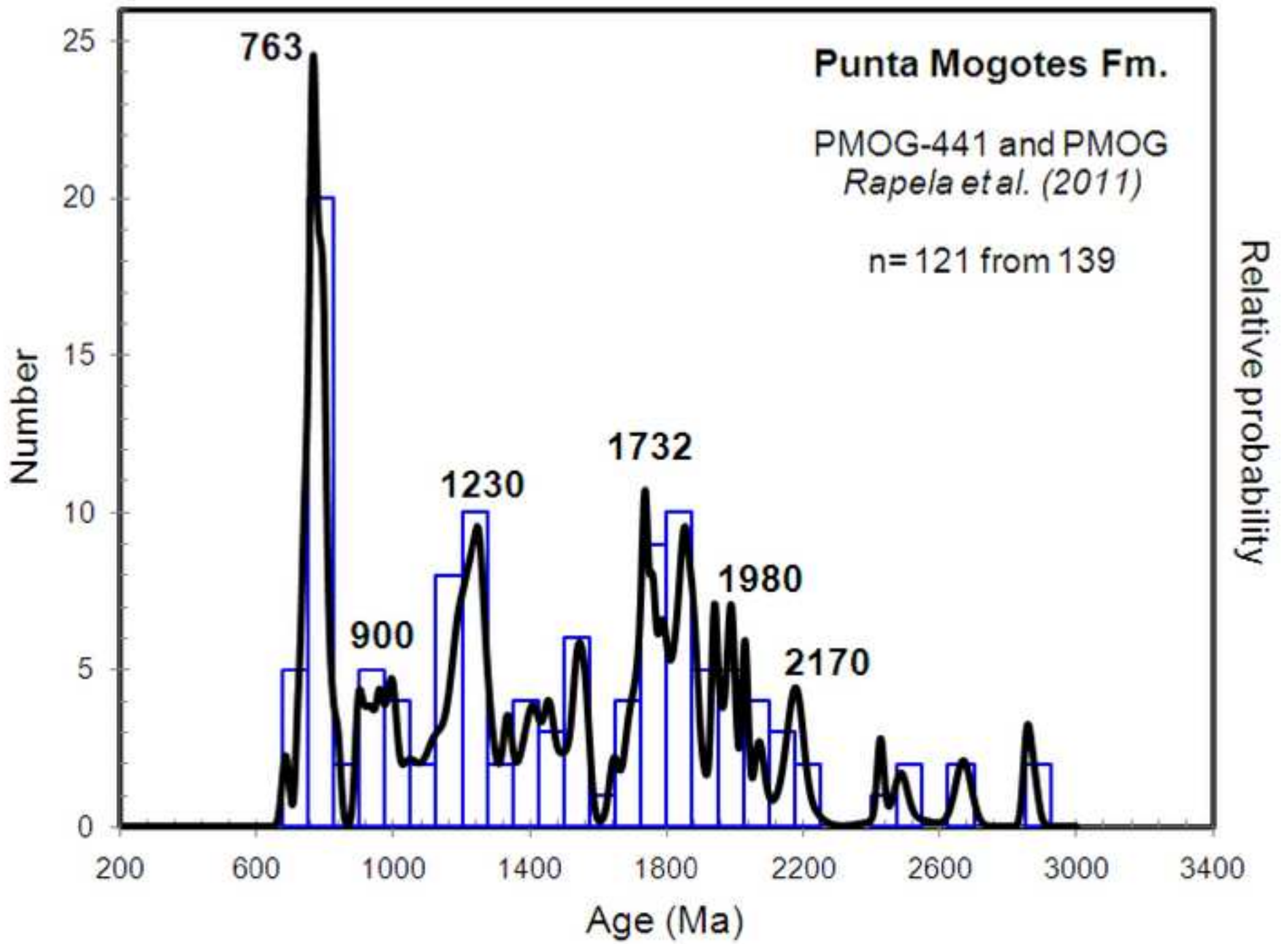


Figure 17
[Click here to download high resolution image](#)





New Figure 19
[Click here to download high resolution image](#)

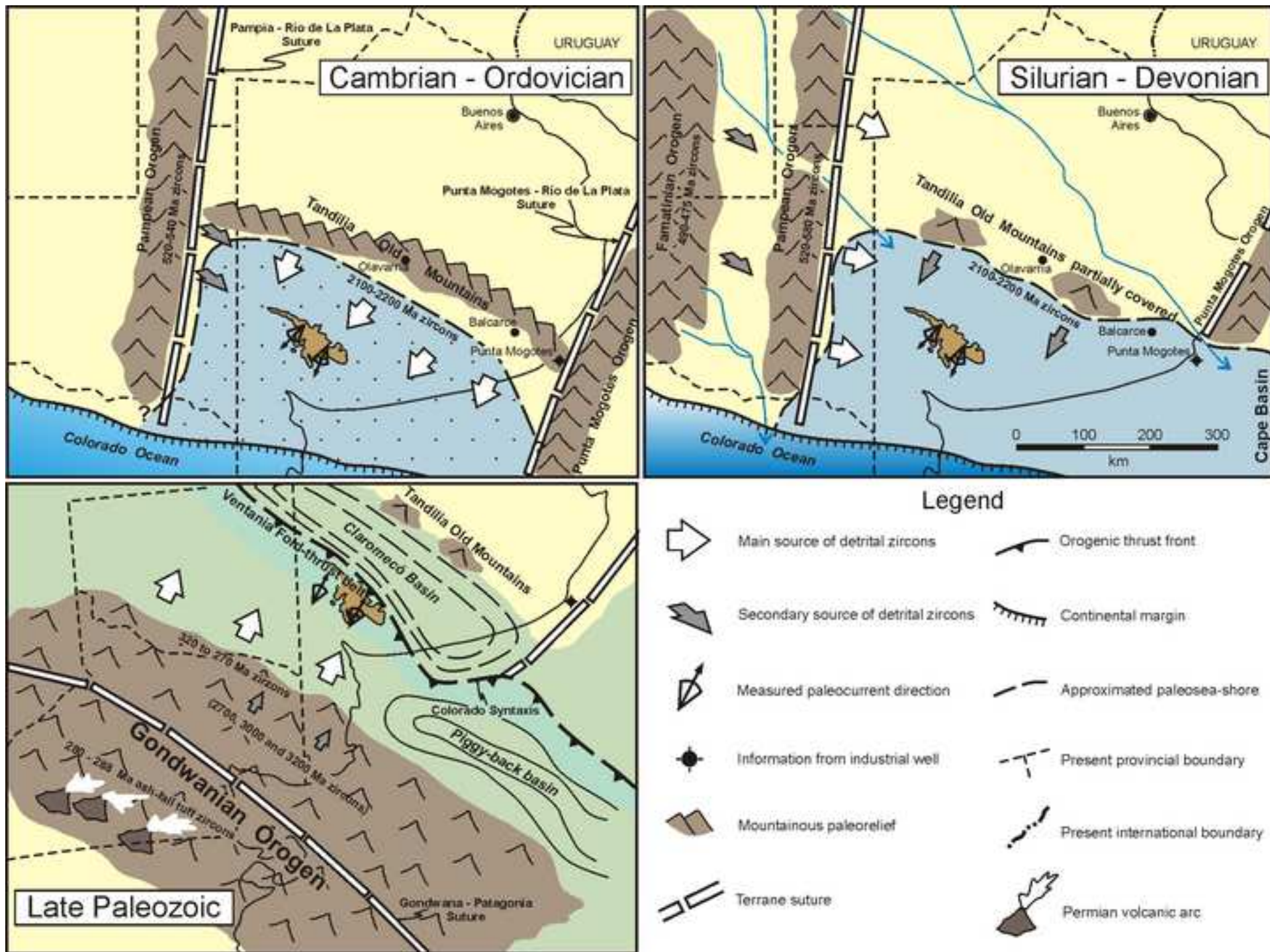
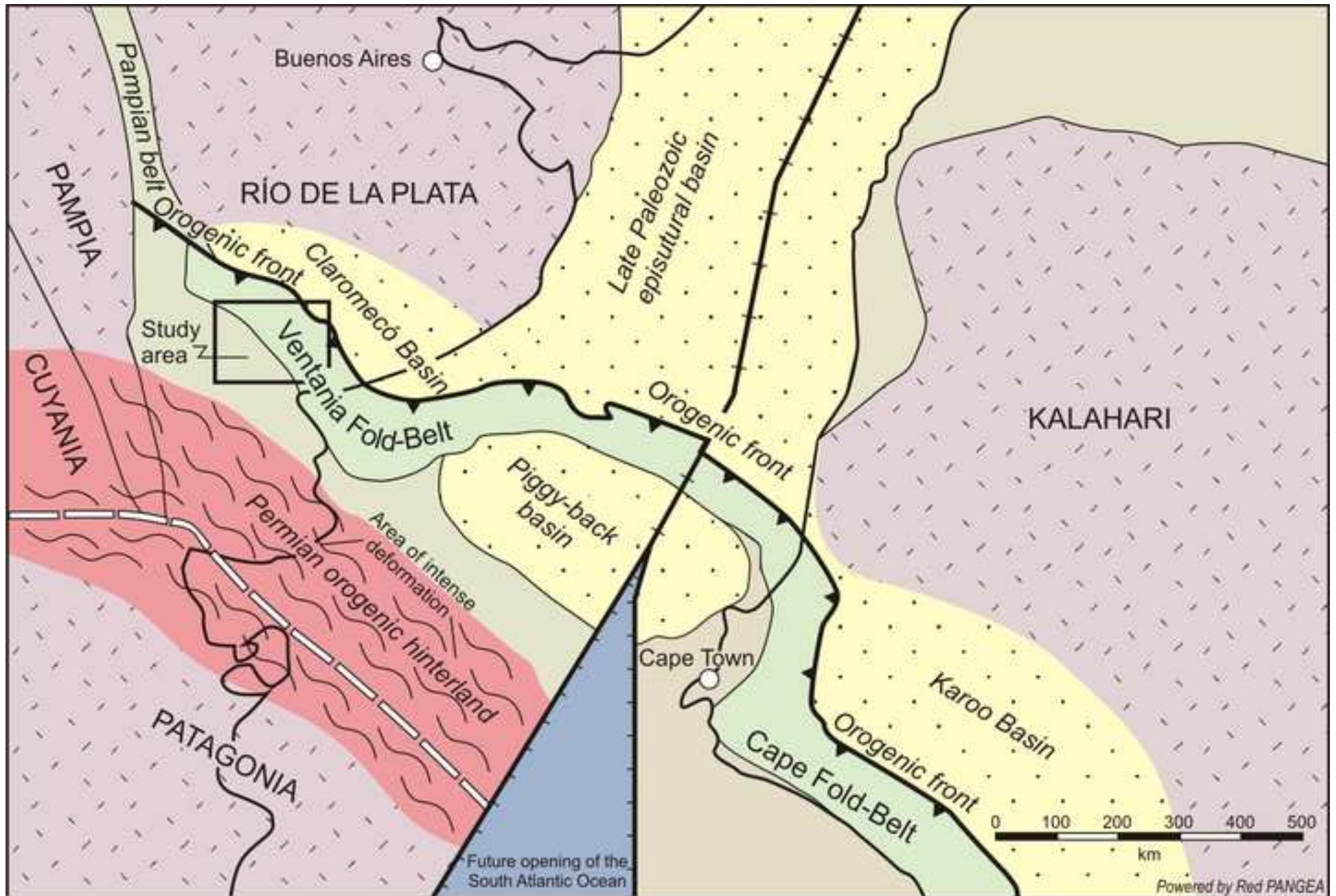


Figure 20
[Click here to download high resolution image](#)



Supplementary Table 1

[Click here to download e-component: Supplementary Table_1_Sample list.pdf](#)

Supplementary Table 2

[Click here to download e-component: Supplementary Table_2_U-Pb data.pdf](#)

Table 3: Lu-Hf dataLu-Hf data obtained by MC-ICPMS in detrital zircons from the quartzite of Lolén Fm, Sierra de la Ventana (**sample SLV-VE-01**)

Name	U/Pb Age (Ma)	$\pm 2\sigma$	Sample (Present day ratios)			Sample Initial Ratios				T DM Ga	Assumed Values			
			$^{176}\text{Hf}/^{177}\text{Hf}$	$\pm 2\text{SE}$	$^{176}\text{Lu}/^{177}\text{Hf}$	$\pm 2\text{SE}$	$^{176}\text{Hf}/^{177}\text{Hf}$ (t)	$\epsilon\text{Hf}(0)$	$\epsilon\text{Hf}(t)$		$\pm 2\text{SE}$	t (Ma)	λ (Ga-1) ^a	
002-A-I-03	2093	106	0.281346	3.61E-05	0.000343	1.93E-05	0.281332	-50.88	-4.04	0.43	2.59	4560		
003-A-I-05	2157	53	0.281476	2.66E-05	0.000319	9.70E-06	0.281463	-46.29	2.08	0.11	2.41		$(^{176}\text{Hf}/^{177}\text{Hf})^0\text{chur}^b$	0.282785
004-A-I-08	2023	43	0.281510	2.84E-05	0.000608	1.16E-05	0.281487	-45.09	-0.18	0.01	2.39		$(^{176}\text{Lu}/^{177}\text{Hf})^0\text{chur}^b$	0.0336
005-A-I-09	2165	62	0.281498	2.99E-05	0.000462	1.44E-05	0.281479	-45.49	2.86	0.17	2.39		$(^{176}\text{Hf}/^{177}\text{Hf})\text{DM}^c$	0.28325
006-A-I-10	461	54	0.282186	3.61E-05	0.000517	1.88E-05	0.282181	-21.19	-11.09	1.70	1.47		$(^{176}\text{Lu}/^{177}\text{Hf})\text{DM}^c$	0.0388
009-A-I-11	2066	59	0.281272	3.67E-05	0.000320	5.66E-06	0.281260	-53.49	-7.23	0.34	2.68		$(^{176}\text{Lu}/^{177}\text{Hf})\text{BSE}^d$	0.015
010-A-I-14	2178	63	0.281183	3.14E-05	0.000432	4.32E-06	0.281165	-56.66	-8.01	0.31	2.81		$^{176}\text{Lu}/^{177}\text{Hf}^e$	0.022
011-A-I-18	569	40	0.282413	3.98E-05	0.000728	1.92E-05	0.282406	-13.14	-0.73	0.07	1.16		$^{176}\text{Lu}/^{177}\text{Hf}^e$	0.010
012-A-I-22	2118	90	0.281476	4.59E-05	0.000703	4.74E-05	0.281447	-46.30	0.63	0.07	2.44			
013-A-I-26	551	26	0.281929	4.09E-05	0.000571	1.23E-05	0.281923	-30.28	-18.22	1.25	1.82			
014-A-I-34	2083	120	0.281417	5.72E-05	0.000228	1.91E-05	0.281408	-48.36	-1.57	0.22	2.49			
015-A-I-36	2136	87	0.281480	2.99E-05	0.000476	3.88E-05	0.281460	-46.16	1.50	0.18	2.42			
016-B-II-02	557	56	0.282283	4.73E-05	0.000812	3.15E-05	0.282275	-17.75	-5.64	0.79	1.35			
017-B-II-08	2092	87	0.281503	3.56E-05	0.000428	1.62E-05	0.281486	-45.35	1.38	0.11	2.39			
018-B-II-14	2092	87	0.281467	4.59E-05	0.000468	7.61E-06	0.281449	-46.60	0.07	0.00	2.43			
033-D-IV-02	433	40	0.282470	3.89E-05	0.000510	2.86E-05	0.282466	-11.15	-1.66	0.25	1.08			
034-D-IV-03	499	64	0.282518	3.77E-05	0.001187	1.47E-05	0.282507	-9.44	1.29	0.18	1.03			
035-D-IV-07	427	56	0.282436	3.97E-05	0.000740	9.41E-06	0.282430	-12.33	-3.04	0.44	1.13			
036-D-IV-22	2688	46	0.281218	5.78E-05	0.000554	1.47E-05	0.281189	-55.42	4.76	0.21	2.77			
037-E-V-11	1320	113	0.282167	5.85E-05	0.000574	4.70E-06	0.282153	-21.84	7.32	0.69	1.50			
038-E-14	486	81	0.282345	6.08E-05	0.000894	3.78E-05	0.282337	-15.54	-5.01	1.05	1.26			
039-F-VI-01	1300	118	0.282310	4.95E-05	0.000767	2.33E-05	0.282291	-16.80	11.77	1.42	1.31			
040-F-VI-04	1104	52	0.282330	4.07E-05	0.000444	6.66E-06	0.282319	-16.10	12.75	1.35	1.27			
041-G-VII-05	1814	54	0.281510	2.98E-05	0.000379	3.06E-05	0.281502	-45.08	-20.68	2.64	2.37			
042-G-VII-06	485	65	0.282454	3.34E-05	0.000524	1.73E-05	0.282436	-11.70	28.71	1.81	1.10			
021-B-II-16	2051	170	0.281480	4.15E-05	0.000482	3.43E-05	0.281461	-46.15	-0.44	0.07	2.42			

022-B-II-21	597	67	0.281529	1.06E-04	0.001158	9.05E-05	0.281516	-44.41	-31.59	6.03	2.39
023-B-II-25	2051	170	0.281570	4.17E-05	0.000882	4.67E-05	0.281536	-42.97	2.21	0.30	2.32
024-B-II-26	500	30	0.281888	3.46E-05	0.000345	1.84E-05	0.281885	-31.72	-20.72	2.35	1.86
025-B-II-31	2082	152	0.281515	4.74E-05	0.000598	1.05E-05	0.281491	-44.92	1.35	0.12	2.38
026-B-II-37	531	37	0.282397	4.55E-05	0.001041	5.61E-05	0.282386	-13.74	-2.27	0.28	1.20
027-C-III-06	500	15	0.281987	3.48E-05	0.000130	1.65E-05	0.281986	-28.21	-17.13	2.69	1.72
028-C-III-18	464	15	0.281527	5.39E-05	0.000409	1.70E-05	0.281523	-44.49	-34.32	2.55	2.35
029-C-III-21	362	15	0.281317	3.22E-05	0.000164	2.98E-06	0.281316	-51.91	-43.93	2.62	2.61
030-C-III-27	617	15	0.281410	1.61E-04	0.000676	1.42E-05	0.281403	-48.61	-35.17	1.61	2.52

Lu-Hf data obtained by MC-ICPMS in detrital zircons from the mylonitic paragneiss of Pan de Azúcar area, Sierra de la Ventana (sample SLV-VE-02)

Name	U/Pb Age (Ma)	$\pm 2\sigma$	Sample (Present day ratios)				Sample Initial Ratios				T DM Ga	Assumed Values	
			$^{176}\text{Hf}/^{177}\text{Hf}$	$\pm 2\text{SE}$	$^{176}\text{Lu}/^{177}\text{Hf}$	$\pm 2\text{SE}$	$^{176}\text{Hf}/^{177}\text{Hf}$ (t)	$\epsilon\text{Hf}(0)$	$\epsilon\text{Hf}(t)$	$\pm 2\text{SE}$		t (Ma)	λ (Ga-1) ^a
065-A-1	979	29	0.281755	4.45E-05	0.000423	7.75E-06	0.281747	-36.43	-14.82	0.71	2.05	$(^{176}\text{Hf}/^{177}\text{Hf})^0\text{chur}$ ^b	0.282785
066-A-6	2690	17	0.280890	3.40E-05	0.000670	6.14E-05	0.280856	-67.00	-7.06	0.69	3.22	$(^{176}\text{Hf}/^{177}\text{Hf})^i\text{chur}$	0.279718
067-A-9	2079	11	0.281501	4.13E-05	0.000678	6.68E-05	0.281475	-45.39	0.69	0.07	2.40	$(^{176}\text{Lu}/^{177}\text{Hf})^0\text{chur}$ ^b	0.0336
068-A-14	2170	20	0.281352	3.78E-05	0.000168	4.40E-05	0.281345	-50.68	-1.80	0.49	2.57	$(^{176}\text{Hf}/^{177}\text{Hf})\text{DM}$ ^c	0.28325
069-A-18	2170	20	0.281472	1.16E-04	0.000548	3.91E-05	0.281449	-46.43	1.90	0.15	2.43	$(^{176}\text{Lu}/^{177}\text{Hf})\text{DM}$ ^c	0.0388
070-B-05	1190	11	0.282073	4.30E-05	0.000477	8.15E-06	0.282063	-25.16	1.15	0.03	1.62	$(^{176}\text{Lu}/^{177}\text{Hf})\text{BSE}$ ^d	0.015
072-B-06	2128	18	0.281491	4.43E-05	0.000634	6.68E-05	0.281465	-45.77	1.48	0.17	2.41	$^{176}\text{Lu}/^{177}\text{Hf}$ ^e	0.022
71-B-07	2897	11	0.280988	3.00E-05	0.000388	1.49E-06	0.280966	-63.55	1.73	0.01	3.06	$^{176}\text{Lu}/^{177}\text{Hf}$ ^e	0.010
075-B-09	2507	36	0.281043	5.70E-05	0.000243	1.99E-05	0.281031	-61.60	-5.11	0.49	2.98		
076-B-11	1811	10	0.281651	3.02E-05	0.000453	3.91E-06	0.281635	-40.11	0.20	0.00	2.19		
078-B-17	2059	8	0.281568	4.61E-05	0.000970	5.93E-05	0.281530	-43.04	2.19	0.14	2.33		
079-C-1	552	20	0.282315	4.55E-05	0.001017	9.96E-05	0.282304	-16.63	-4.70	0.63	1.31		
080-C-3	552	20	0.282294	4.95E-05	0.000939	4.69E-05	0.282284	-17.36	-5.40	0.47	1.34		
081-C-4	552	20	0.282366	5.76E-05	0.001587	6.14E-05	0.282350	-14.80	-3.08	0.23	1.26		
082-C-10	1539	18	0.281893	3.73E-05	0.000565	1.23E-05	0.281876	-31.56	2.51	0.08	1.87		
083-C-16	1782	11	0.281532	5.83E-05	0.001186	4.43E-05	0.281491	-44.33	-5.57	0.24	2.39		
084-C-17	552	20	0.282353	3.46E-05	0.001000	2.37E-06	0.282343	-15.27	-3.33	0.13	1.26		
085-D-1	2111	19	0.281505	4.61E-05	0.000442	7.73E-06	0.281487	-45.27	1.88	0.05	2.38		

Lu-Hf data obtained by MC-ICPMS in detrital zircons from the tuffs of Tunas Fm., Sierra de la Ventana (sample SLV-VE-20 and SLE-VE-21)

Name	U/Pb Age (Ma)	$\pm 2\sigma$	Sample (Present day ratios)				Sample Initial Ratios				T DM Ga	Assumed Values	
			$^{176}\text{Hf}/^{177}\text{Hf}$	$\pm 2\text{SE}$	$^{176}\text{Lu}/^{177}\text{Hf}$	$\pm 2\text{SE}$	$^{176}\text{Hf}/^{177}\text{Hf}$ (t)	$\epsilon\text{Hf}(0)$	$\epsilon\text{Hf}(t)$	$\pm 2\text{SE}$		t (Ma)	
045-ZR-8-A-17	317	15	0.282623	4.38E-05	0.000979	1.97E-05	0.282617	-5.74	1.11	0.07	0.88	λ (Ga-1) ^a	4560
046-ZR-8-A-40	316	8	0.282888	3.68E-04	0.000824	9.75E-05	0.282883	3.64	10.51	1.52	0.51	$(^{176}\text{Hf}/^{177}\text{Hf})^0\text{chur}$ ^b	0.01867
047-ZR-8-B-II-35	311	20	0.282661	7.86E-05	0.000787	1.21E-05	0.282657	-4.38	2.38	0.19	0.82	$(^{176}\text{Hf}/^{177}\text{Hf})^i\text{chur}$	0.282785
048-ZR-8 C-III-18	290	20	0.282678	4.89E-05	0.000926	6.47E-05	0.282673	-3.77	2.50	0.35	0.80	$(^{176}\text{Lu}/^{177}\text{Hf})^0\text{chur}$ ^b	0.0336
049-ZR-8-C-III-13	311	19	0.282594	8.77E-05	0.001079	3.57E-05	0.282588	-6.74	-0.05	0.00	0.92	$(^{176}\text{Hf}/^{177}\text{Hf})\text{DM}$ ^c	0.28325
050-ZR-8-C-III-6	300	22	0.282547	1.05E-04	0.000664	2.15E-05	0.282543	-8.41	-1.87	0.20	0.98	$(^{176}\text{Lu}/^{177}\text{Hf})\text{DM}$ ^c	0.0388
051-ZR-8 E-V-3	303	11	0.282552	3.36E-05	0.000596	1.64E-05	0.282548	-8.25	-1.63	0.10	0.97	$(^{176}\text{Lu}/^{177}\text{Hf})\text{BSE}$ ^d	0.015
052-ZR-8 E-V-7	312	9	0.282545	6.66E-05	0.000718	1.06E-05	0.282541	-8.48	-1.69	0.07	0.98	$^{176}\text{Lu}/^{177}\text{Hf}$ ^e	0.022
053-ZR-8 E-V-9	340	8	0.282565	4.99E-05	0.000991	2.99E-05	0.282559	-7.78	-0.44	0.02	0.96	$^{176}\text{Lu}/^{177}\text{Hf}$ ^e	0.010
036-Zr 8 E-V-11	303	6	0.281914	2.71E-05	0.000096	1.33E-05	0.281913	-30.82	-24.11	3.81	1.82		
056-ZR-8 F-VI-18	420	18	0.282633	5.55E-05	0.001006	4.83E-05	0.282625	-5.36	3.71	0.34	0.87		
057-ZR-8 F-VI-01	468	16	0.282643	3.56E-05	0.000627	1.86E-05	0.282637	-5.02	5.22	0.33	0.85		

a ^{176}Lu decay constant (Söderlund et al., 2004)

b Chondritic values (Bouvier et al., 2008)

c Present day Depleted Manlte (Griffin et al., 2000; updated by Andersen et al., 2009)

d Goodge and Vervoort, EPSL 243, 711-731 (2006)

e $^{176}\text{Lu}/^{177}\text{Hf}$ ratios of mafic and felsic crust from Pietranik et al. (2008)

